IET #12 /

[redacted]

~~[redacted]~~

APEX
445
Cy. 1

~~[redacted]~~

H. Peterson 12-7-88

~~H. Peterson 8-31-89~~

LOAN COPY
return to
TECHNICAL LIBRARY

DECLASSIFIED

Research and
Development Report

Final Report
First Meltdown Experiment
(Operation Boot)

LOAN COPY
THIS REPORT MAY BE RECALLED
AFTER TWO WEEKS. PLEASE
RETURN PROMPTLY TO:
INL TECHNICAL LIBRARY

R.E.Baker
C.C.Gamertsfelder R.F.Gentzler

UNCLASSIFIED

classification cancelled
per TID-1299 4-30-64
by Connie Erickson 9-28-64

G. Staymates 1-24-05

GENERAL ELECTRIC
ATOMIC PRODUCTS DIVISION
AIRCRAFT NUCLEAR PROPULSION DEPARTMENT

SPECIAL REVIEW
FINAL DETERMINATION
Len Koch
DATE 4-12-94

CLASSIFIED
AUTHORITY
H. F. CARROLL
CONFIDENTIAL

[redacted]

TAN-P084

[redacted]L

Apex-445

Nuclear Technology – Reactor
Engineering and Technology
M-3679 (25th Ed.)

DECLASSIFIED

Final Report First Meltdown Experiment
(Operation Boot)

R.E. Baker **C.C. Gamertsfelder** **R.F. Gentzler**

Radiation and Criticality Safety

January 2, 1959

United States Air Force — Contract No. AF 33(600)-38062

United States Atomic Energy Commission — Contract No. AT (11-1)-171

GENERAL ELECTRIC
ATOMIC PRODUCTS DIVISION
AIRCRAFT NUCLEAR PROPULSION DEPARTMENT
Cincinnati 15, Ohio

Published by
Technical Publications Sub-Section

DECLASSIFIED

[redacted]

1-2

GROUP 1
EXCLUDED FROM AUTOMATIC DOWNGRADING
AND DECLASSIFICATION.

[redacted]

DECLASSIFIED

C-44c

Standard Distribution

Copies	
1	ACF-South Albuquerque Works
1	Aerojet-General, Azusa (BUWEPS)
1	Aerojet-General Nucleonics
1	Aeroprojects, Inc.
2	AiResearch Manufacturing Company of Arizona
1	Air Force Cambridge Research Laboratories
2	Air Force Special Weapons Center
1	Air Technical Intelligence Center
2	Albuquerque Operations Office
1	Alco Products, Inc.
1	Allis-Chalmers Manufacturing Company
1	Allis-Chalmers Manufacturing Company, Washington
1	Allison Division–GMC
2	Argonne National Laboratory
1	Armour Research Foundation
1	Army Air Defense School
1	Army Chemical Center
1	Army Engineer Research and Development Laboratories
1	Army Medical Research Laboratory
5	Atomic Energy Commission, Washington
1	Atomic Power Development Associates, Inc.
1	Atomics International
2	Babcock and Wilcox Company
1	Battelle Memorial Institute
1	Bendix Aviation Corporation (ALOO-705)
1	Bridgeport Brass Company
2	Brookhaven National Laboratory
1	Bureau of Naval Weapons
1	Bureau of Ships
1	Bureau of Yards and Docks
1	Central Intelligence Agency (NED)
2	Chicago Operations Office
1	Chicago Patent Group
1	Columbia University (NYOO-187)
1	Combustion Engineering, Inc.
2	Combustion Engineering, Inc. (NRD)
1	Convair Division, Fort Worth
1	Convair Division, San Diego (BUWEPS)
1	Cornell University (Wilson)
1	Defense Atomic Support Agency, Washington
1	Department of the Army
1	Director of Defense Research and Engineering (OSD)
1	Division of International Affairs, Brussels
1	Division of International Affairs, Tokyo
4	duPont Company, Aiken
1	duPont Company, Wilmington
1	Edgerton, Germeshausen and Grier, Inc., Goleta
1	Electric Boat Division
1	Franklin Institute of Pennsylvania
1	General Atomic Division
4	General Electric Company (ANPD)
6	General Electric Company, Richland
1	General Nuclear Engineering Corporation
1	Gibbs and Cox, Inc.
1	Hanford Operations Office
1	Iowa State University
1	Jet Propulsion Laboratory
1	Johns Hopkins University (ORO)
6	Knolls Atomic Power Laboratory

Copies	
4	Los Alamos Scientific Laboratory
1	Lowry Air Force Base
1	Marquardt Corporation
1	Martin Company
1	Martin Company, Baltimore (BUWEPS)
1	Massachusetts Institute of Technology (Evans)
1	Massachusetts Institute of Technology (Thompson)
1	Mound Laboratory
1	NASA Ames Research Center
1	NASA Flight Research Center
1	NASA George C. Marshall Space Flight Center
1	NASA Langley Research Center
1	NASA Lewis Research Center
1	National Aeronautics and Space Administration, Washington
1	National Bureau of Standards
1	National Lead Company of Ohio
1	Naval Air Development Center
1	Naval Air Material Center
1	Naval Medical Research Institute
1	Naval Ordnance Laboratory
1	Naval Postgraduate School
1	Naval Radiological Defense Laboratory
2	Naval Research Laboratory
1	Naval Training Device Center
1	New York Naval Shipyard
1	New York Operations Office
1	North American Aviation, Inc., Downey
1	Nuclear Development Corporation of America
1	Nuclear Materials and Equipment Corporation
1	Nuclear Metals, Inc.
1	Oak Ridge Operations Office
1	Office of the Chief of Naval Operations
1	Olin Mathieson Chemical Corporation
1	Patent Branch, Washington
5	Phillips Petroleum Company (NRTS)
1	Power Reactor Development Company
1	Pratt and Whitney Aircraft Division
1	Princeton University
1	Public Health Service
1	San Francisco Operations Office
1	Sandia Corporation
1	Sargent & Lundy
1	Savannah River Operations Office
1	Secretary of the Air Force, R&D
1	Surgeon General
2	Union Carbide Nuclear Company (ORGDP)
5	Union Carbide Nuclear Company (ORNL)
1	USAF Headquarters (ODCE)
1	University of California, Berkeley
1	University of California, Livermore
1	Walter Reed Army Medical Center
6	Westinghouse Bettis Atomic Power Laboratory
1	Westinghouse Electric Corporation
1	Westinghouse Electric Corporation (Biondi)
8	Wright Air Development Division
1	Yankee Atomic Electric Company (NYOO-222)
40	Office of Technical Information Extension

3-4

[redacted]L

DECLASSIFIED

[redacted]

DECLASSIFIED

Abstract

An experiment is described which was conducted to determine the extent of damage to a high performance aircraft type reactor and the degree of radiological hazard which resulted from airborne fission products released as a consequence of severely restricting coolant air.

The facility, field sampling network, conduct of the experiment, and results are presented. Release fractions of fission products, reactor damage, radiological hazards, and the prediction of the distribution of airborne activity using meteorological diffusion theory are discussed.

DECLASSIFIED

[redacted]

[redacted]

[redacted]

[redacted]

DECLASSIFIED

Contents

Introduction 9
The Problem 9
Desired Conditions 9
Description of Experiment 11
General Test Requirements 11
Geographical Aspects 12
Reactor Test Facilities 17
Reactor and Insert 17
General Nuclear Data 17
Power Distribution 27
Insert Temperature Measurements 27
Stage Radial Temperature Profiles 27
Cartridge Temperature Relationships 31
Performance Characteristics 31
CTF Effluent Sampling and Monitoring Devices 31
Field Sampling Network 31
Meteorological Instrumentation 38
Idaho Test Station Facilities 38
Supporting Instrumentation from USWB 41
Conduct of Experiment and Results 43
Reactor Operations and CTF Data 43
Reactor Operating History and Iodine Inventory 43
Events Following the Valve Closing 43
Scram Significance 46
Changes in Excess Reactivity 46
Reactor Damage 52
Handling and Analyses of Samples 62
CTF Source Data 62
Atmospheric Conditions at Test Time 67
Description of Weather Regime 67
Cloud Trajectory and Diffusion Parameters 74
Field Sampling Data 83
Fallout Plates 83
High Volume Air Samples 92
Vegetation Samples 100
Carbon Traps 100
Pocket Ionization Chambers and Film Badges 100
Inoperative Instrumentation 100
Other Measurements 103

[redacted]

DECLASSIFIED

[redacted]

I^{131} Release Fraction Estimate by Residue Analysis 103
Chemical Separations 103
I^{131} Fractional Release Estimation 106
Contamination of Facilities 106
Comparison of Measured Data with Predicted Values 109
Airborne Activity Distribution 109
Activity and Wind Direction Fluctuation Distribution 126
Discussion 133
Reactor Damage 133
Source Measurements and Fractional Release 133
Residue Analysis 134
Effluent Samples (Duct) 134
Diffusion Theory and Isopleths 135
General 135
Environmental Measurements 135
Vegetation 135
Fallout Activity 136
Particle Size Distribution 136
HVA Samples 136
Conclusions 136

[redacted]

[redacted]

DECLASSIFIED

Introduction

THE PROBLEM

Operation BOOT (burnout one tube) was an experiment designed to obtain information relative to the radiological hazards associated with the release of fission products from a high-performance air cycle reactor. Fission products may be released as a consequence of reactor malfunctions which result in rupturing, melting, burning, or excursion of the reactor core. This experiment was an attempt to ascertain the consequences of severely restricting the coolant airflow through an operating reactor.

The radiological hazards associated with the release of the fission products are dependent upon the amount and kinds of isotopes released, the physical form of the released materials, the methods of dissemination, and certain biological factors. From several independent experiments one can obtain estimates for the many factors pertinent to the hazards of releases from reactors, but, since long extrapolations and many assumptions are necessary, an integrated experiment which incorporated all factors in one system appeared necessary.

DESIRED CONDITIONS

As originally conceived, the plan* was to operate an air-cooled reactor long enough to produce a satisfactory inventory of fission products and while still at full power to restrict the coolant airflow through one cartridge (fuel element), thereby causing it to melt or burn with subsequent release of part of the fission product inventory. Monitoring within the facility, postexperiment examination of the reactor, and field measurements would indicate the magnitude and distribution of the fission product release.

The Initial Engine Test Facility (IET) permits the fission products released from the reactor to be routed through a 150-foot stack before being released to the atmosphere. A sampling network downwind of the stack was planned to establish fallout and aerosol-integrated concentration patterns. Dissemination of aerosols have been described by O. G. Sutton over several kilometers by a diffusion equation, but the adequacy of the equation to predict concentrations at several miles downwind has not been established. It was therefore desirable to select a neutral or weak lapse meteorological condition for the time of release to obtain the simplest dissemination patterns for subsequent analytical treatment.

Prior to the planning of this experiment, a few small samples (~ 0.1 gram of UO_2) of Ni-Cr fuel elements (used by GE-ANPD) were sent to ORNL where they were irradiated in the graphite pile and subsequently melted and analyzed to determine the fractional release of some of the fission products. Fractional release estimates were made for two conditions: (1) a single, very quick melt (~ 30 seconds) with subsequent cooling and (2) a sustained melt over a period of several hours until the sample was essentially entirely

*C. C. Gamertsfelder, et. al, "Private Communication," February 5, 1958.
C. C. Gamertsfelder and R. E. Baker, "Private Communication," April 7, 1958.

[redacted]

DECLASSIFIED

oxidized. The results of these experiments, as given by G. Creek and G. Parker,* are listed in Table 1.

TABLE 1

FRACTIONAL RELEASE

	Quick Melt	Prolonged Melt
Gross gamma	0.004	0.08
Xenon	0.10	0.77
Iodine	0.04	0.77
Cesium	0.005	0.016
Strontium	10^{-6}	10^{-4}

If the differences involved between the experimental conditions of the Creek and Parker release fraction determination and the condition one might expect in a reactor melt are considered, it is obvious that at best the Creek and Parker data could only be expected to be approximations of the expected conditions. After considering the range of iodine release fraction values for the quick and prolonged melts, an estimate of 0.25 was made for the experimental condition.

Samples used for the ORNL laboratory experiments contained approximately 0.1 gram of UO_2, whereas the cartridge to be damaged during this experiment contained about 950 grams of UO_2. The extrapolation with respect to estimating quantity of the iodine release was about four orders of magnitude.

*Private Communication.

DECLASSIFIED

Description of Experiment

GENERAL TEST REQUIREMENTS

The objective of Operation BOOT was to obtain information about the many parameters necessary in predicting the radiological hazards associated with reactor damage caused by insufficient cooling during power operation. Specifically, more information was sought in the following areas:

1. Reactor damage caused by restriction of the coolant air during power operation.
2. Fractional release of specific fission products as a consequence of reactor damage.
3. Physical characteristics of the effluent released from the reactor while it was being damaged.
4. Correlation between measured meteorological quantities and dissemination of activity at ground level, as shown by isopleth patterns.
5. Correlation between ground-level isopleths of airborne activity and isopleths due to fallout and "scrubbing" action of fission products on vegetation.
6. Correlation between isotope concentrations collected by air-sampling devices and isotope concentrations in animal lungs as a consequence of inhalation during passage of the cloud of fission products.

In order to ascertain this information, there were certain requirements for the experiment; these include:

1. Reactor. Theoretical thermodynamic studies can predict temperatures encountered in a reactor during steady-state conditions, but the transient conditions encountered at the time of melting or burning of fuel elements are difficult to analyze with any degree of certainty. In order to be meaningful, the condition of reactor damage due to insufficient cooling had to be accomplished in an operating reactor. The Heat Transfer Reactor Experiment No. 2 (HTRE No. 2) power plant was available, and an insert formerly used for criticality studies was modified for power operation and instrumented with valving and thermocouples to provide evidence of damage to high-performance air-cooled reactors similar to those considered for use in nuclear propulsion.

2. Fractional Release and Physical Characteristics. In order to determine the fractional release of specific fission products and the physical characteristics, effluent sampling and analytical capabilities were required prior to the release of the effluent to the atmosphere.

3. Meteorological Aspects. Correlations between dissemination patterns and meteorological measurements required atmospheric measuring devices. Interpretation capabilities were required in order to establish compliance with control requirements at the time of release and to insure proper cloud trajectory after release of the effluent to the atmosphere.

4. Isopleth Patterns. A sizable field-sampling network was necessary to determine

DECLASSIFIED

ground-level isopleth patterns of interest in this experiment. The dimensions of the network and the specific location of sampling stations were determined by compromise between the finite amount of instrumentation and the desire to have a network large enough to encompass the cloud-trajectory variations and the predicted isopleth patterns.

5. Biological Measurements. In order to determine the validity of using air-sampling devices for obtaining samples characteristic of inhalation retentions, animals were required as an integral part of the sampling network and capabilities for biological studies were necessarv. These were furnished by the University of Rochester.

6. Source Strength. A predetermined fission product inventory was desirable in order to facilitate the determination of the fractional release of radioiodine from the fuel elements. Iodine release is of special importance because it is generally the limiting quantity with respect to the release of airborne fission products for this type of reactor considered for aircraft propulsion. The original plan was to establish a fission product inventory during two reactor-power operations: the first, a period of 2 hours at full power 2 days before the planned release date; the second, a period of 1/2 hour at full power just prior to restricting the coolant air.

7. Acceptable Meteorological Conditions During Release. Since the experimental data from measurements taken during the diffusion of a cloud of fission products in the atmosphere is extremely complex in general, the neutral or weak lapse atmospheric condition was originally selected for time of release. This condition would permit the most accurate analysis and, according to theoretical calculations, would produce the desired dispersion of fission products so that there should be no radiological hazards beyond the sampling network.

8. Last Minute Changes. In order to obtain permission from the Idaho Operations Office, Atomic Energy Commission, to proceed with the experiment, the reactor history just prior to the release was changed from 1/2 hour at full power to 10 minutes equivalence at full power. The meteorological requirement at the time of release was also changed from neutral-weak lapse to a strong lapse condition. These changes reduced the activity that was available for collection, produced more dilution (diffusion), and complicated the analyses of the diffusion data.

GEOGRAPHICAL ASPECTS

The experiment was conducted at the Initial Engine Test (IET) Facility and over a test grid to the northeast of the Aircraft Nuclear Propulsion Department's test site at the National Reactor Testing Station (NRTS), Idaho Falls, Idaho. The NRTS lies on the west side of the Snake River Plain in southeastern Idaho and has an average elevation of 5000 feet above mean sea level. Figure 1 shows the location of the NRTS in southeastern Idaho and its relation to the surrounding terrain. The ANPD site, other major installations, and main highways at the NRTS are shown in Figure 2. The region is semiarid, and desertlike characteristics prevail.

The ANPD area has the lowest elevation of the NRTS and was at one time the site of end points, or sinks, of several rivers or creeks. The entire area is underlaid by a series of lava flows, and outcroppings can frequently be seen. The ground is sparsely covered with vegetation, which is predominantly sagebrush and other desert plants. Figure 3 shows typical ground cover.

The terrain over which the radioactive cloud passed is generally a valley floor which rises gradually toward the northeast from the release point. This valley is bounded by mountain ranges about 10 to 15 miles to the northwest, approximately 30 miles to the north, and roughly 50 miles to the east. Figure 4 presents an aerial photo of the valley

DECLASSIFIED

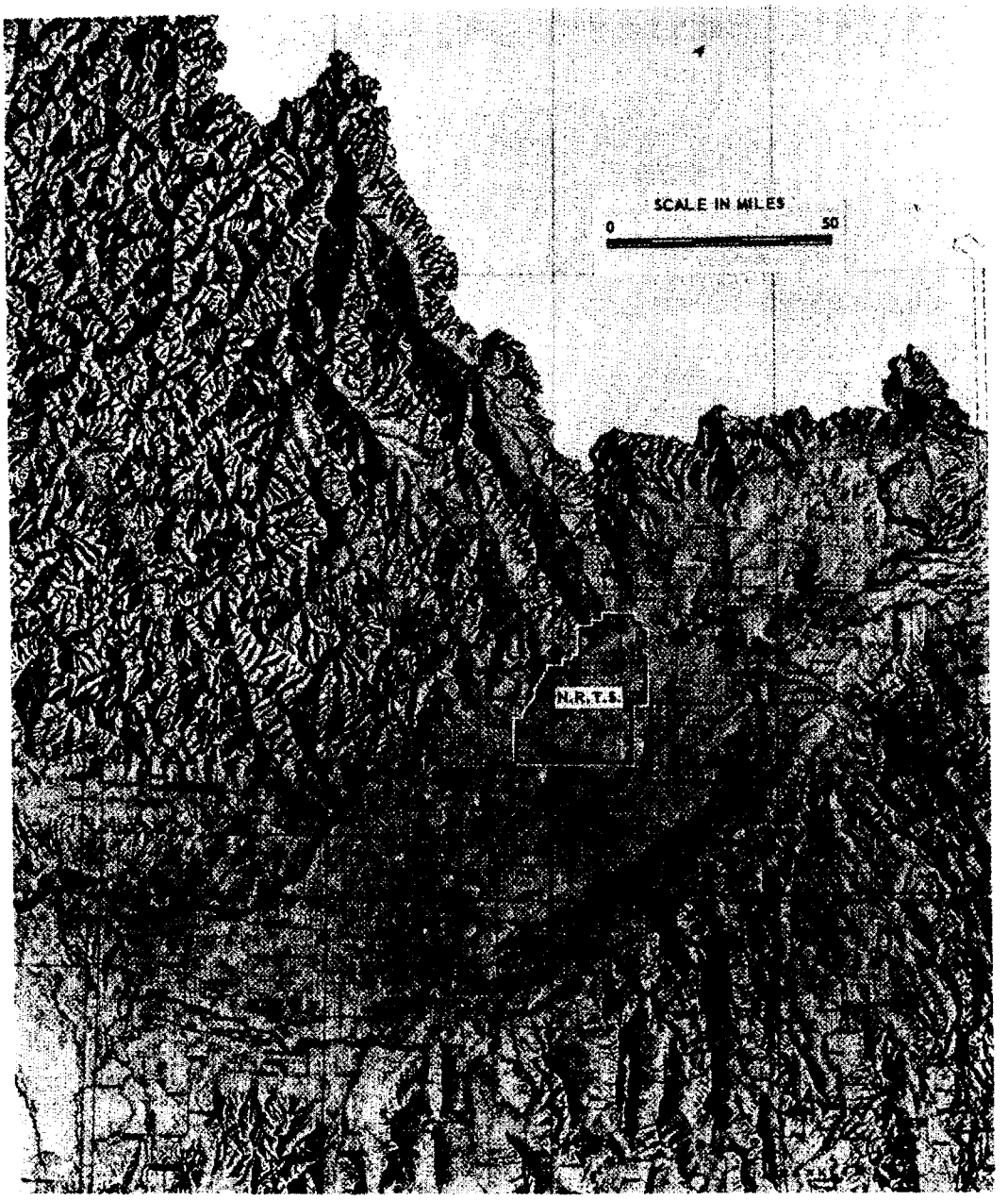

Fig. 1—NRTS and its relation to surrounding terrain

DECLASSIFIED

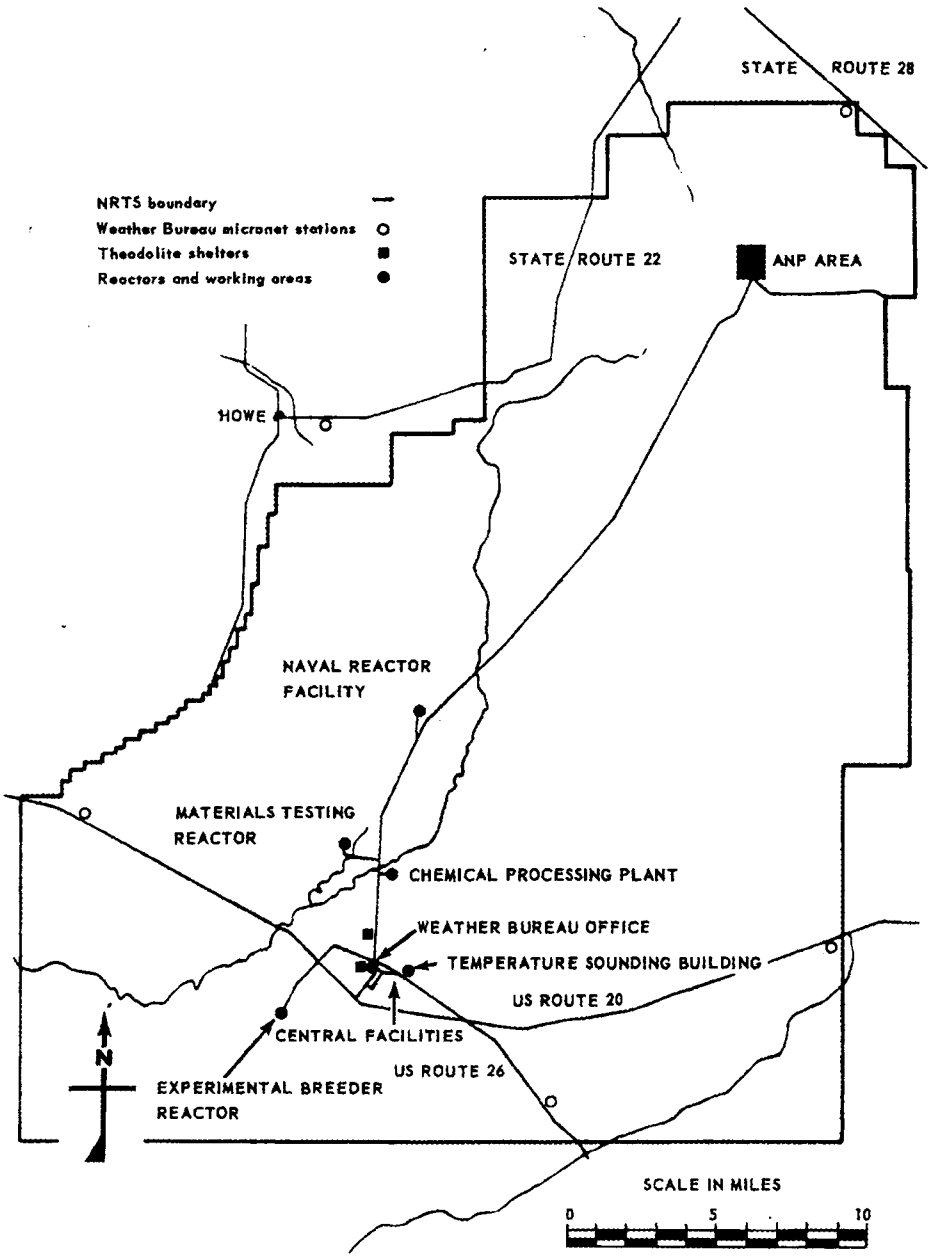

Fig. 2—Location of ANPD area at NRTS

DECLASSIFIED

DELETED

DECLASSIFIED

DELETED

DECLASSIFIED

with the IET in the foreground, sampling network outlined, and mountain ranges in the background.

THE REACTOR TEST FACILITIES

The complete Heat Transfer Reactor Experiment (HTRE) power plant which was used for Operation BOOT is shown in Figure 5 as it was being moved to the Initial Engine Test (IET) facility. For Operation BOOT, the HTRE includes the Core Test Facility (CTF), a parent reactor (HTRE No. 2), and an insert for the parent reactor (Insert 1d). The CTF is the identification given to the apparatus that contains the reactor and includes the supporting instrumentation, turbomachinery, and auxiliary equipment. HTRE No. 2 is an air-cooled reactor containing a solid moderator and has a built-in void volume into which a partial reactor core may be placed for particular studies. Figure 6 is a schematic drawing of the CTF. A ctuaway drawing of HTRE No. 2 reactor is shown in Figure 7, and Insert 1d, which fits inside HTRE No. 2, is shown in Figure 8.

Effluent from CTF jet engines is sent through a 76-inch-diameter duct to a 150-foot stack where it is exhausted to the atmosphere. Figure 9 shows the shed (used to cover the CTF), the ducting, and the 150-foot stack.

REACTOR AND INSERT

The HTRE No. 2 parent reactor was used with the Insert 1d to provide the source of fission products for this experiment. The Insert 1d was the Insert 1a (critical experiment version of the 1b), which had been modified for power operation. A complete description of HTRE No. 2 and the Insert 1b is given in APEX-268.* Insert 1d contained six fuel cartridges (elements), three of the set-1 type (11 fuel rings), and three of the set-2 type (10 fuel rings). A set-1 type of stage layout is shown in Figure 10. A cartridge contains 18 stages. The set-1 and -2 type of stages are shown in Figure 11. Fuel cartridges were installed in insert holes 2 through 7, with the center hole (hole 1) containing a beryllium moderator bar. Figure 12 is a drawing of the Insert 1d cross section.

Insert tubes 2 and 6 were fitted with remotely controlled air-activated valves, shown in Figure 13, which were used to instantaneously block a fixed fraction (about 0.66 percent) of the air supply to the fuel tube. This air blockage was designed to produce a rapid increase in temperature of the fuel cartridge, culminating in partial destruction of the cartridge, and yet provide sufficient airflow to flush the gaseous fission products from the moderator tube. Only one fuel cartridge was melted during the experiment, but two fuel cartridges were equipped with valves to provide backup in the event one of the air-valve actuating mechanisms failed.

Insulation was omitted from the external surfaces of the insert to allow the moderator block, in which melting took place, to operate at a lower temperature than it might otherwise.

General Nuclear Data

Uranium inventory (HTRE No. 2 core)	72.9220 lb (93.4% enriched)
Uranium inventory (three-insert set-1 fuel cartridges)	5.4978 lb (93.4% enriched)
Uranium inventory (three-insert set-2 fuel cartridges)	5.2878 lb (93.4% enriched)
Total	83.7076 lb

*"HTRE No. 2 Hazards Evaluation," APEX-268, Aircraft Nuclear Propulsion Department, General Electric Company, November 12, 1956.

DECLASSIFIED

DECLASSIFIED

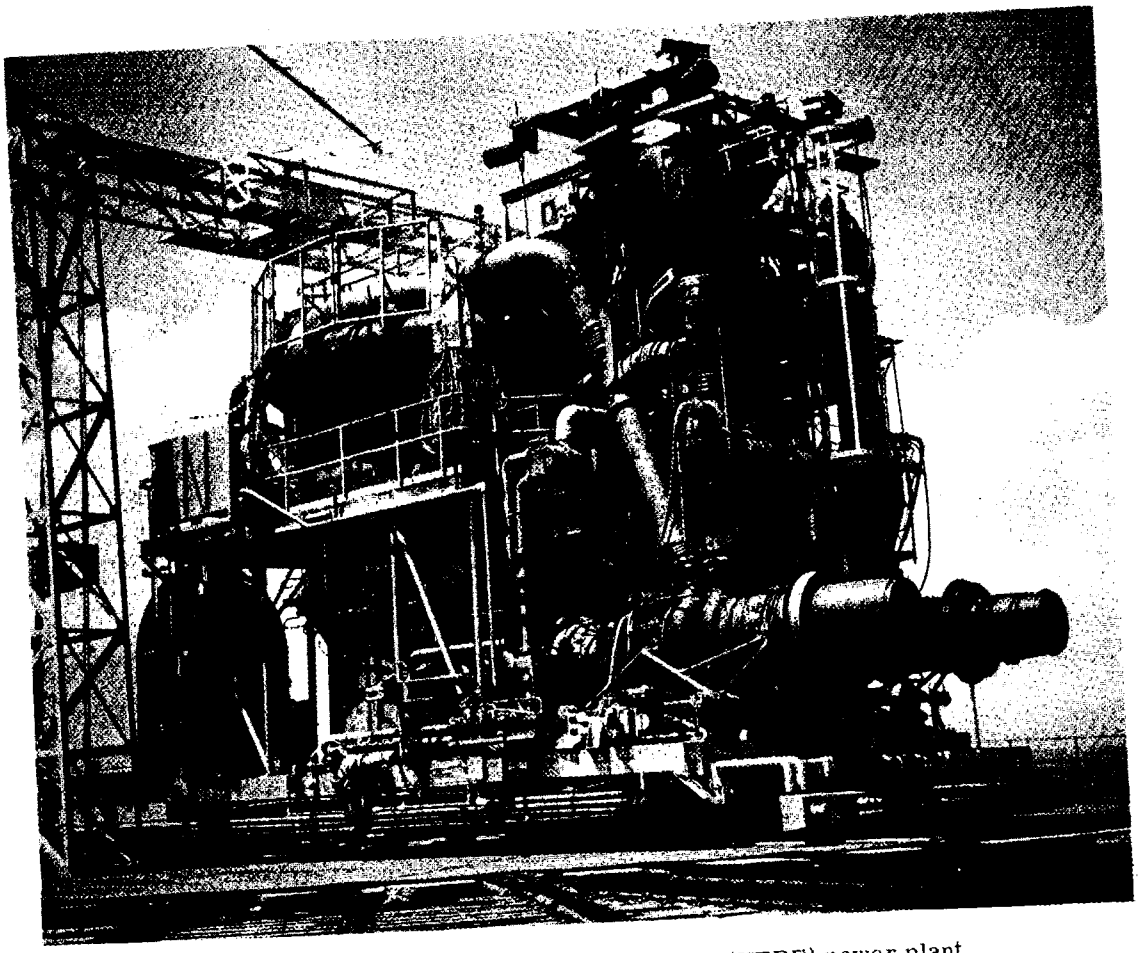

Fig. 5 - Heat transfer reactor experiment (HTRE) power plant

DECLASSIFIED

DECLASSIFIED

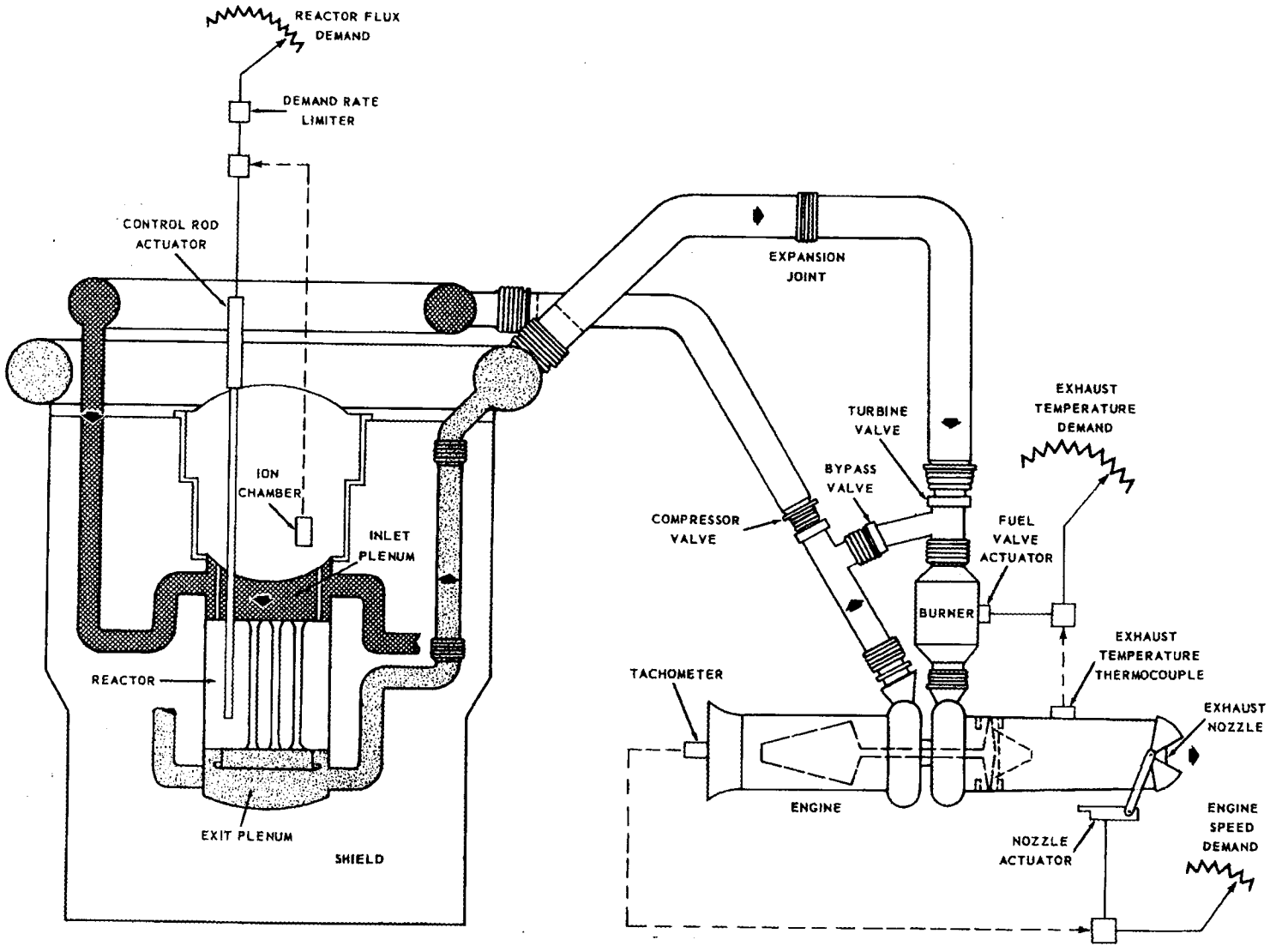

Fig. 6 Core Test Facility (CTF) Schematic

DECLASSIFIED

DECLASSIFIED

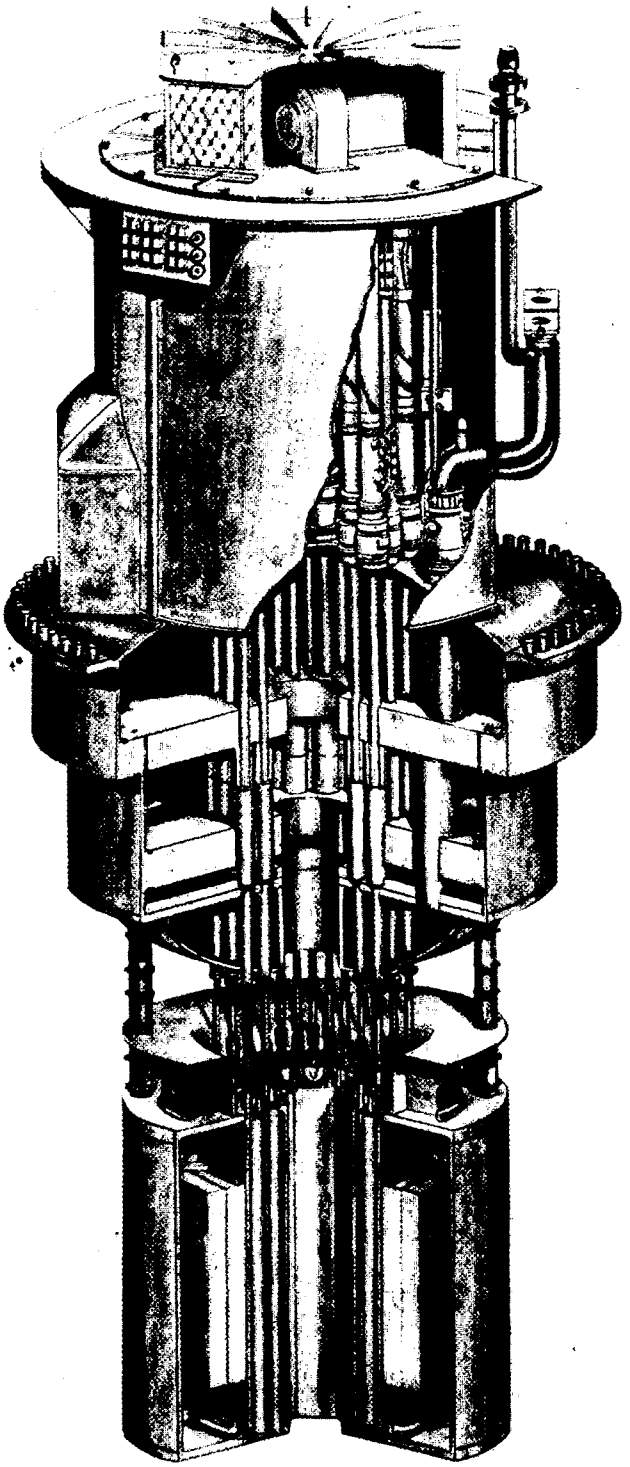

Fig. 7 - Heat transfer reactor experiment No. 2 (HTRE No. 2) Reactor

Fig. 8 – Insert 1d before assembly in HTRE No. 2

DECLASSIFIED

DELETED

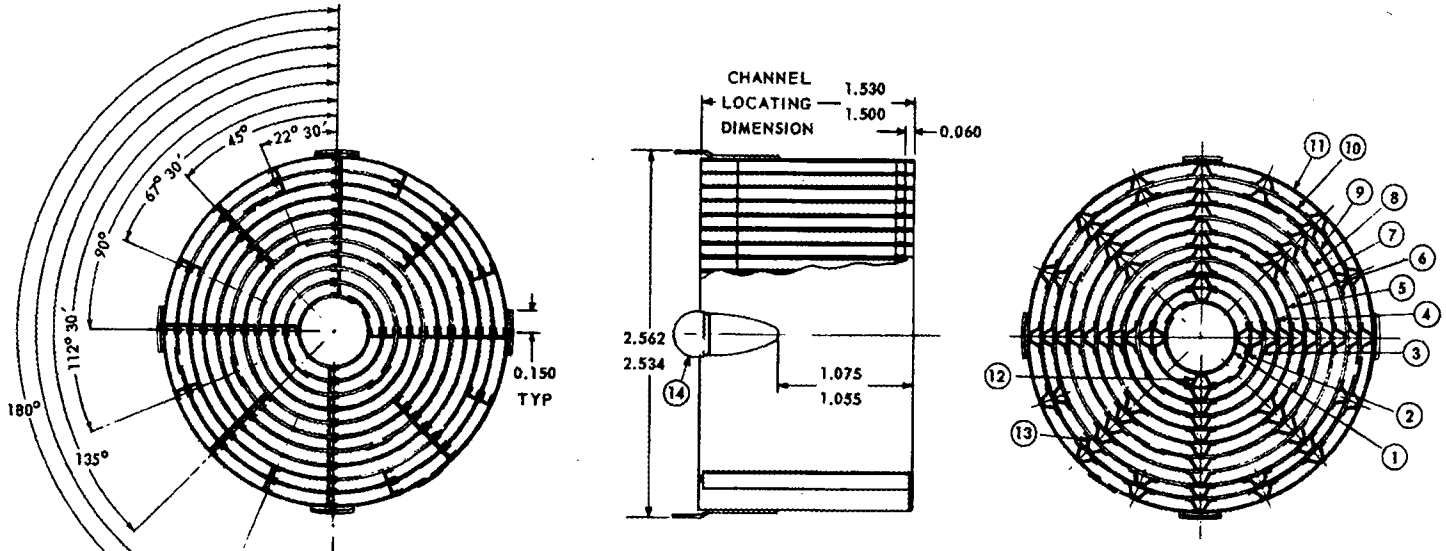

PART NO.	OUTSIDE DIAMETER	PLATE THICKNESS ±0.001	CUT LENGTH ±0.015	CORE WEIGHT FRACTION UO_2/TOTAL	WEIGHT UO_2 IN GRAMS	FUELED AREA IN.^{2} REF	AREA DENSITY GRAMS UO_2/IN.^{2} FUELED AREA
1	0.468	0.0210	1.3173	0.40	1.4950	1.9233	0.7773
2	0.670		1.9519	0.42	2.3260	2.8498	0.8162
3	0.872		2.5865		3.0822	3.7763	0.8162
4	1.074		3.2211		3.8384	4.7028	0.8162
5	1.276		3.8557		4.5946	5.6293	0.8162
6	1.478	0.0210	4.4903		5.3508	6.5558	0.8162
7	1.678	0.0200	5.1238		5.6360	7.4808	0.7534
8	1.878	0.0200	5.7521		6.3271	8.3981	0.7534
9	2.076	0.0190	6.3793		6.4321	9.3138	0.6906
10	2.272	0.0180	7.0002		6.4163	10.2203	0.6278
11	2.468	0.0180	7.6159	0.42	6.9806	11.1192	0.6278

Fig. 10 – Set-1 type of stage layout

DECLASSIFIED

DECLASSIFIED

DECLASSIFIED

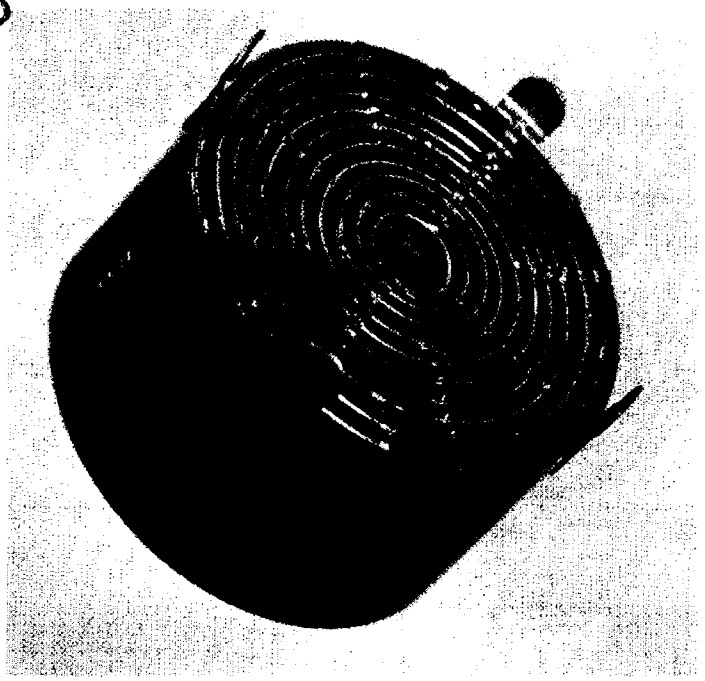

DECLASSIFIED

Fig. 11 – Insert 1d, set-1 and -2 type stages

DECLASSIFIED

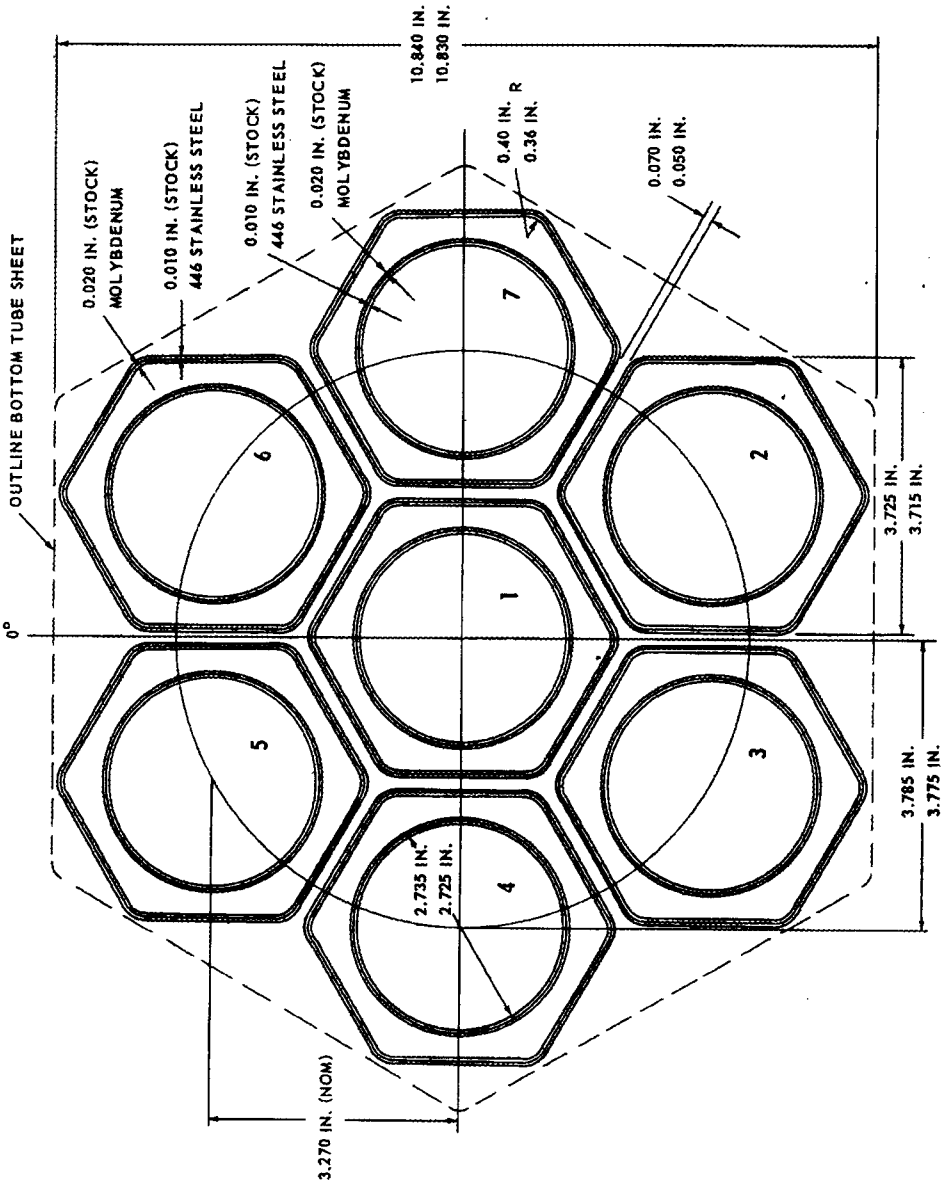

Fig. 12 – Insert 1d cross-sectional drawing

DECLASSIFIED

DECLASSIFIED

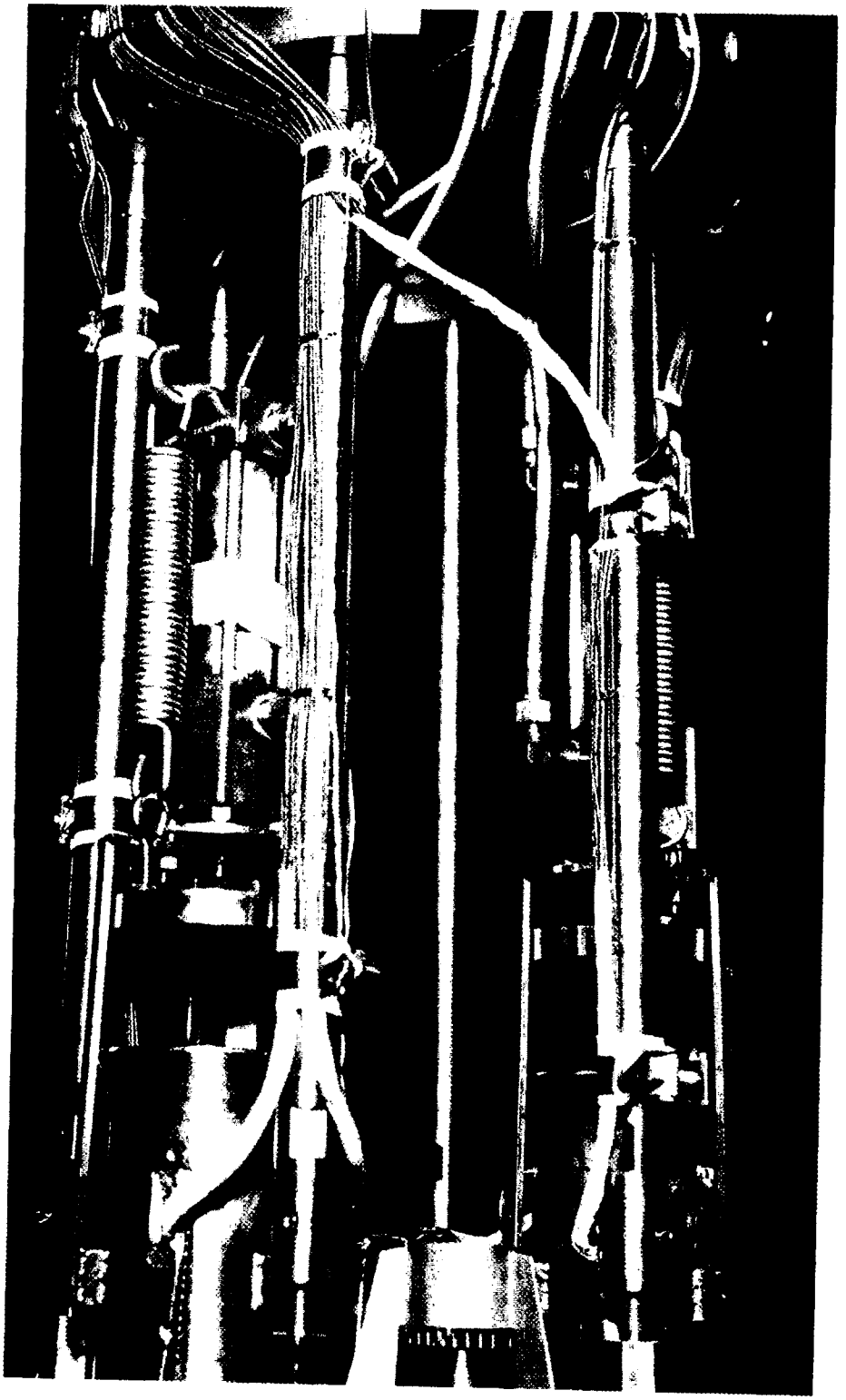

Fig. 13—Remotely controlled air-activated valves on Insert 1d

DECLASSIFIED

DECLASSIFIED

Volume parent core (active region)		19,753.21 in.^{3}
Volume insert test hole (active region)		3,251.66 in.^{3}
N_H of zirconium	Nominal	3.95×10^{22} atoms/cm^3

Material in Insert 1d. (Active Region)

Material	Volume Fraction[a]	Weight	Specific Gravity
Hydrided zirconium	0.417	282.97	6.05
Uranium (93.4%)	0.0055	10.786	18.68
80 Ni - 20 Cr	0.0375	39.00	8.62
Stainless steel	0.014	13.00	7.78
Molybdenum	0.028	30.00	9.01

[a]Volume fractions based on 3251.66-in.^{3} Test-hole volume.

Power Distribution

The gross radial relative power distribution in the HTRE No. 2 Insert 1d assembly was essentially the same as that calculated for the 1c insert. The relative longitudinal power distribution for the 1c is shown in Figure 14. The circumferential power distribution was probably similar to that measured in the Insert 1a critical experiment and is shown in Figure 15.

The total power generated in the fuel cartridge was designed to be between 1.5 and 2.0 percent of the total reactor power; e.g., at 10 megawatts the fuel cartridges in tubes 2_i and 6_i were designed to be generating 150 and 200 kilowatts each. This power range represented a nominal 5.4×10^{15} fissions per second.

Insert Temperature Measurements

It was desirable to measure the temperature excursions from the moment the air supply to the fuel cartridge was cut off. For this purpose the following instrumentation was installed in the 1d insert:

1. The fuel cartridge melted was installed in insert tube 6_i. This cartridge was a set-1 type A and was instrumented for radial temperature distributions on stages 9 and 18.
2. The second fuel cartridge, to be melted in the event the first one failed, was a set-1 cartridge, type B which was installed in tube 2_i. This cartridge had thermocouples positioned to measure a longitudinal temperature profile on the outer rings.
3. The moderator cells were instrumented with seven or more thermocouples on the outer moderator cladding to measure the longitudinal temperature profile.

Stage Radial Temperature Profiles

Radial profiles of temperatures measured on cartridge 6_i, stages 9 and 18 are shown in Figure 16 for two separate operating runs preliminary to the experiment power operations. These profiles indicate the temperature gradient across the rings of stages 9 and 18; the highest temperatures occurred in the outermost rings. The temperatures were measured during reactor operation with the valve open. When excessive cartridge temperatures were encountered during the actual melt, the temperature gradients were somewhat modified by the presence of the cooled moderator block in the proximity of the 11th ring of all stages. The cooled moderator block, to some extent, lowered the temperature of rings 10 and 11.

DECLASSIFIED

DECLASSIFIED

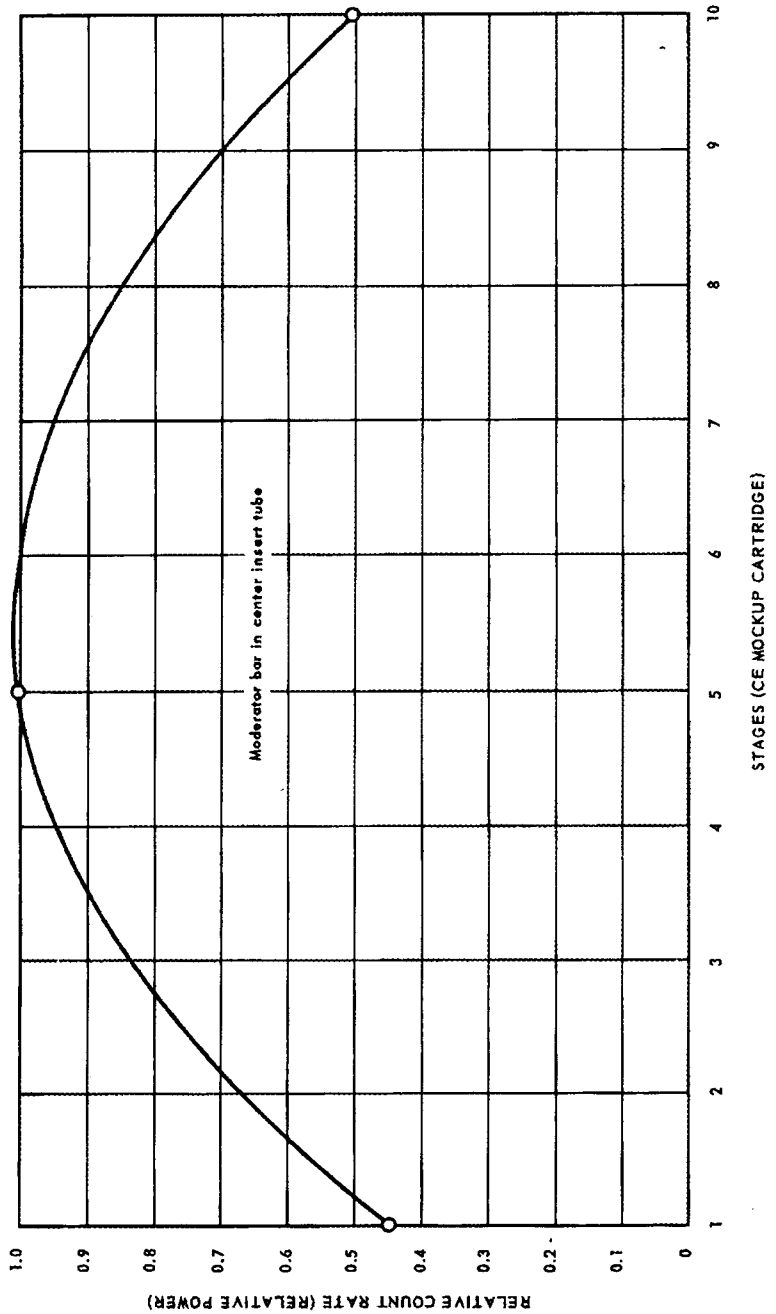

Fig. 14 – Longitudinal power distribution – Insert 1c, tube 6

DECLASSIFIED

DECLASSIFIED

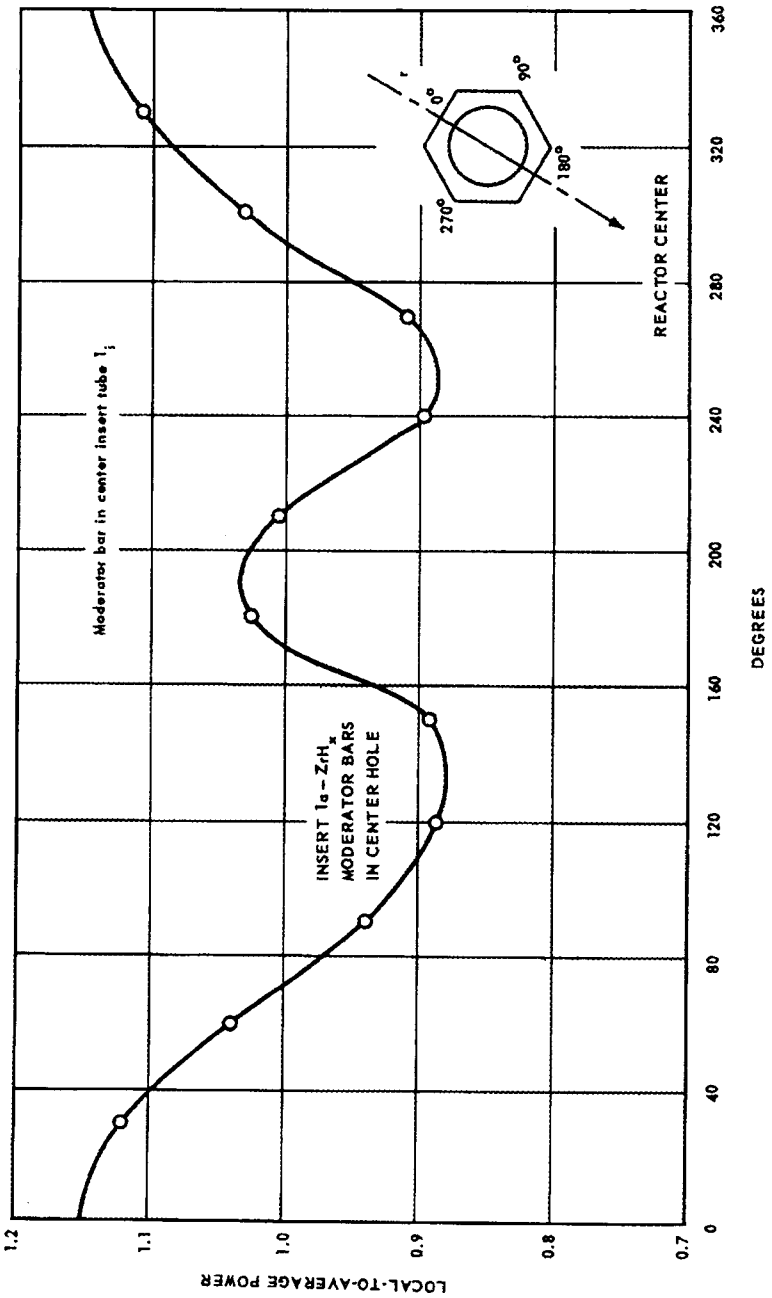

Fig. 15 – Circumferential power distribution – Insert 1c, tube 6

DECLASSIFIED

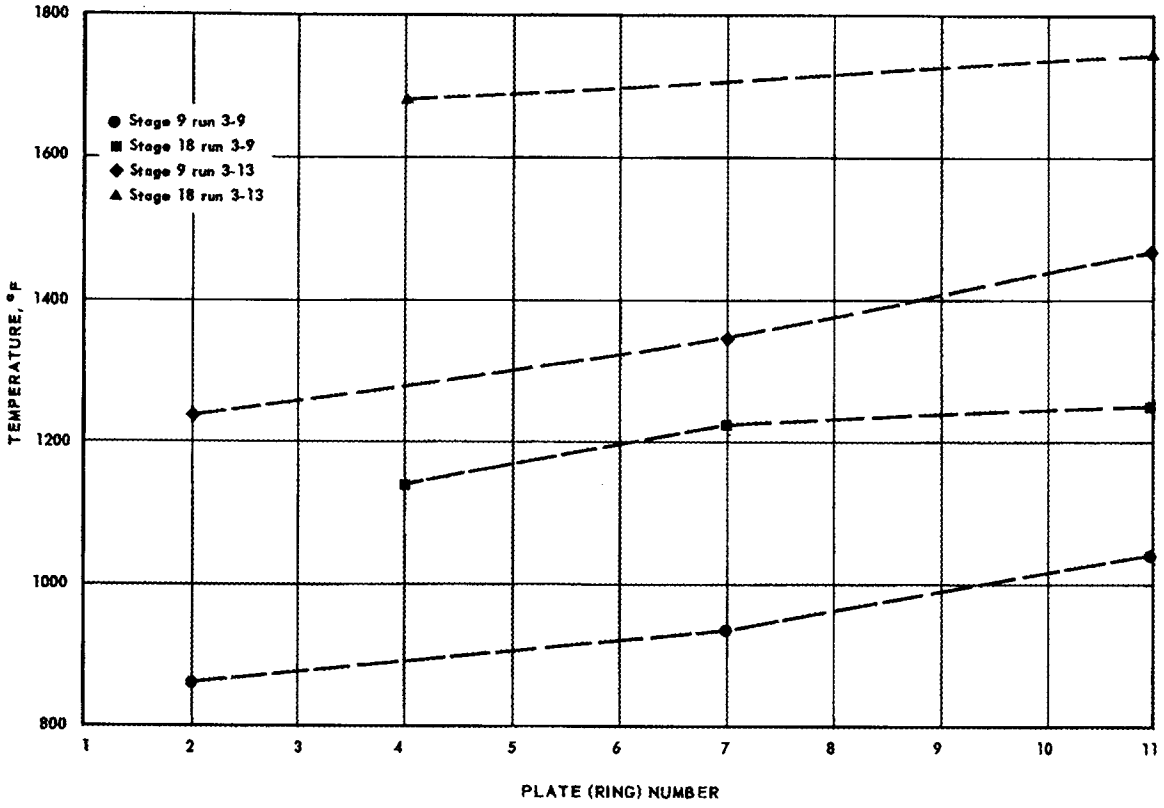

Fig. 16 – Radial temperature profiles – Cartridge 6_i, stages 9 and 18

DECLASSIF

Cartridge Temperature Relationships

The reactor was operated at low power in order to obtain temperature relationships between cartridges of the insert and temperature profile differences for the affected element with the valve open and closed. These measurements, shown in Figure 17, indicated that the desired 3000°F or more could be attained without exceeding other fuel element temperatures. The measurements were made using steady-state airflow conditions; but, since this could not be expected while the melting condition prevailed, the measurements could be considered qualitative only.

Performance Characteristics

The following is a list of the operating characteristics for the power operation of the 1d insert.

1. Total power (parent and insert)	11.4 mw
2. Design insert power	11% of total
3. Insert moderator temperature (design)	1000° to 1500°F
4. Insert fuel cartridge temperature (tube 2_i or 6_i). Normal operating maximum.	1750°F
5. Insert fuel cartridge temperature (tubes 3, 4, 5, 7). Operating maximum.	1300° to 1500°F
6. Insert fuel cartridge temperature. Peak during melt.	>3000°F
7. Parent core fuel cartridge temperature. Design maximum average.	1300° to 1500°F
8. Parent core fuel cartridge temperatures. Hot spots.	1750°F
9. Insert center moderator rod temperature. Design maximum.	900° to 1100°F

CTF Effluent Sampling and Monitoring Devices

Several effluent sampling devices were used in the CTF in an attempt to determine the magnitude and characteristics of the fission products released from the reactor during the experiment. The type and location of the sampling probes or chambers and collecting devices are given in Table 2.

Just prior to the start of the experiment, velocity profiles were measured in the 76-inch duct leading from the engines to the stack and at the 80-foot level in the stack. Measuring points are indicated in Figure 18. Figures 19, 20, and 21 indicate the velocity variations encountered. Prior facility commitments did not permit a delay of the experiment in order to relocate sampling probes. Since all prior information concerning the calibration and use of the sampling system was obtained with the sampling probe positions as they were, and since the sampling within the facility was only one phase of the experiment, no changes were made prior to the melt.

Corrections for nonisokinetic sampling are not available because the physical properties of the effluent are not sufficiently well known and sufficient flow measurements were not made.

FIELD SAMPLING NETWORK

The field sampling network used in the experiment covered a 60-degree angle clockwise from the north with the origin at the IET. It is shown schematically in Figure 22. The sector was oriented in accordance with meteorological data obtained from wind instru-

DECLASSI

DECLASSIFIED

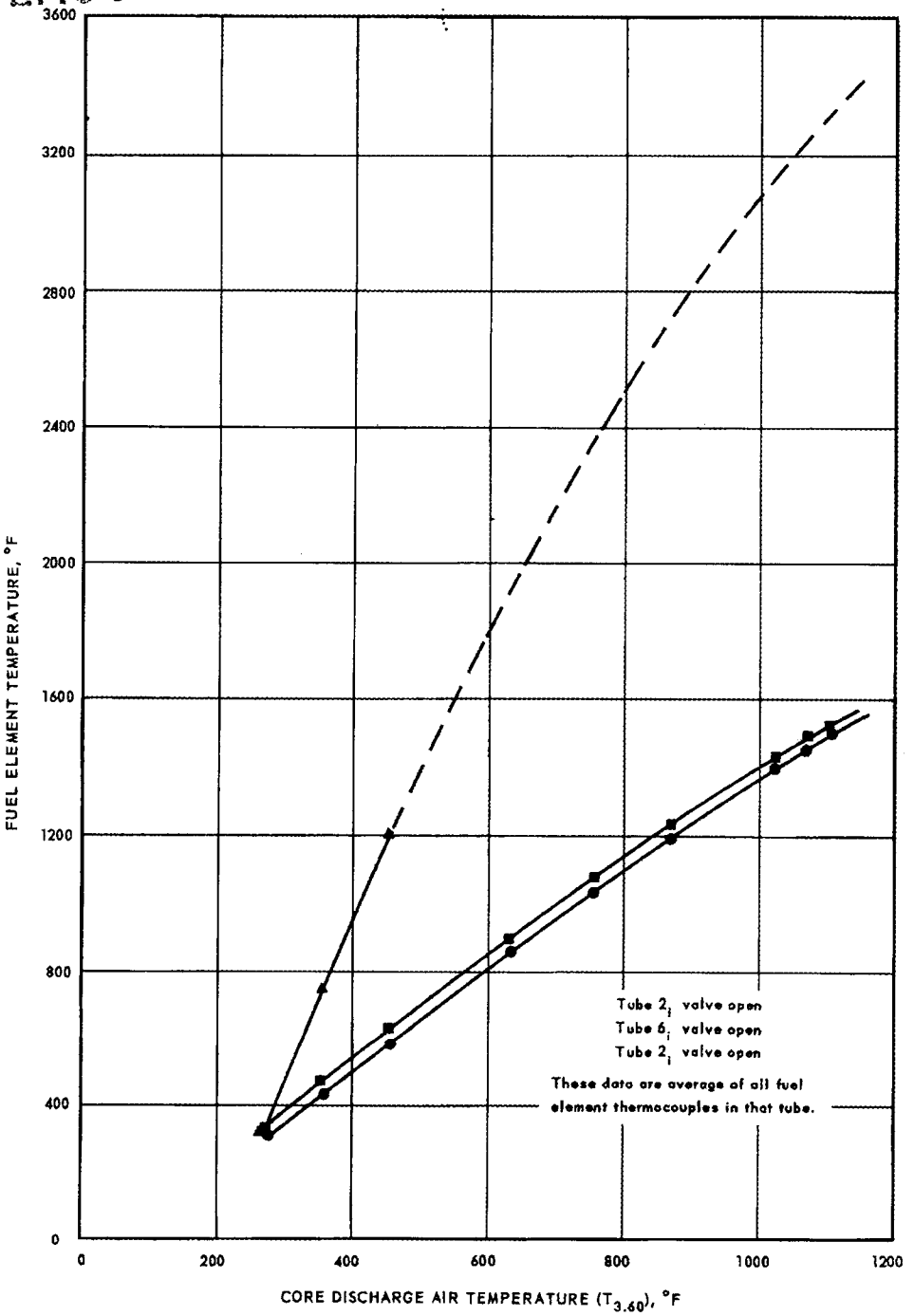

Fig. 17 – Cartridge temperature relationships with valve open and closed

DECLASSIFIED

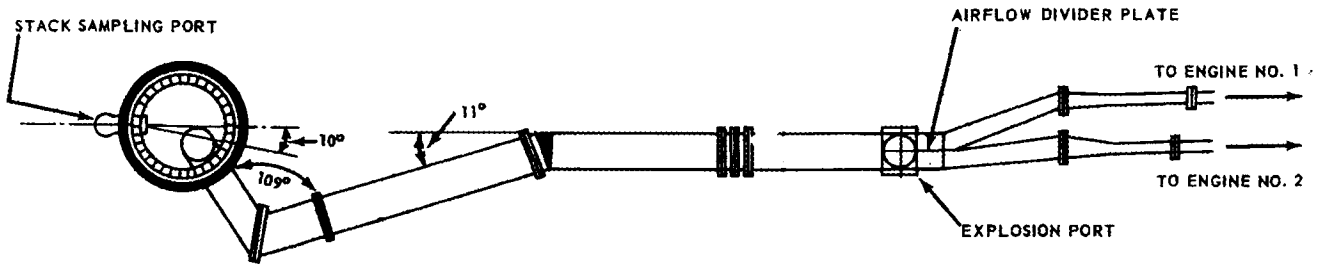

Fig. 18 - IET Gas Exhaust Ducting

DECLASSIFIED

DECLASSIFIED

DECLASSIFIED

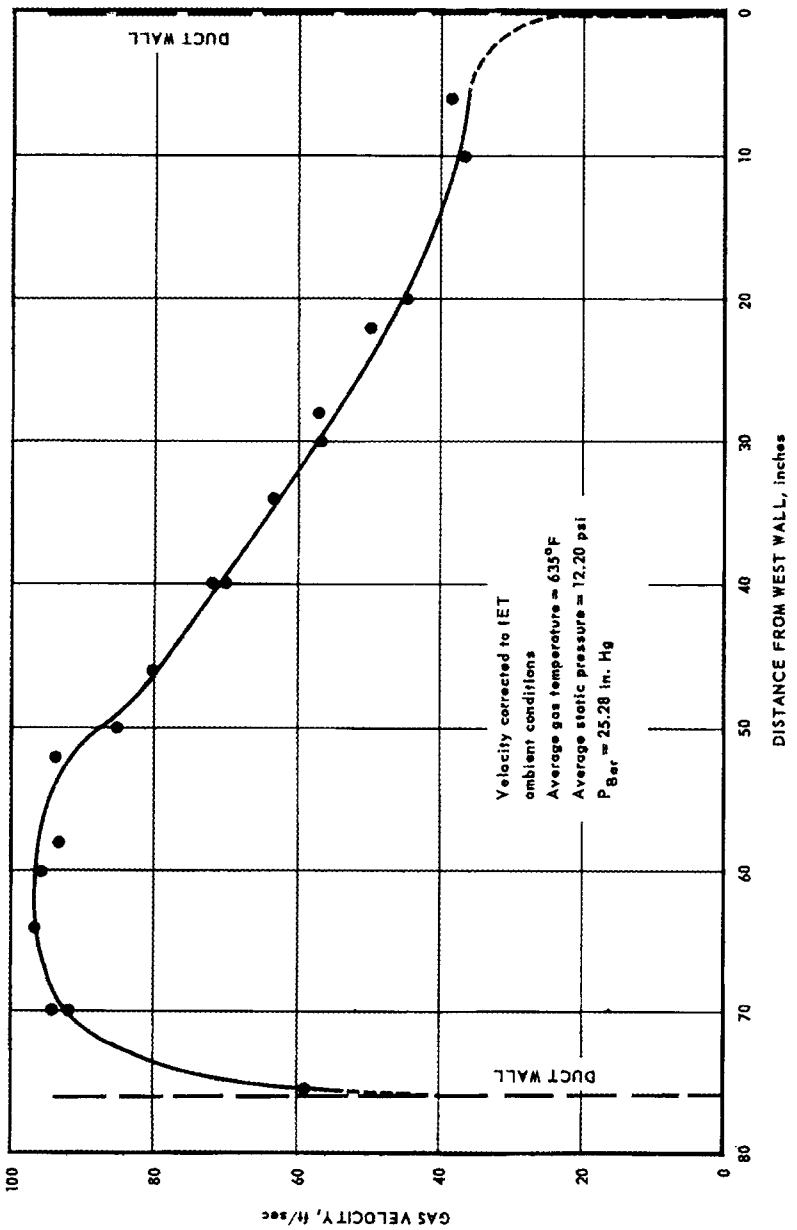

Fig. 19 – Gas velocity profile. Horizontal traverse in 76-inch duct

DECLASSIFIED

DECLASSIFIED

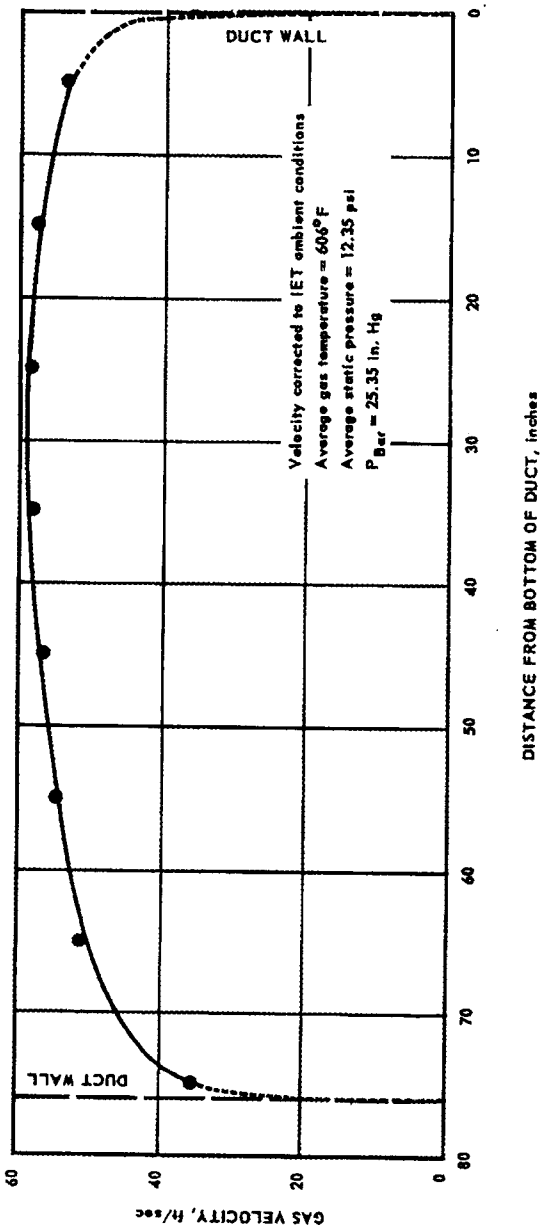

Fig. 20—Gas velocity profile. Vertical traverse in 76-inch duct.

DECLASSIFIED

DECLASSIFIED

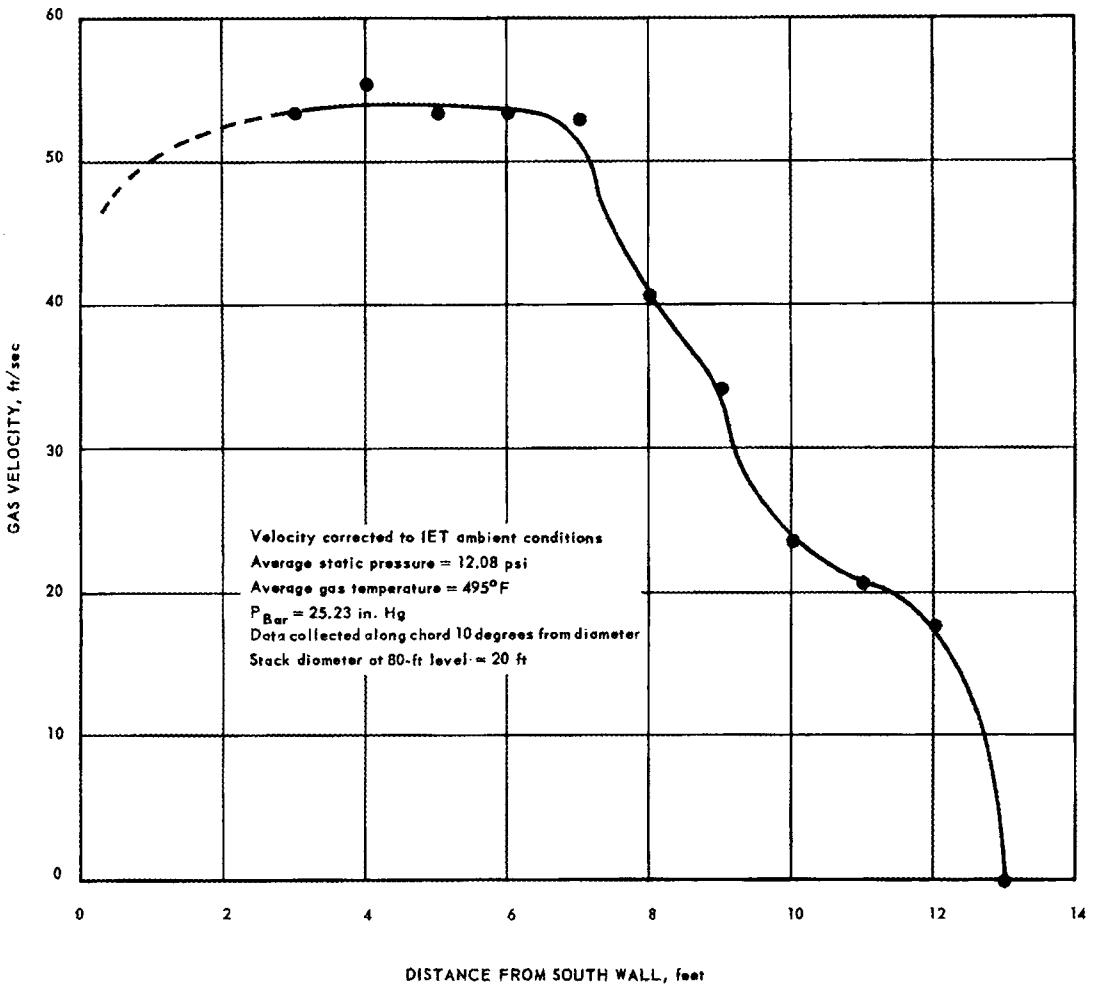

Fig. 21 – Gas velocity profile at 80-foot level of the IET stack

DECLASSIFIED

DECLASSIFIED

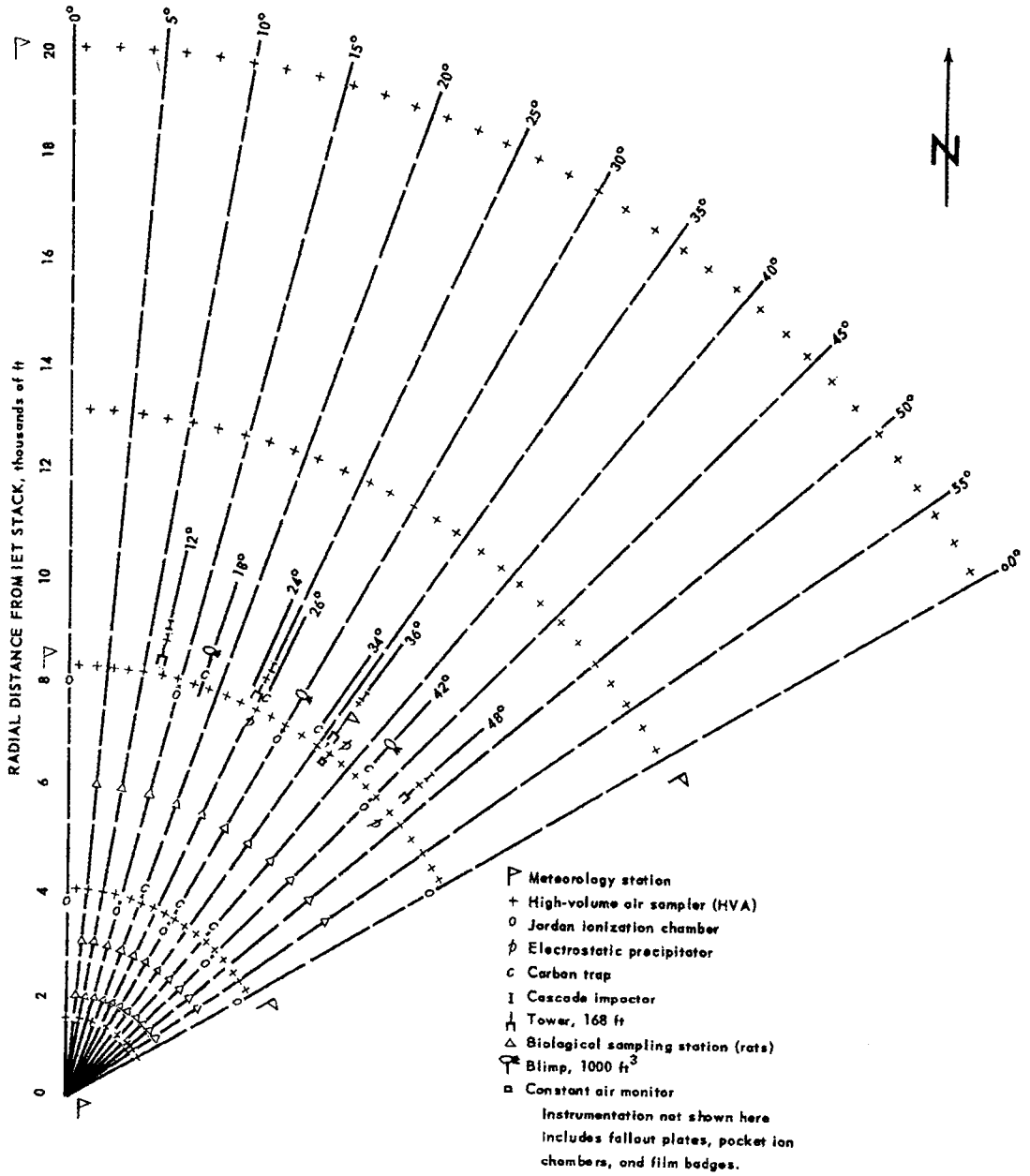

Fig. 22 – Field sampling network

DECLASSIFIED

DECLASSIFIED

mentation at the 20-foot level of the IET weather tower for the period 1953 - 1956. Appropriate wind roses are shown in Figure 23. Radial arcs for various types of sampling instrumentation, to be described later, were located at radial distances of 100; 1,500; 2,000; 3,000; 4,000; 8,250; 13,000; and 20,000 feet from the IET exhaust stack.

The system of arcs was established by a compromise after considering the many complex factors affecting the desired measurements. One of the major factors considered was the meteorological condition expected at the time of release. Because the neutral condition is the simplest for analysis purposes, the indicated spacing of arcs was chosen.

Access roads were constructed along each of the radial arcs and a central road along the north-south boundary of the network to permit rapid sampling gathering and communication to the laboratory areas after the test had been run.

Operational control of the experiment was maintained by personnel in the IET control room. Instructions to and operational readiness reports from field personnel were accomplished by means of a two-way radio communication system. This system also provided assurance that all personnel were at the specially designated safety positions at the extremities of the sampling arcs prior to conduct of the action that would cause the release of fission products. Entry and exit to the experiment area were controlled by health physics personnel.

Several types of devices were used to measure the dissemination of the airborne material, but high-volume air samplers (HVA) were favored as standard sampling devices. The number and specific kinds of sampling devices at various distances from the stack are listed in Table 3.

Four 168-foot towers were placed on the 8250-foot arc. Each tower had one HVA on the top and cylindrical fallout plates at vertical intervals of 15 feet. All HVA samplers used BM-2133 MSA filters.

HVA samplers were selected as the basic air-sampling devices because they sample at about 35 cubic feet per minute - a much greater rate than most devices. BM-2133 MSA filters for the HVA's were selected for their ability to operate under heavy dust loadings and for their efficiency in the collection and retention of iodine.

Fallout plates were simple 14-inch by 11-inch sheets of sticky paper placed horizontally on wooden supports approximately 1 meter above the ground.

METEOROLOGICAL INSTRUMENTATION AND SERVICES

Idaho Test Station Facilities

A 200-foot meteorological tower located at the IET near the point of release and equipped for measurement of wind direction and speed and air temperature was utilized. Wind instruments (Bendix-Friez Aerovanes) were located at the 20-foot, 75-foot, 150-foot, and 200-foot levels; artificially aspirated thermocouples for air-temperature measurements were located at the 5-foot, 20-foot, 50-foot, 60-foot, 140-foot, 150-foot, 180-foot, and 200-foot levels. These data were continuously recorded at the IET control room. Barometric pressure and the temperature of the dew point at the 5-foot level were also continuously recorded in the control room.

For purposes of this experiment, a wind direction bivane for measurement of horizontal and vertical wind-direction fluctuations was mounted at the 200-foot level of the IET tower with recording equipment at the control room. The instrument recording system and data reduction and their use are in the development stages.

DECLASSIFIED

DECLASSIFIED

TABLE 2

LOCATION AND TYPES OF SAMPLING DEVICES - CTF FACILITY

Location of Sampling Probe	Collecting Device
Beneath cartridge 6_i.	Carbon trap in an ice bath.
Hot duct, just before unit combustor.	Carbon trap in an ice bath. Electrostatic precipitator in series with a chilled carbon trap. Cascade impactor (four stages plus millipore filter).
76-inch duct between test cell and stack.	Six carbon traps in ice baths.
80-foot level of stack	Stack monitor (continuous filter). Spot sample collector. Two carbon traps in series - the first in an ice bath, the second in a liquid nitrogen bath.
Parent core sampling manifold and on the hot torus	Rupture detectors - continuous collection and recording
Below 76-inch duct (chamber)	Duct Jordan - Ionization chamber

All carbon traps used in the CTF were 0.86-inch inside diameter and 14 inches long. The traps were filled with 20 - 30 mesh carbon.

TABLE 3

TYPES, NUMBERS, AND LOCATION OF SAMPLING DEVICES

Type of Sample	Radial Distance from IET Stack, feet							
	100	1500	2000	3000	4000	8250	13000	20000
High-volume air samplers	0	0	0	0	17	27	27	33
Carbon traps	0	0	0	3	4	0	0	0
Flat fallout plates	9	17	17	17	17	27	27	33
Cascade impactors	0	0	0	0	3	0	0	0
Electrostatic precipitators	0	0	0	0	0	3	0	0
Continuous air monitor	0	0	0	0	0	1	0	0
Pocket ion chambers	9	17	17	17	17	27	27	33
Film badges	9	17	17	17	17	27	27	33
Vegetation samples	9	17	17	17	17	27	27	33
Cylindrical fallout plates	0	0	0	0	0	27	0	0
Animal cages	0	0	11	11	0	0	0	0

DECLASSIFIED

DECLASSIFIED

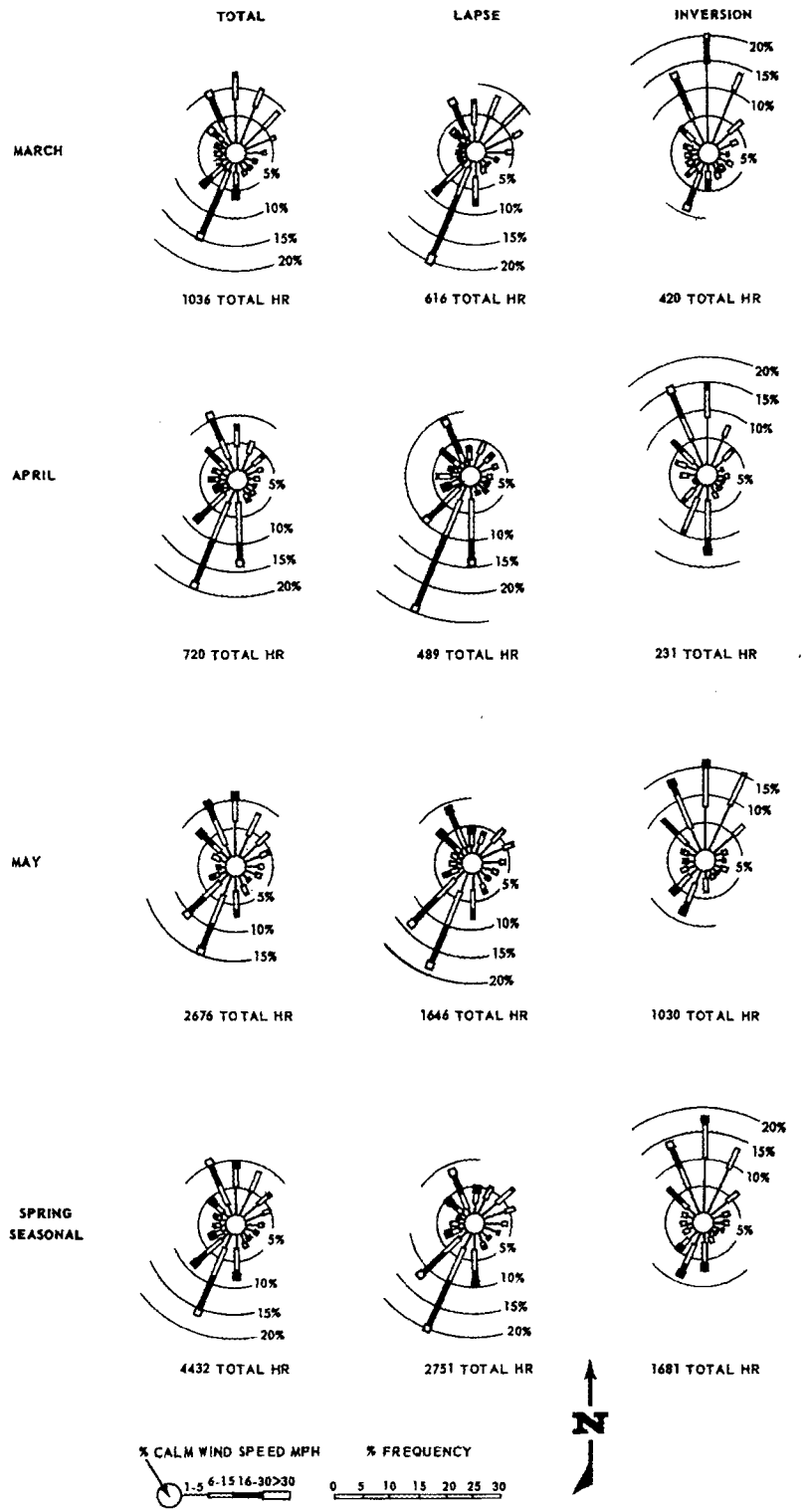

Fig. 23 – Spring season and monthly wind roses at ANPD-IET site, 20-foot level for the period 1953–1956.

DECLASSIFIED

Temporary devices for observers to make crude measurement of wind velocity on the sampling network were located at alternate ends of the sector arcs. Wind direction was obtained by noting the position of lightweight cloth streamers attached to stakes about 5-feet high in relation to compass points marked on the ground. Wind speed was measured with a portable pocket meter that was held in the observer's hand and pointed into the wind whose force deflected a small, plastic ball encased in a calibrated channel. The readings were transmitted to the control center by radio and were used to determine that the wind pattern over the sampling net was suitable for the experiment just prior to the melting of the tube.

Supporting Services from USWB

Supporting meteorological equipment and services were provided by the U.S. Weather Bureau organization at the NRTS. These included a weather station at approximately 29,400 feet from the IET along the centerline of the grid equipped with sensitive strip-chart recording instrumentation (Beckman-Whitley) for measurement of wind velocity at the 20-foot level; tethered-balloon temperature-sounding equipment near the point of release for measurements above the height of the IET tower; a pilot-balloon winds-aloft observation prior to the experiment; data collection, analysis, and forecasting services of the over-all weather regime; and determination of diffusion coefficients used for test control and operational calculations.

DECLASSIFIED

Conduct of Experiment and Results

REACTOR OPERATIONS AND CTF DATA

The procedure for the performance of the experiment is described in the following paragraphs.

The reactor and engine instrumentation was checked out. The power level was increased to produce a maximum temperature on fuel tube 6_i of 1750°F; other insert fuel cartridges were operating cooler because of lower resistance to flow (the venturi installed on tubes 2_i and 6_i somewhat restricted the flow to these tubes).

The reactor was operated at the power level that produced the above temperature-limiting condition (~ 11.4 mw) for a period of time in order to store a predetermined fission product inventory in the fuel cartridge.

At the end of this period the airflow to tube 6_i was restricted (approximately 2/3) causing the fuel cartridge temperature to increase to a point at which a portion of the cartridge was destroyed and carried into the airstream.

During the temperature excursion, attempts were made to maintain the power level of the reactor with automatic shim rod controls. Tentative plans were made to shut down the reactor using standard shutdown procedures at the conclusion of the experiment.

Reactor Operating History and Iodine Inventory

The reactor was operated for an equivalence of 2 hours at 11.4 megawatts on April 30, 1958 in order to establish a satisfactory inventory of I^{131} and other fission products of relatively long half life in the fresh cartridge to be melted. The reactor was then shut down and allowed to decay until May 2, 1958, when it was once again operated for an equivalence of 12 minutes at full power to establish an inventory of fresh fission products. Figure 24 shows the reactor history during the experiment.

The inventory of the various iodine isotopes in the cartridge is shown graphically in Figure 25 as a function of time since the beginning of the first power operation (assumed to be approximately 1220, April 30, 1958 for purposes of calculations). The valve limiting the coolant air to cartridge 6_i was closed at the end of the second (shorter) power operation while the reactor was still operating at a total power of 11.4 megawatts.

Events Following the Valve Closing

The sequence of events following the closing of the valve was quite significant and rather surprising. Some of the more important recordings were taken on a recording oscillograph in order to minimize instrument response time and to synchronize recordings. Because cartridge 6_i was selected as the initial cartridge to be melted, signals from thermocouples from various stages of the cartridge, the moderator surrounding it, and the exit air were recorded simultaneously with linear flux, control rod frame position, duct Jordan response, and other reactor information.

DECLASSIFIED

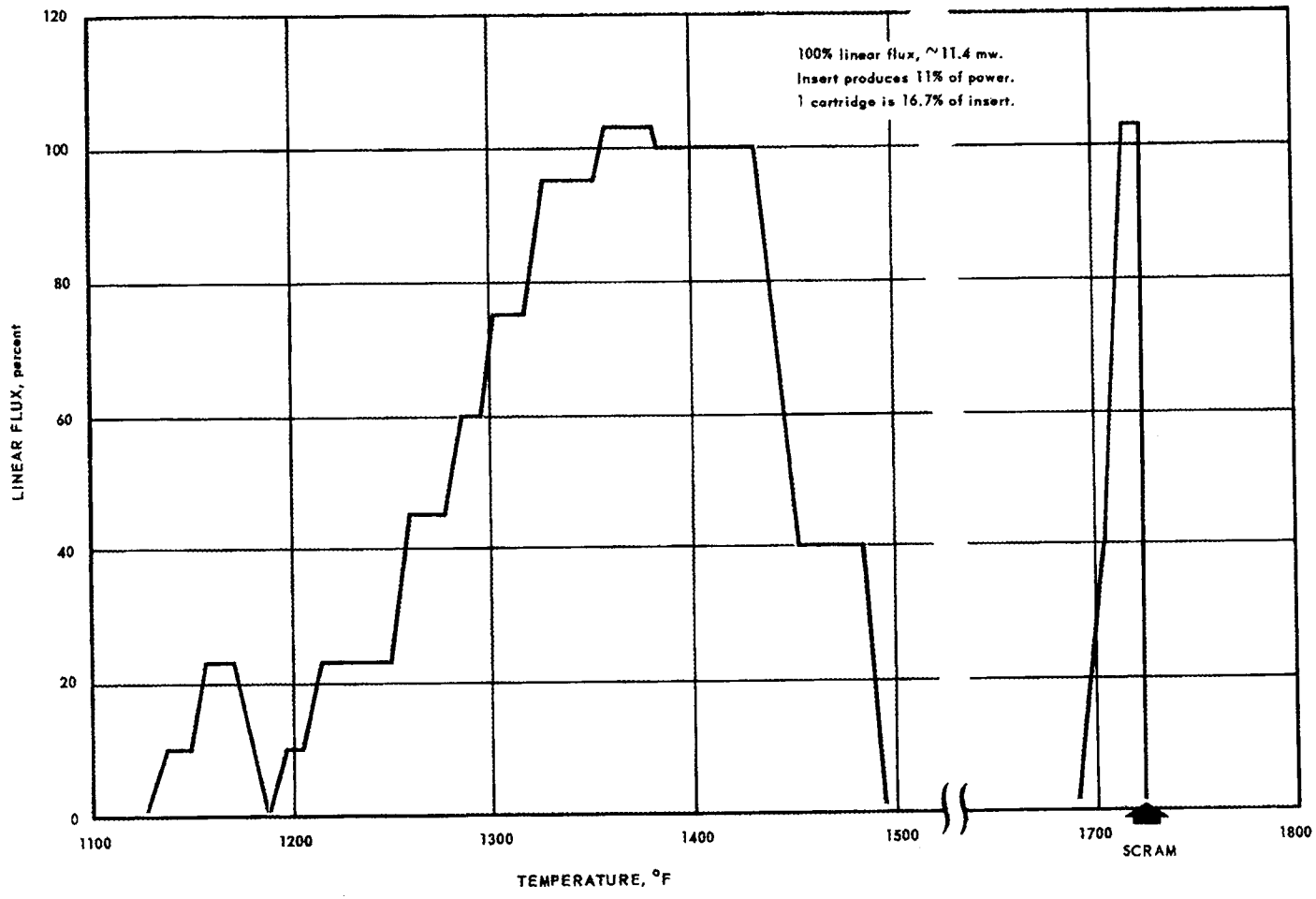

Fig. 24 – Reactor history during inventory and melt runs

DECLASSIFIED

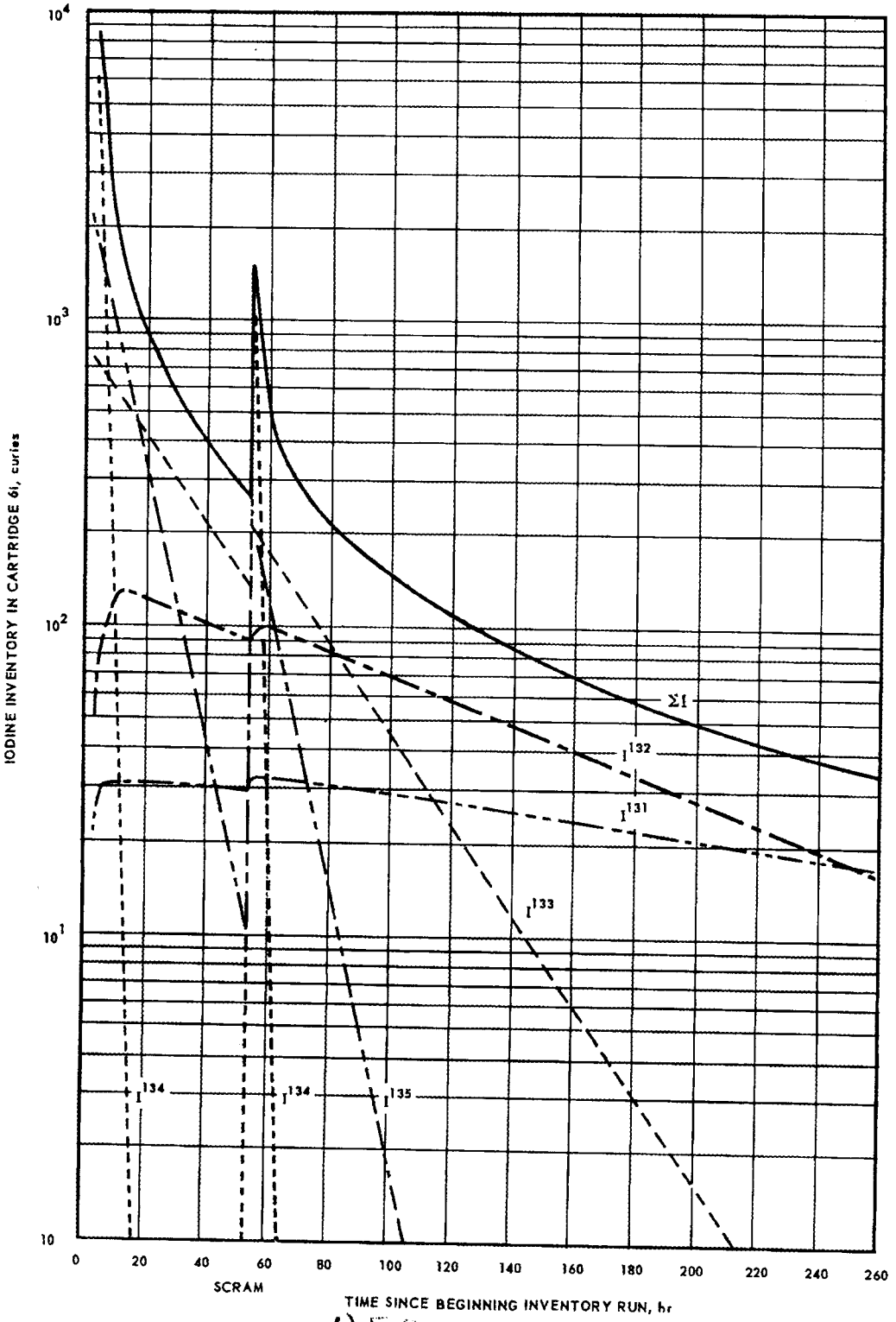

Fig. 25 – Iodine inventory in cartridge 6_i as a function of time after startup

DECLASSIFIED

DECLASSIFIED

The closing of the valve caused the cartridge 6_i temperatures to rise about 70°F per second until stages started melting and losing fission products and uranium. There was a slight loss of power 8 seconds after the valve was closed, initiating some fluxation in the frame positions, but the power remained relatively constant for the first 10 seconds. At 10.5 seconds there was a sharp loss of about 6 percent in linear power. At 11.5 seconds there was another power loss of about 1 percent, and at 12.5 seconds there was another loss of about 6 percent followed by a continuous drop of 3 percent over the next 1-1/2 seconds. At 15 seconds the reactor scrammed.

The frame positions indicate that the automatic controls attempted to maintain power, but the loss of reactivity overwhelmed the system before the scram occurred. Both power and frame position changes are shown in Figure 26.

The duct Jordan indicated a first sharp peak of activity 13 seconds after the valve was closed. A second peak was recorded at 17 seconds, and a third peak at 21 seconds followed by a rather gradual decrease. The duct Jordan response dropped to "background" by the 56th second. A delay between the time of release and any indication by the duct Jordan may be expected because considerable ducting had to be traversed before the Jordan chamber was affected by the radiation from the airborne residue. The duct Jordan response is shown in Figure 27.

The temperature of the moderator around the cartridge remained essentially constant during the course of the experiment. The slight changes of moderator temperature may be attributed to the fact that it was not yet in equilibrium when the valve was closed. Excessive temperatures and physical changes experienced within the insert during the experiment caused many of the thermocouples to become inoperative. Fortunately, some remained intact, and measurements for some of the locations in cartridge 6_i, the moderator block, and the exit air are shown in Figure 28.

Scram Significance

During routine reactor operation at the CTF there are rupture detectors which can cause the reactor to scram in the event of excessive airborne activity in the effluent. These systems were bypassed for the experiment because activity was an expected and desirable part of the experiment. However, fission chambers located in the upper section of the shield assembly (which normally monitor the period of the parent reactor) were still operative and capable of scramming the reactor in the event of excessively short parent-core periods.

Fifteen seconds after the valve was closed, the reactor was scrammed automatically by the parent core instrumentation, which had apparently received a false parent-core short period signal. Postexperiment examination of the facility and calculations indicate that the fresh fission products being swept up through the hot torus emitted sufficient delayed neutrons to cause an increase in the neutron flux at the fission chambers equivalent to a 5-second period of the parent reactor.

The response of the rupture detector is shown in Figure 29, and the stack monitor response is shown in Figure 30.

Changes in Excess Reactivity

The melt having been attempted, and the unexpected reactor scram having been experienced, the immediate concern was knowledge of the amount of damage to the reactor. The reactor was once again made critical to determine the fraction of fuel removed from the active core region. From prior experiments, cartridge 6_i was determined to be worth approximately 1.24 percent $\Delta k/k$. Three typical control rods were calibrated, but each

DECLASSIFIED

DECLASSIFIED

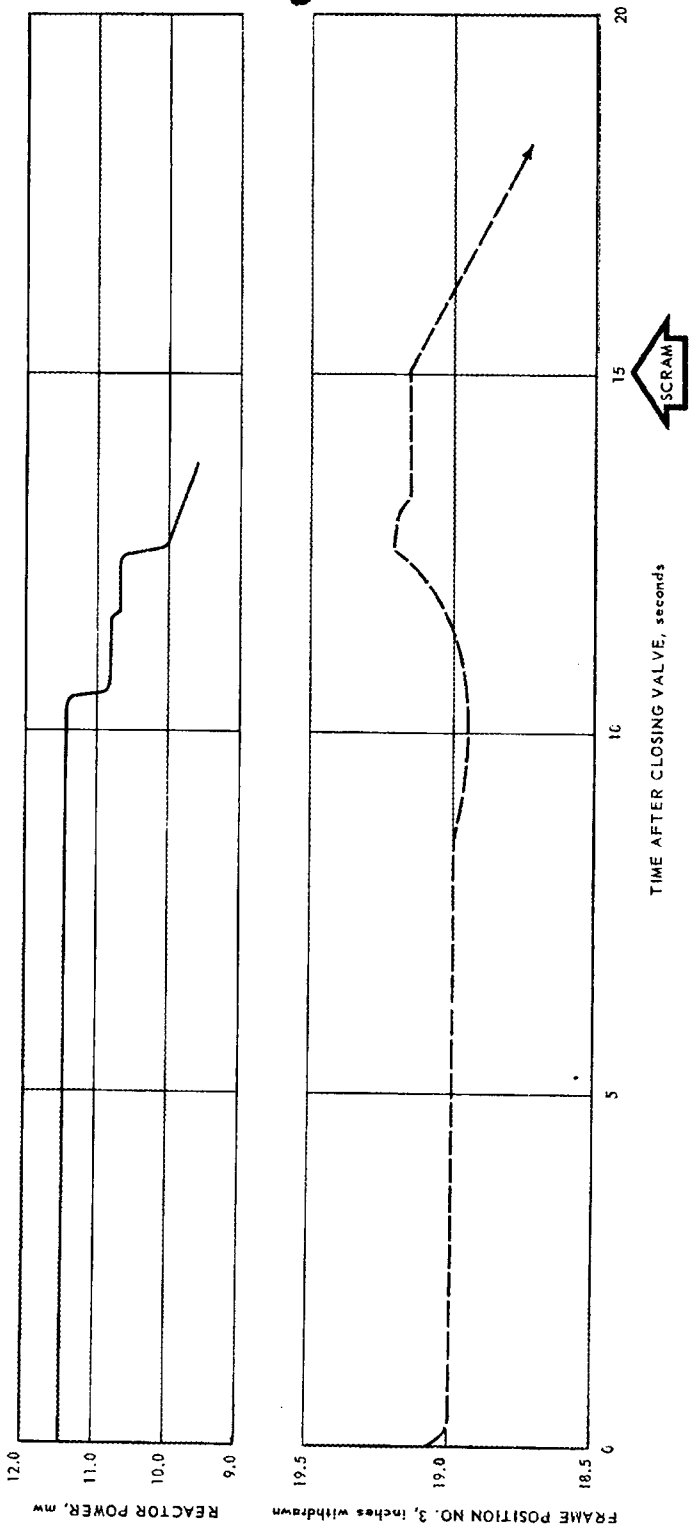

Fig. 26 — Reactor power and frame positions during melt

DECLASSIFIED

DECLASSIFIED

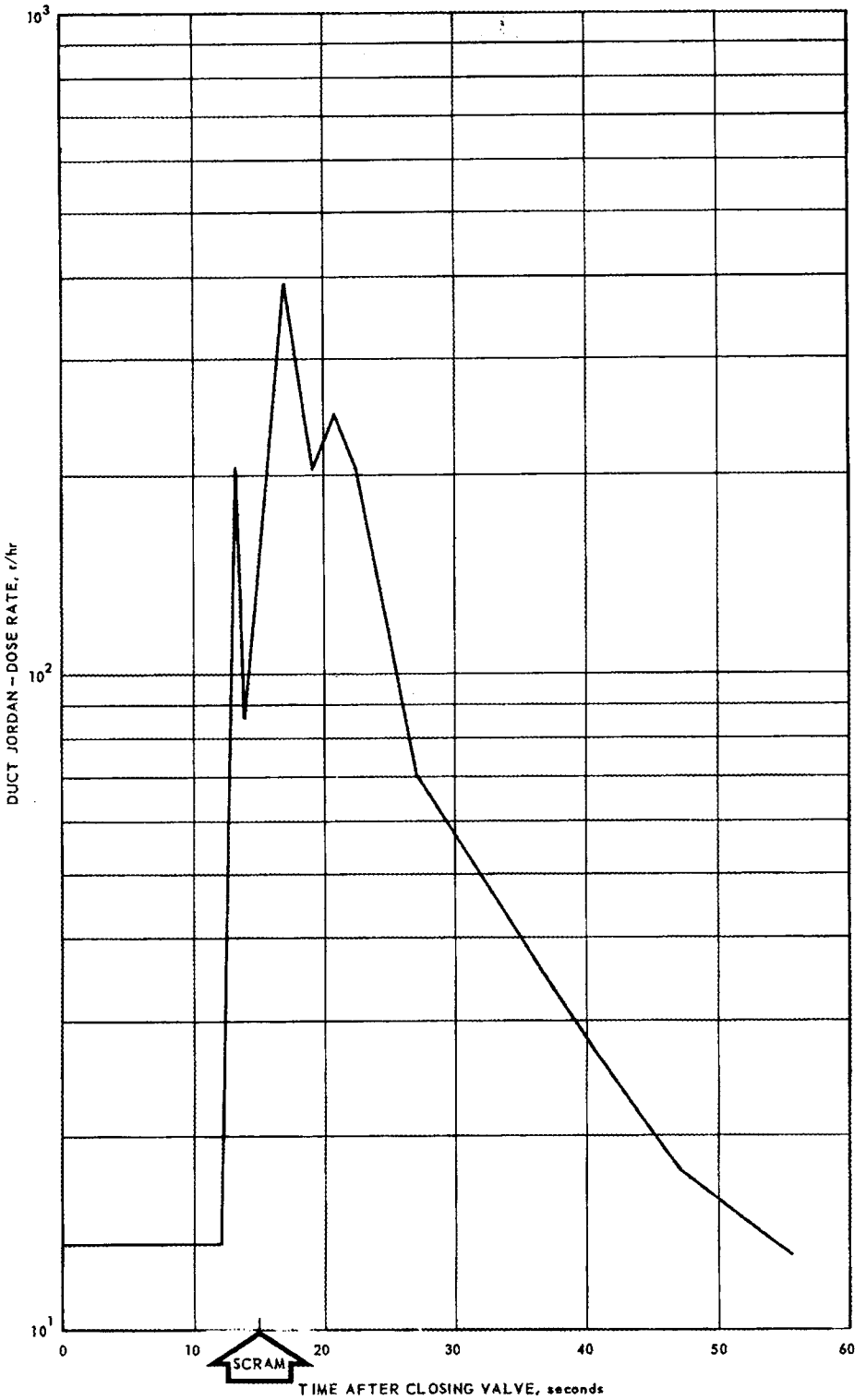

Fig. 27 – Duct Jordan response during melt

DECLASSIFIED

DECLASSIFIED

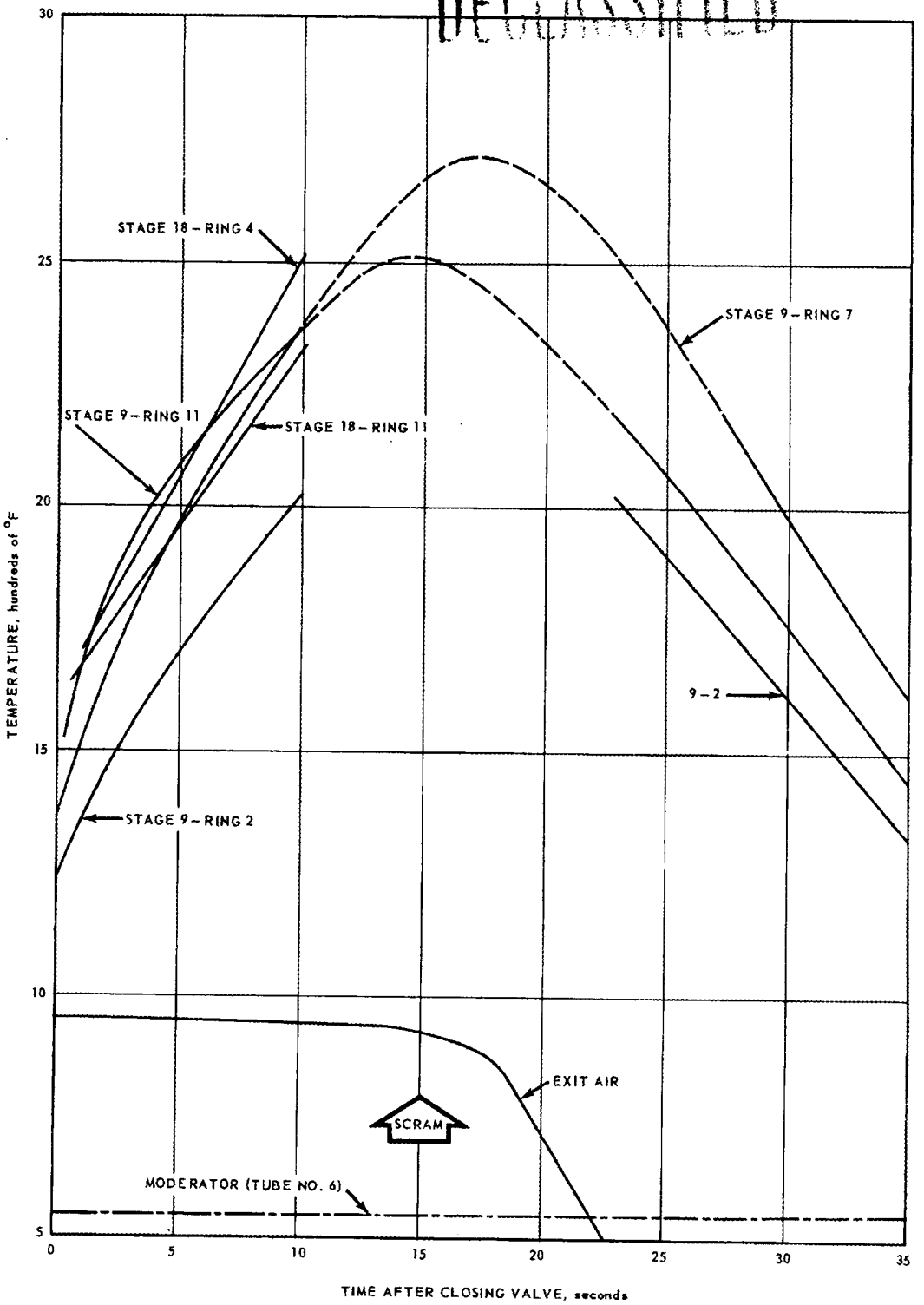

Fig. 28 – Cartridge 6_i, air, and moderator temperatures during melt

DECLASSIFIED

DECLASSIFIED

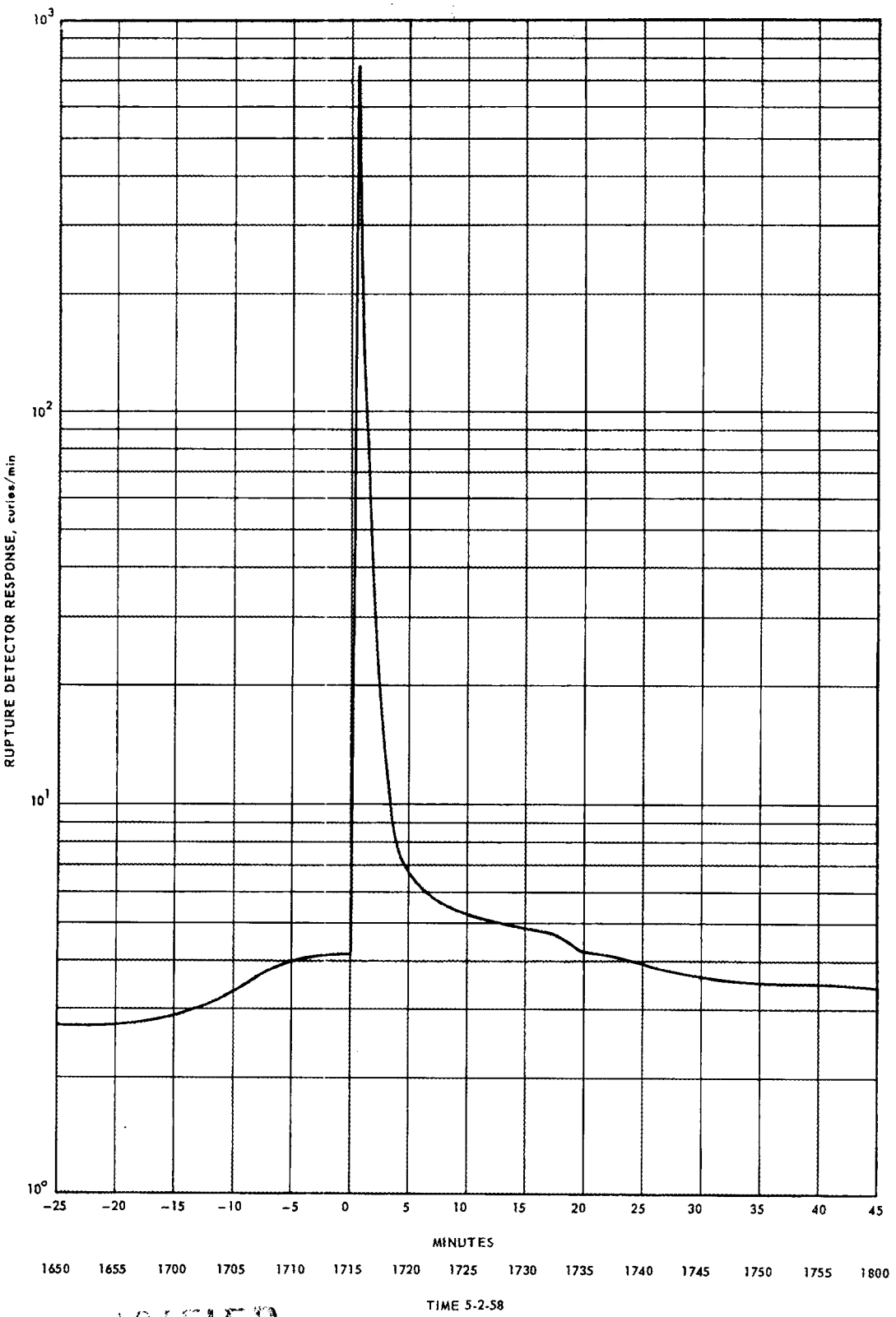

Fig. 29--Rupture detector response during melt

DECLASSIFIED

DECLASSIFIED

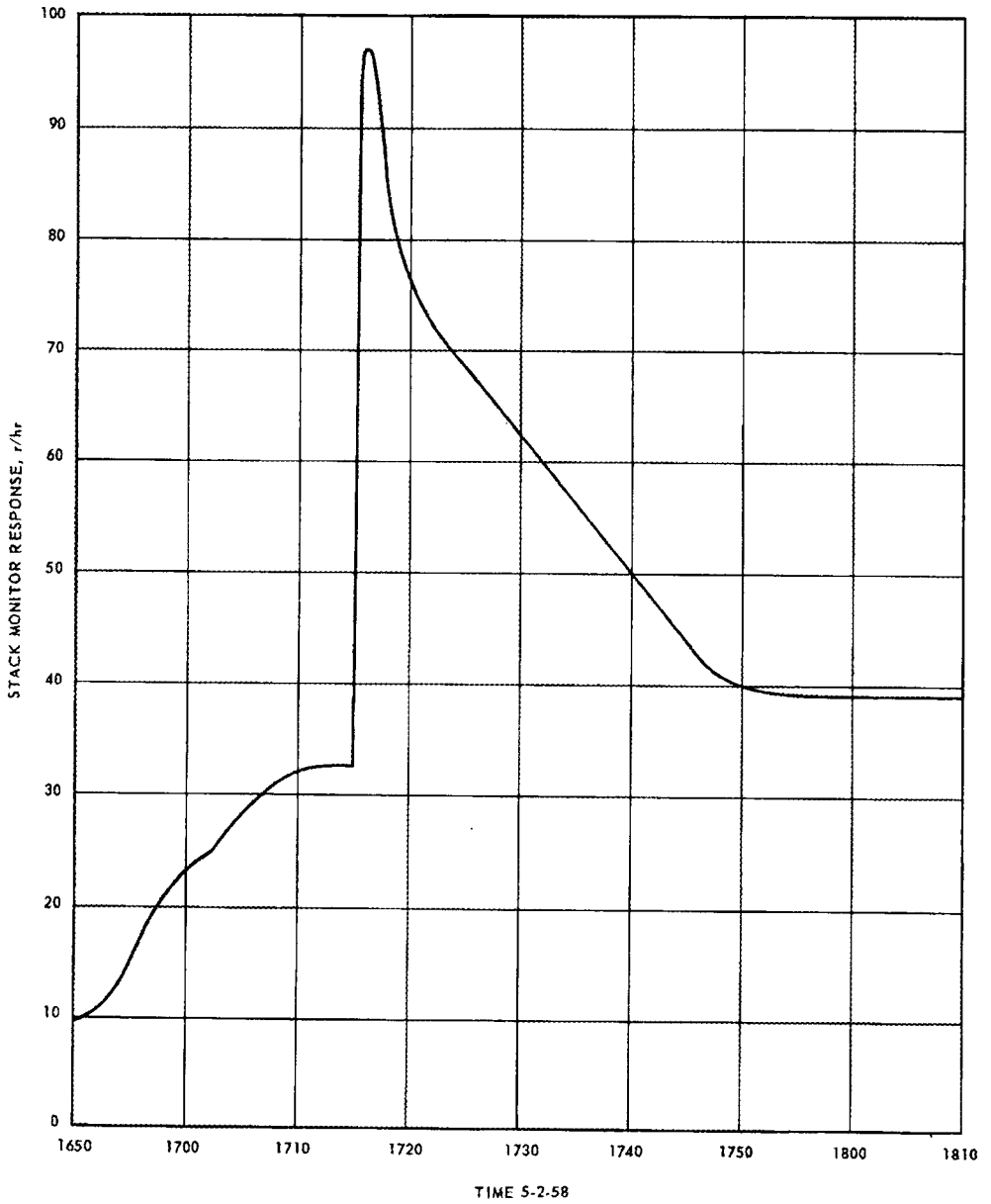

Fig. 30 – Stack monitor response during melt

DECLASSIFIED

DECLASSIFIED

rod worth was 17 percent below the values obtained during earlier tests. In spite of the rod discrepancies, the measurement of excess reactivity was considered desirable. The data points in Table 4 were measured before and after the melt.

A comparison of similar conditions before and after the experiment indicates that there was a loss of from 0.154 to 0.262 percent $\Delta k/k$. This represents from 12 to 21 percent of the total worth of the cartridge. Values indicating a loss of 21 percent of the cartridge appear to be more consistent, and therefore more confidence was placed in this estimate.

Postexperimental visual examination of the cartridge indicated a loss of about 40 percent of the fuel from the active region of the core - an appreciable amount of it remaining in the plug found in the tailcone of the tube. Since the contribution to Δk by material in the tailcone section is rather small, the factor of 2 discrepancy between observed material loss and estimated material loss by $\Delta k/k$ methods is not understood.

Reactor Damage

After cartridge 6_i was melted, consideration was given to the thought of melting cartridge 2_i as it was already instrumented and had an independent valve system. The valve used to restrict the air to cartridge 6_i was opened on May 6, 1958, and the reactor was taken stepwise to 1, 5, 20, and 40 percent of full power. Thermocouples still in working order on cartridge 6_i indicated temperature rises comparable to those noted when the valve restricting the air to tube 6 was closed. Detection instruments also indicated increased activity in the effluent. It was concluded that a restriction somewhere in tube 6 was limiting the coolant so severely that any additional power would cause cartridge 6_i to remelt, thereby nullifying any chances of gaining information from either the first melt or the proposed second one. The decision was then made to return the reactor to the hot shop for dismantling and examination.

In the hot shop the insert was removed from the parent core to determine whether it would be feasible to remove the restriction causing the excessive temperatures in tube 6.

When the insert was removed from the parent core, it was noted that a hole had been burned through the side of the moderator tailcone of tube 6 (Figure 31). Examination of the aft end of the insert revealed an appreciable plug of molten residue and partial stages in the moderator tailcone. Figure 32 is a photo of the underside of tube 6_i showing the plug. An attempt to remove this plug by pressure using a probe was unsuccessful. The decision was made to cancel any further attempts to melt cartridge 2_i and to proceed with dismantling the reactor to determine further reactor damage.

The insert was removed to the Radioactive Materials Laboratory, where the moderator tube was cut longitudinally to expose the cartridge. The cartridge was subsequently cut apart to reveal damage to the individual stages. Figure 33 shows the split moderator block 6_i and the cartridge within. The plug in the tailcone (Figure 34) was also revealed by splitting the tailcone.

The cartridge contained 18 stages. Negligible damage could be detected through the first 7 stages. Stage 7 is shown in Figure 35. Stage 8, Figure 36, showed the first signs of "blister" formation. Stage 9, Figure 37, was severely blistered to the point that it could have been a major cause of the airflow restriction noted when the reactor was operated at partial power after the melt. Stages 10 through 18, shown in Figures 38 through 46, were damaged to the extent that in a few cases there was not much more than a portion of the outer rings remaining. Most of the inner rings from these stages had partially melted and fused into a mass which had solidified in the tailcone, forming the plug which had been observed in the hot shop but could not be loosened by probing.

DECLASSIFIED

DECLASSIFI

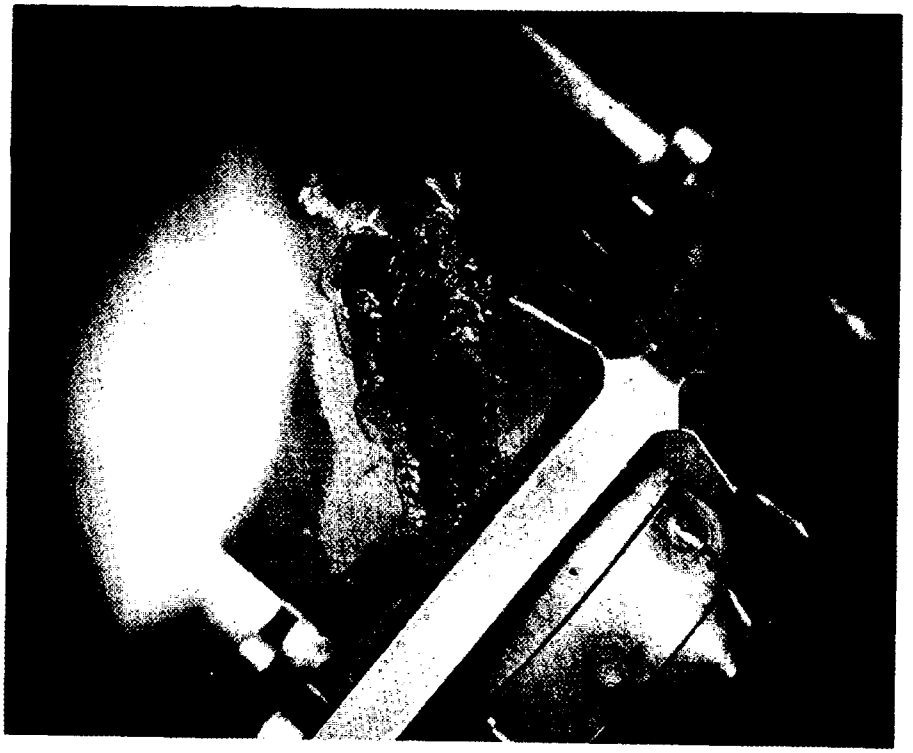

Fig. 31 – Hole burned through moderator tailcone of tube 6_j, Insert 1d

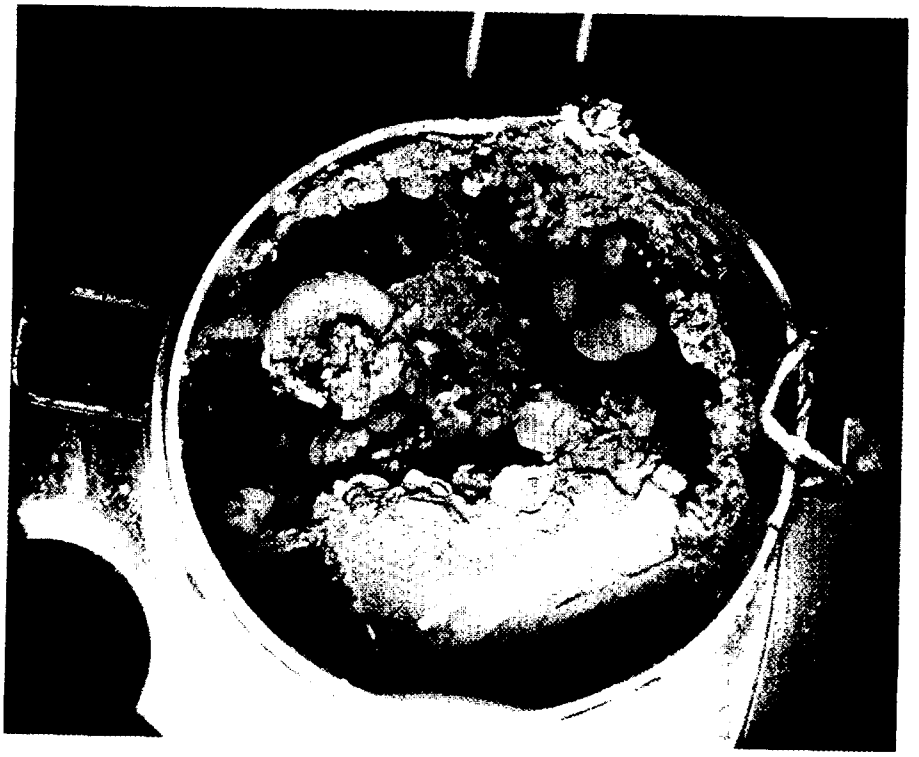

Fig. 32 – Moderator block 6_j, showing remains of cartridge 6_j

D

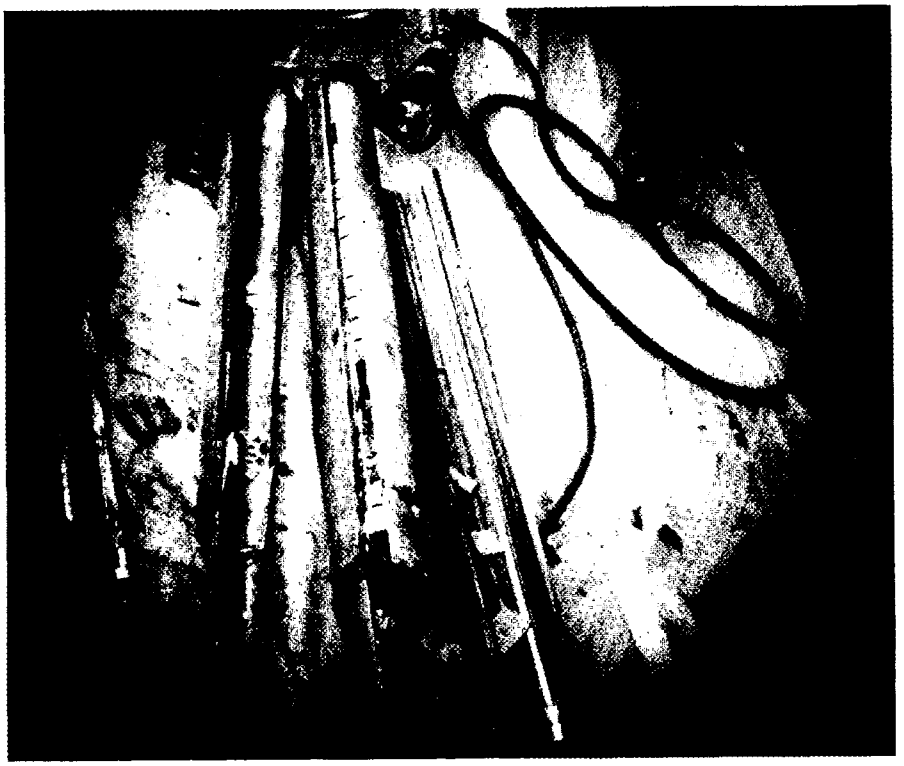

Fig. 33 – Fused plug in tailcone of tube 6_i, Insert 1d

Fig. 34 – Plug of slag in tailcone of tube 6_i, Insert 1d

DECLASSIFIED

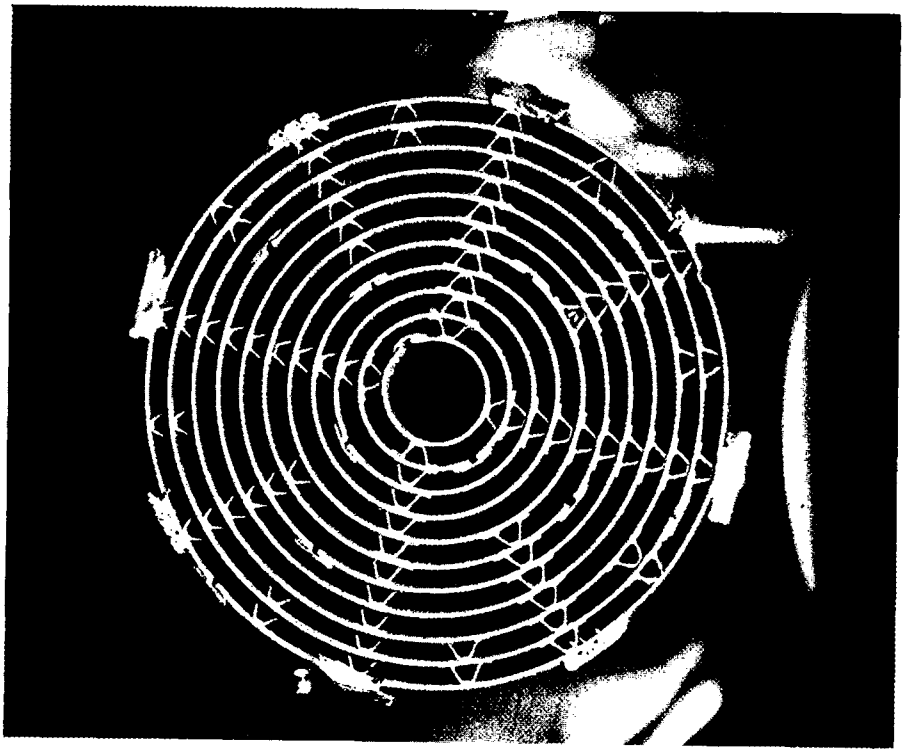

Fig. 35 – Cartridge 6_i, stage 7, Insert 1d

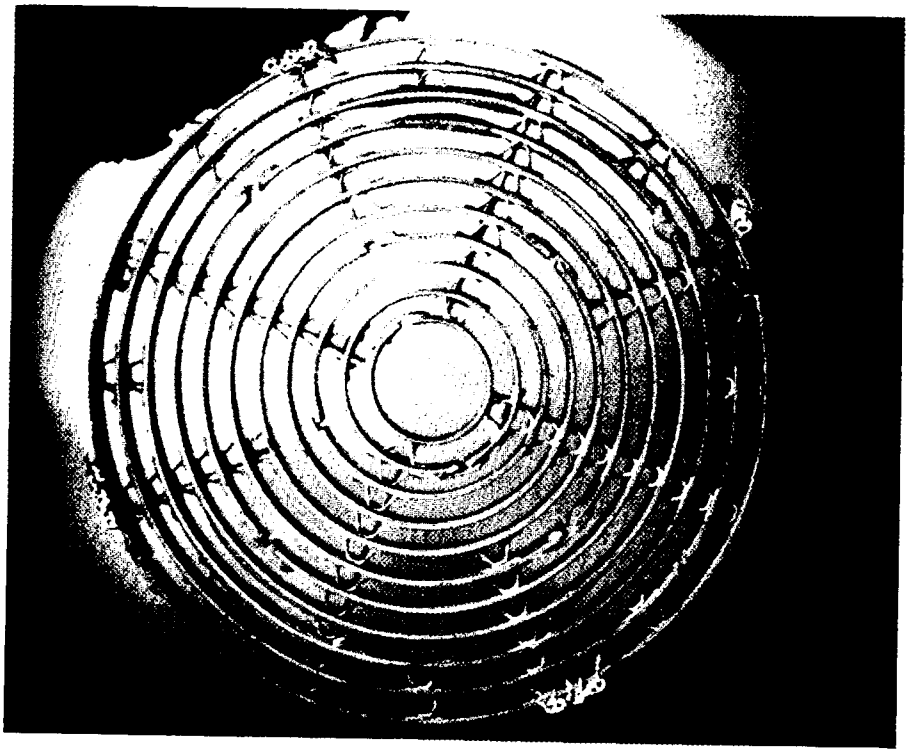

Fig. 36 – Cartridge 6_i, stage 8, Insert 1d

DECLASSIFIED

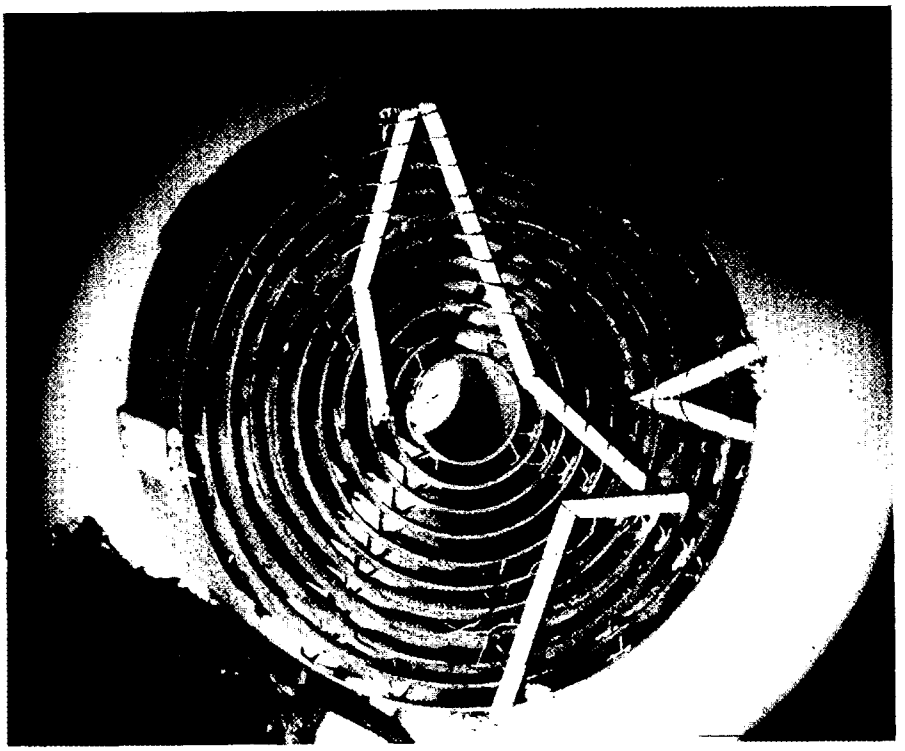

Fig. 37 – Cartridge 6_i, stage 9, Insert 1d

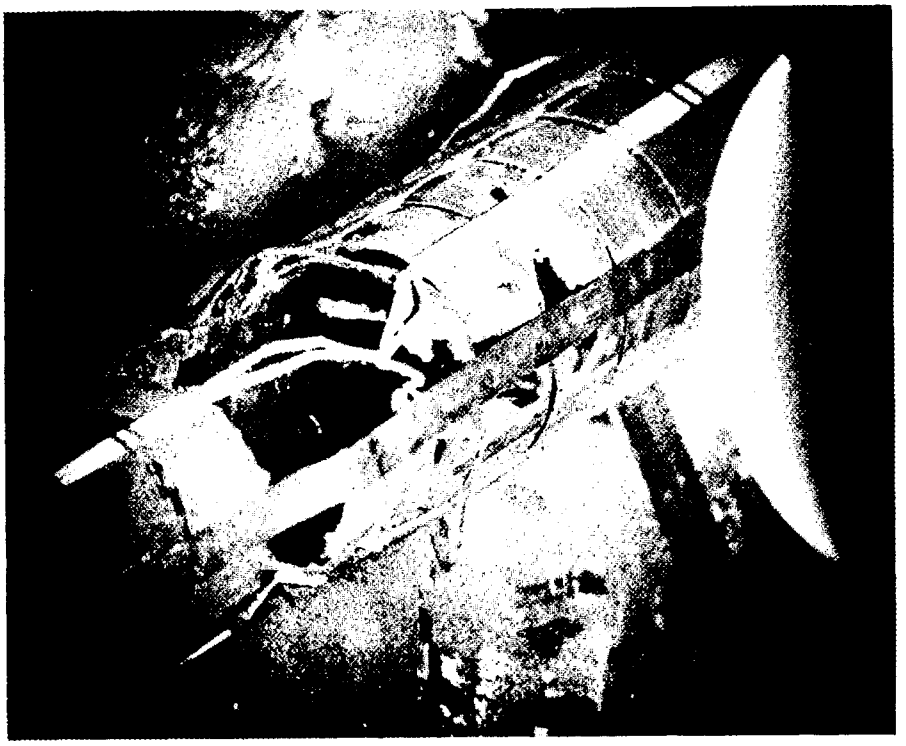

Fig. 38 – Cartridge 6_i, stages 10, 11, 12, 13, 14, and 15, Insert 1d

DECLASSIFIED

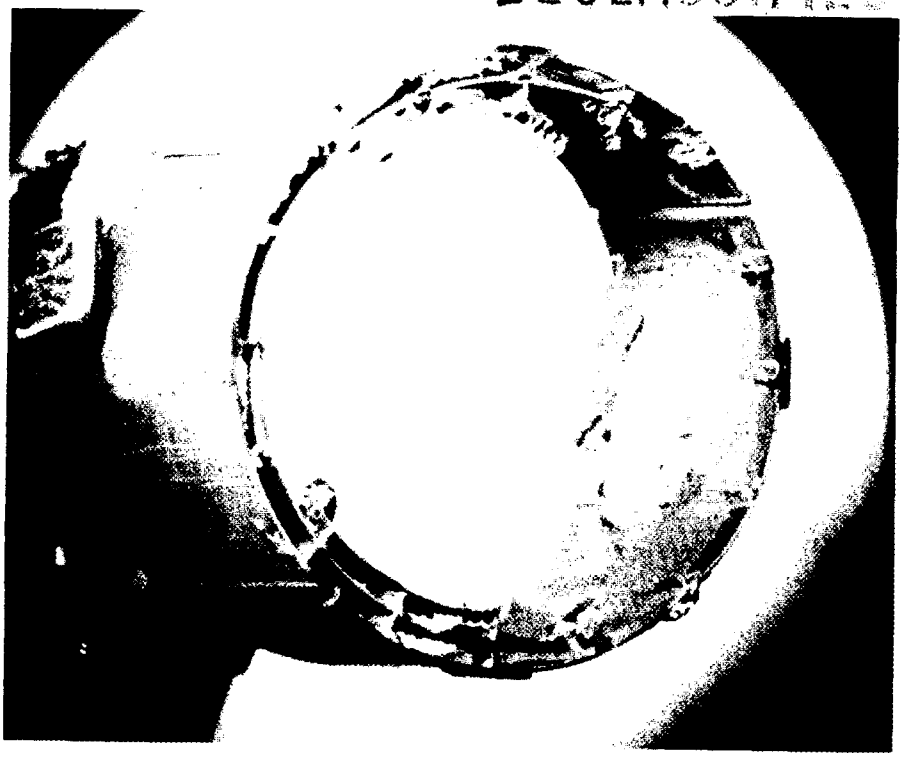

Fig. 39 – Cartridge 6_i, stage 10, Insert 1d

Fig. 40 – Cartridge 6_i, stage 11, Insert 1d

DECLASSIFIED

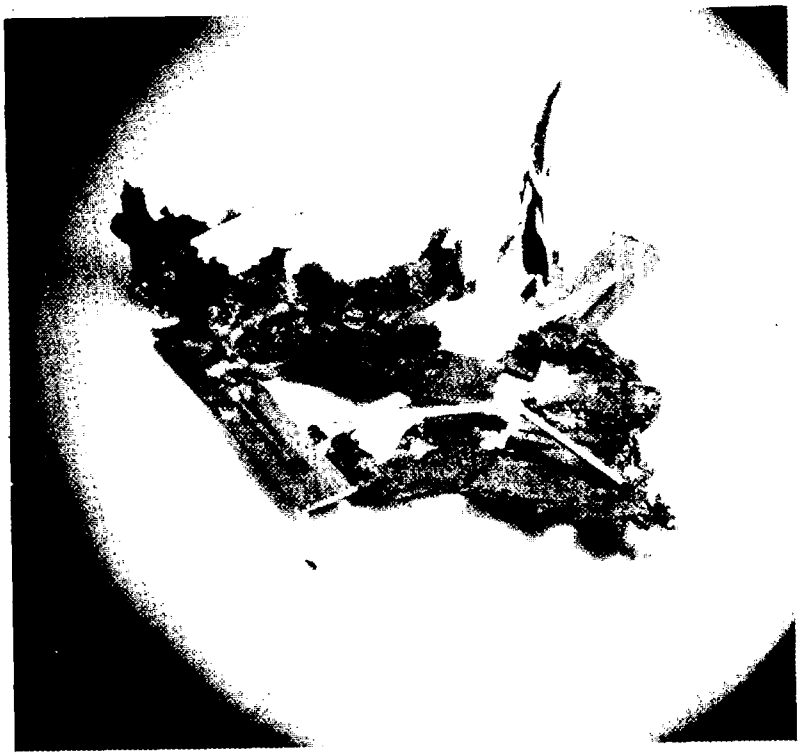

Fig. 41 – Cartridge 6_i, stage 12, Insert 1d

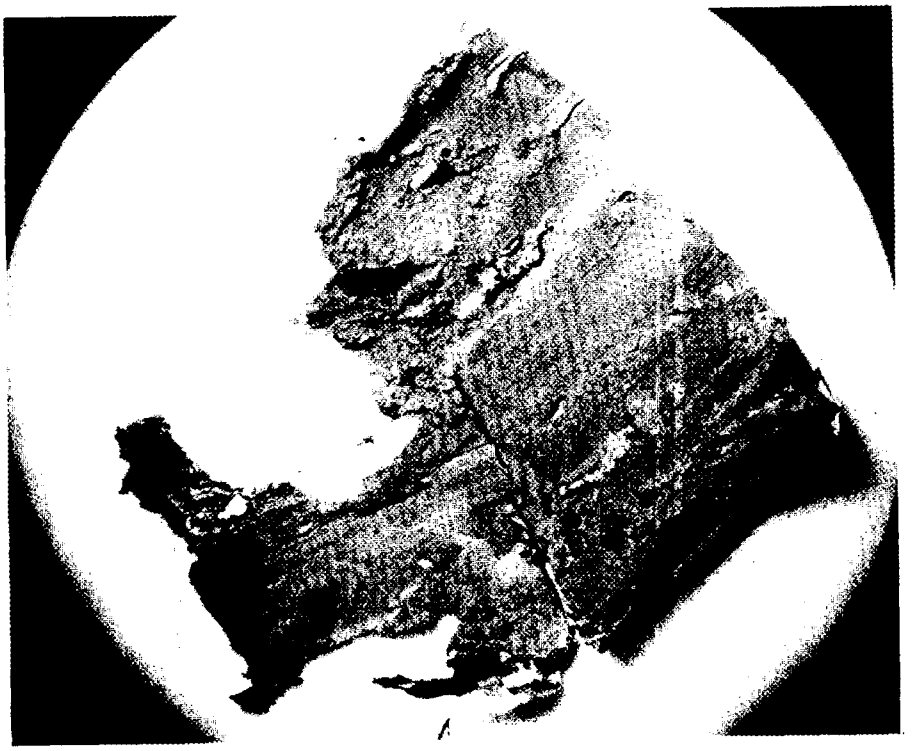

Fig. 42 – Cartridge 6_i, stage 13, Insert 1d

DECLASSIFIED

DECLASSIFIED

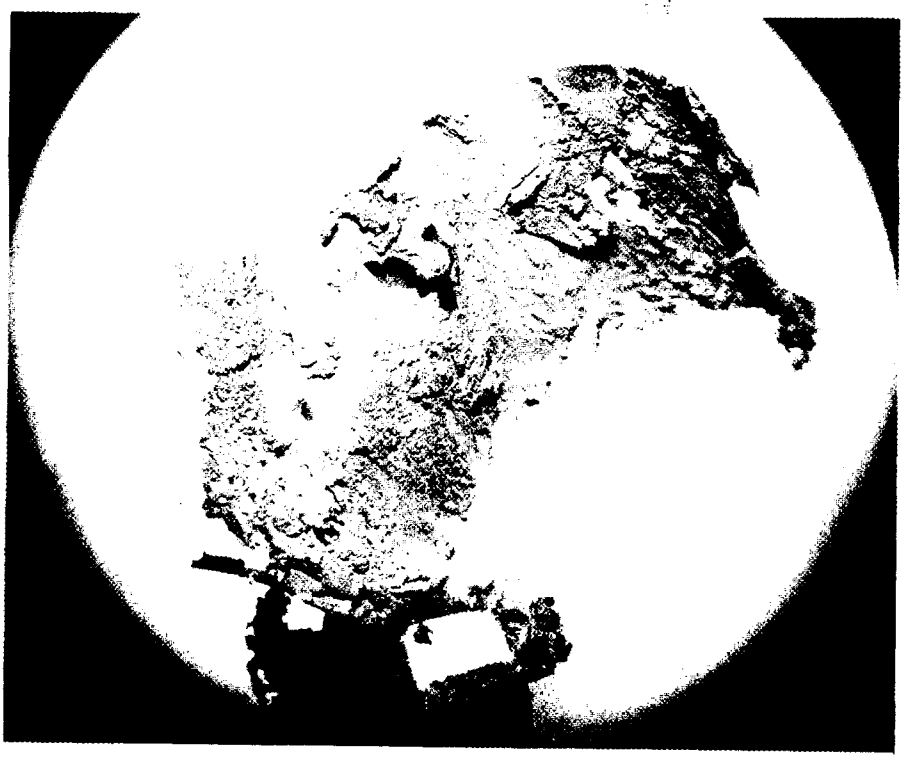

Fig. 43 – Cartridge 6_i, stage 14, Insert 1d

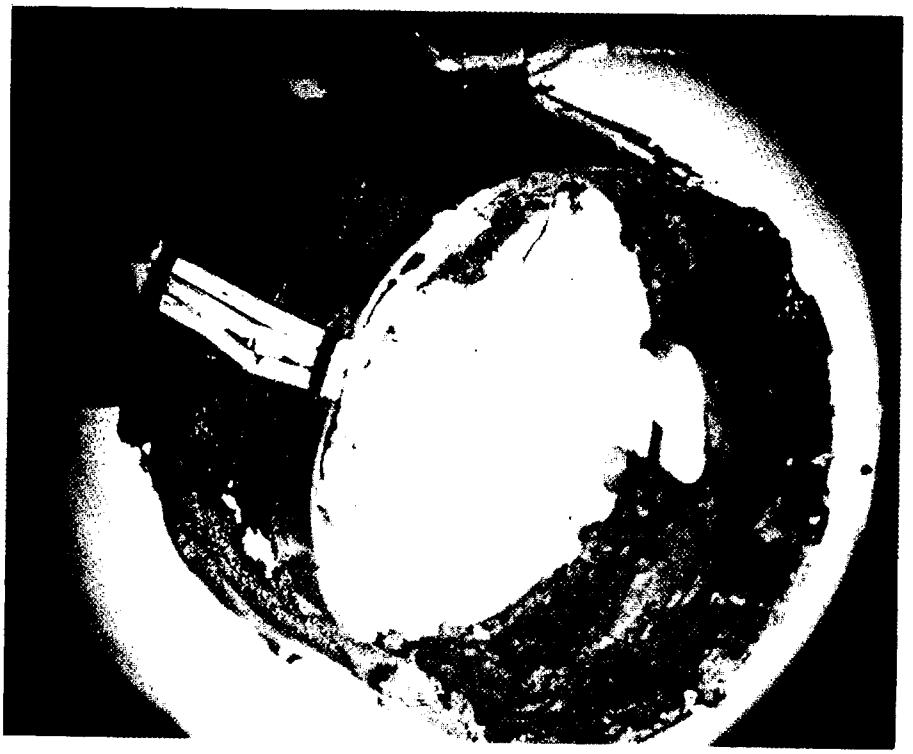

Fig. 44 – Cartridge 6_i, stage 15, Insert 1d

Fig. 45 – Cartridge 6_j, stage 16, Insert 1d

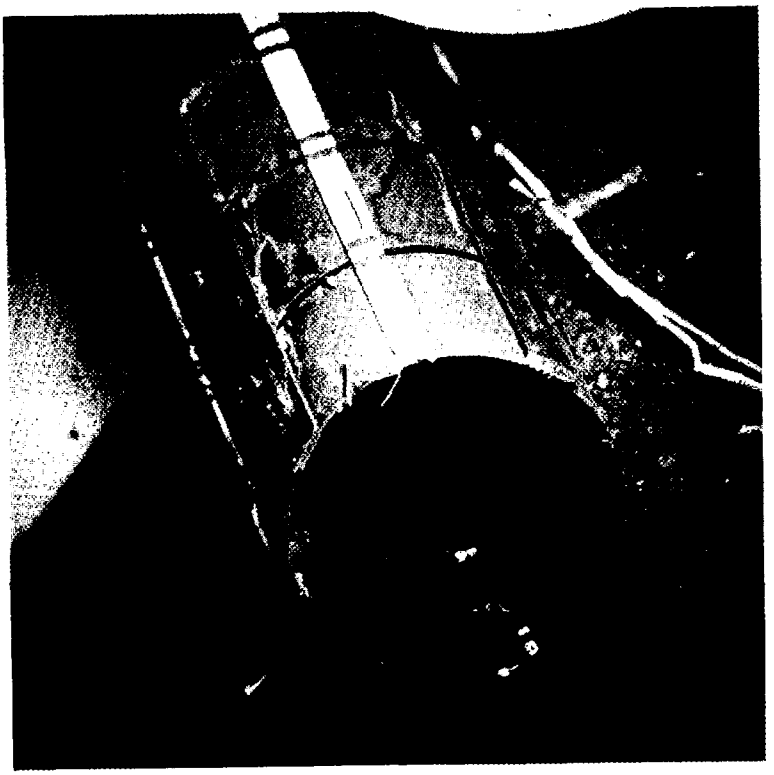

Fig. 46 – Cartridge 6_j, stages 16, 17, and 18, Insert 1d

TABLE 4

EXCESS REACTIVITY MEASUREMENTS

Date	Percent Δk/k	Condition
4-26-58	2.038	Cold reactor - no flow
4-26-58	2.028	Cold reactor - no flow
4-30-58	2.082	Intermediate power - engine flow
5-2-58	1.540	Cold reactor - engine flow
5-2-58	2.148	Full power - engine flow
- Experiment Performed -		
5-2-58	1.386	Cold reactor - engine flow
5-5-58	1.766	Cold reactor - no flow
5-5-58	1.776	Cold reactor - no flow

TABLE 5

PERCENT FRACTIONAL RELEASE[a]

Location of Sample		I^{131}	I^{133}	I^{134}	I^{135}	Ba^{139}	Ba^{140}	Sr^{91}
76-in. duct loop 1	(carbon trap)	9.20	9.27	26.4	28.8	--	0.866	2.66
76-in. duct loop 2	(carbon trap)	1.70	0.924	11.7	8.64	--	0.296	1.03
76-in. duct loop 3	(carbon trap)	1.66	1.64	6.84	4.32	--	0.205	0.717
76-in. duct loop 4	(carbon trap)	5.76	5.15	1.56	0.984	--	0.088	0.235
76-in. duct loop 5	(carbon trap)	1.26	1.16	2.50	2.35	--	0.205	0.370
76-in. duct loop 6	(carbon trap)	0.274	0.228	0.492	0.286	--	0.064	0.018
Vault	(carbon trap)	0.550	0.600	0.649	0.271	1.44	--	0.236
Vault backup	(carbon trap)	0.097	0.098	0.184	0.058	0.190	--	0.029
Rupture detector 6_i	(carbon trap)	7.64	--	--	--	--	0.153	0.531

[a]"Fractional Release" used here is the amount of the isotope released divided by the amount theoretically contained in the entire cartridge and multiplied by 100.

DECLASSIFIED

The plug was broken loose in the Radioactive Materials Laboratory and is shown in Figures 47 and 48. Notice the clusters of rings from several stages that are still recognizable.

A wire basket, which was placed aft of the tailcone of the tube in an attempt to catch a sample of the slag, was missing when the insert was examined in the hot shop. It was later found in the instrument harness below the insert. The wire had partially melted, but the basket still contained an appreciable sample of stage-18 residue. The basket and sample are shown in Figure 49.

Examination of the moderator and the rest of the reactor indicated no further damage.

Handling and Analyses of Samples

Following the test, the carbon traps in the exhaust system and in the field were taken to the radiochemical laboratory where the radioactive iodine, barium, and strontium were separated from an aliquot of the first 5 inches of the carbon traps. The resulting separations were taken to the counting laboratory where they were counted or analyzed, using a 256-channel, gamma-ray-spectrum analyzer. From these data the disintegration rate of the particular isotope was determined. By taking the ratio of the amount of the specific isotope in the effluent to the amount calculated to be present in the whole fuel cartridge, the release fraction was determined. Uranium separations were also performed on the carbon traps.

Flat fallout plates (11 in. by 14 in.) and the high-volume air samples (3.5-in. diameter) were collected and counted for gross beta activity using Geiger-Müller (G-M) counters. The cylindrical fallout plates (3.5-in. diameter by 6.75 in.) and the vegetation samples, collected before and after the test, were counted for gross gamma activity in crystal well counters. The samples that showed sufficient activity for radiochemical separations were taken to the radiochemical laboratory where the separations were performed.

Decay curves were produced from representative samples to permit normalization of activities to a specific time. Because of the high radiation level encountered in the test cell, some of the CTF samples were not collected until the following day.

CTF Source Data

Fission Product Release - The fractional release of specific fission products, as determined by radiochemical separation and analyses of carbon traps in the CTF are given in Table 5.

Velocity profile measurements made in the 76-inch duct indicated that the sampling probe for duct loop 1 was in a very poor location with respect to obtaining representative samples. The results of the analyses indicate that the sampling device for duct loop 6 was not functioning properly. If the results of analyses of samples from duct loops 1 and 6 are disregarded, the average and root-mean-square deviations for percent fractional release as indicated by duct loops 2, 3, 4, and 5 are:

I^{131}	2.60 ± 1.84	Ba^{140}	0.199 ± 0.007
I^{133}	2.22 ± 1.71	Sr^{91}	0.588 ± 0.310
I^{134}	5.65 ± 4.01		
I^{135}	4.07 ± 2.90		

Major factors leading to discrepancies in the results are the location of the sampling probes, the sampling efficiencies for the various isotopes, and analytical techniques.

Uranium Release - The average uranium release as indicated by the first 5 inches of

DECLASSIFIED

DECLASSIFIED

Fig. 47 – Plug of slag and residue from tailcone of tube 6_i, Insert 1d

Fig. 48 – Alternate view of plug of slag and residue from tailcone of tube 6_i, Insert 1d

Fig. 49 – Remains of wire basket containing residue from stage 18

TABLE 6

GROSS BETA ACTIVITY COUNT FOR CASCADE IMPACTOR PLATES

	Counts Per Minute at 18 Hours	Counts Per Minute at 41 Hours
Stage 1	310,348	204,596
Stage 2	5,059	3,059
Stage 3	6,357	4,126
Stage 4	27,862	19,209
Millipore filter	1,013,022	747,153

DECLASSIFIED

the duct loop carbon traps was 1.47 grams with a mean deviation of ± 0.51 grams. This release represents approximately 3 percent of one stage. Postoperational examination indicated that more uranium undoubtedly passed through the exhaust system. It is entirely possible that much of the uranium lost was in the form of molten slag or heavy particulate which was not sampled well by the duct loop probes. The first 5 inches of the carbon traps contained 95 percent of the uranium in the entire trap; therefore the efficiency of entrapment appeared to be quite good once the uranium entered the trap.

Source Strength - The curie source strength was determined by a Jordan ionization chamber located beneath the 76-inch duct and the stack monitor located in the vault. The stack monitor is a scintillation counter which measures activity from filter paper through which effluent from the 80-foot stack level has been filtered.

Using calibration obtained during Insert 2b power testing, the total number of curies released at the top of the stack was determined. The duct Jordan indicated a release of approximately 2.1×10^4 curies, and the stack monitor indicated a release of from 1.30×10^4 to 2.1×10^4 curies.

During the melt a spot sample of effluent was taken and the gross beta decay curve was determined for 63 hours.

This decay was then compared with a calculated gross beta decay curve. The two curves compare reasonably well, but the data are not sufficiently refined to permit more than the general statement.

Particle Size Distribution - A cascade impactor and an electrostatic precipitator were installed on the hot duct between the hot torus and the engine unit combustor in an attempt to determine particle size distribution. The cascade impactor plates were counted for gross beta activity approximately 18 hours after the test with a repeat count 41 hours after the test. The relative activities found on the various stages are given in Table 6.

The cascade impactor stages had not been calibrated for the conditions it encountered during the test; however, by use of the calibration supplied by the manufacturer and by the modification of these results for the density of the metal sampled (assumed to be $9.0\ g/cm^3$) the particle size distribution shown in Figure 50 was determined. From this distribution the comparison of numbers of particles of a given size as determined above are compared to the number of particles of a given size one might expect were there equal activity on all stages. This comparison is made normalizing the activities of 10-micron-diameter particles. It is evident that much of the effluent activity is associated with extremely small particles. The individual stages of the cascade impactor were analyzed spectrographically. The predominant isotopes producing the activity were Mo^{99}-Tc^{99}, Te^{132}-I^{132}, and I^{133}.

The electrostatic precipitator liner collected relatively little material during the test. No particle sizing was accomplished due to insufficient concentration of particles. Spectral analysis 19 days after the test indicated that the major gamma activity at that time was from Mo^{99}-Te^{99}, Te^{132}-I^{132}, and Ba^{140}-La^{140}. Analysis of the carbon trap backup for the precipitator indicated that most of the activity on the carbon was from I^{131} with some Ba^{140}-La^{140}.

Retention of I^{131} in IET Ducting - An attempt was made to obtain as estimate of the amount of I^{131} that became attached to the wall of the 76-inch duct between the engines and the stack. A metal plate 4 inches in diameter was set in the wall of the duct about 25 feet upstream from the stack intercept. Spectral analyses of the activity on the plate indicated that at least 0.08 curie of I^{131} was deposited in the duct. Uncertainty factors indicated that the amount deposited could be higher by about a factor of 2.

DECLASSIFIED

DECLASSIFIED

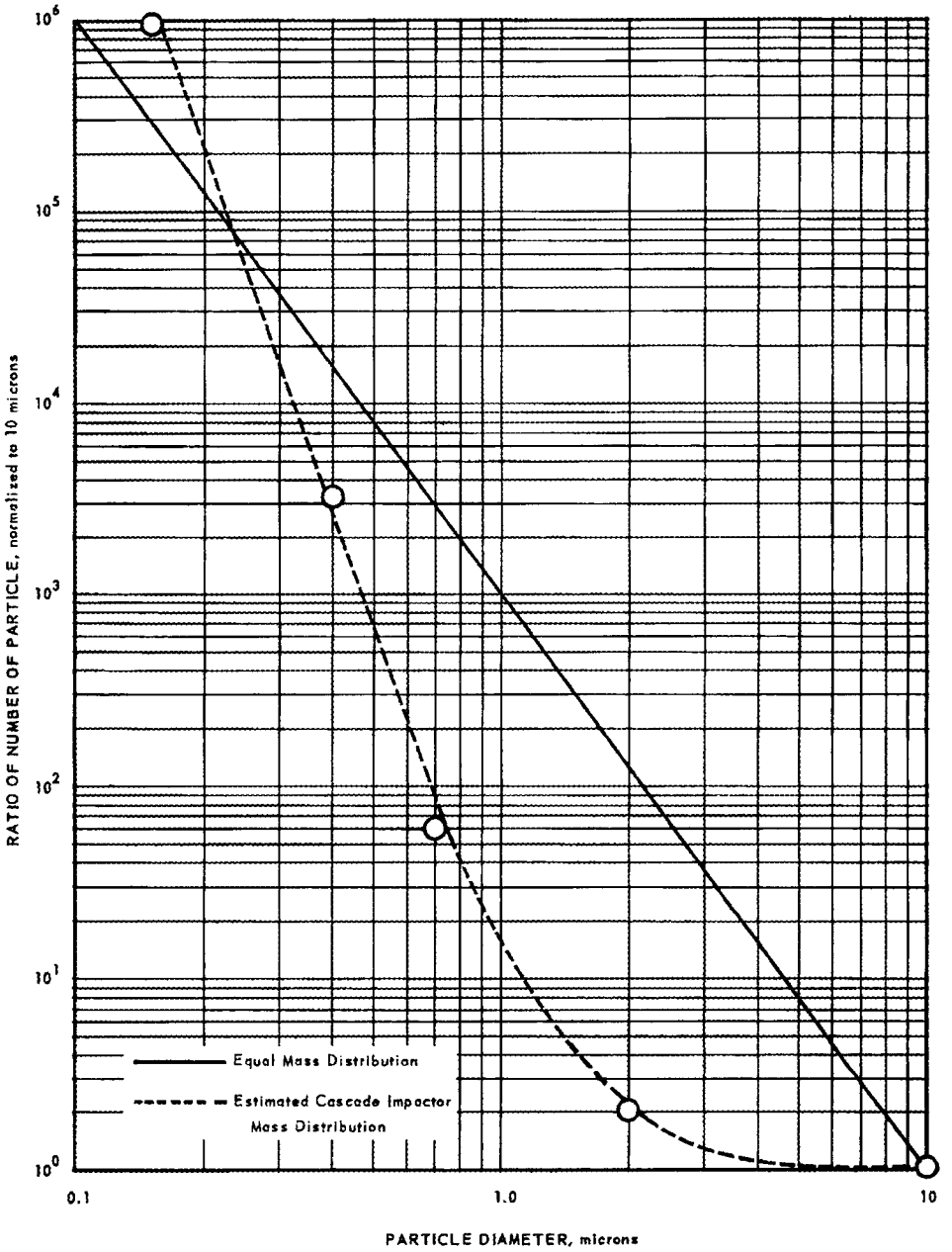

Fig. 50 – Estimated particle size distribution on cascade impactor compared to equal mass distribution

DECLASSIFIED

DECLASSIFIED

No data are available for estimating the amount of iodine retained at other locations in the IET facility.

ATMOSPHERIC CONDITIONS AT TEST TIME

Description of Weather Regime

The general weather pattern existing during conduct of the experiment was characterized by a relatively weak pressure gradient with a low pressure center located about 110 miles to the northwest of the NRTS. The air mass contained little moisture, and only a few scattered clouds were observed. Surface winds in the nearby surrounding area were from the south to southwest. Figure 51 shows the 1700 MST surface weather chart for May 2, 1958 with the upper-level wind-flow pattern at about 10,000 feet mean sea level indicated for the area of interest.*

Meteorological measurements, smoke photography, and visual observations made in the test area before and after the experiment confirm that the atmosphere in which the effluent was released was typical of a strong lapse or "looping" condition. When atmospheric instability such as this exists, strong effluent concentrations can be brought to the ground near the stack and can result in irregular patterns on ground sampling networks.

Figure 52 shows mean temperature profiles for 30-minute periods observed at the IET weather tower before, during (the approximate period of time the radioactive cloud was over the grid), and after the experiment and the dry adiabatic lapse rate for comparison. It can be seen that a superadiabatic lapse rate existed in the time period prior to the experiment and that during the experiment (1715-1745) it was superadiabatic to the 140-foot level and near isothermal to the 200-foot level. It can also be seen that after the experiment relative surface cooling occurred in the first 20 feet, giving an inversion to the 20-foot level (this did not exist during the entire 30-minute period), a superadiabatic lapse rate to the 140-foot level, and near isothermal to the 200-foot level. In all three profiles the rapid decrease in temperature in the first 60 feet, the over-all shapes of the profiles, and the mean temperature differences between the 5-foot level and the 200-foot level, which in each case is greater than the dry adiabatic, shows that parcels of air were being heated at the earth's surface by incoming solar radiation, expanding and rising where they were caught in the mean wind. These air parcels are known as thermal eddies which expand adiabatically and continue to rise until the temperature of the parcel is equal to or less than that of its environment. Rising air parcels are replaced by descending and horizontal air motion. This convective process results in the condition known as "looping" for stack effluents and can be noted on wind-direction recording charts by the angular width of the trace fluctuations which at times will exceed 90 degrees. In this particular experiment fluctuations of 70 degrees were observed at the 200-foot level during the period the radioactive cloud was over the sampling network. Figures 53, 54, 55, and 56 present ground and aerial photographs of smoke plumes generated by injection of engine oil in the exhaust system of CTF. The photographs were taken at the approximate midpoint in time of the temperature profiles discussed above and were selected to describe the type of atmosphere that existed during the test period. The oscillating or "looping" motion, which is shown by the smoke plumes, is produced by thermal eddies which are rising and moving with the mean wind. The aerial photographs have been retouched to denote the approximate sector layout and direction orientation. The looping pattern observed in Figure 53 is exceptionally well defined by the smoke-plume shadow, which can be detected to approximately 1 mile from the release point. In Figure 55 the smoke plume may be detected at considerable distances over the sampling network, and varying intensities of smoke concentration within the plume structure at the same radial distance can be seen. Vertical cross sections of

*Data provided by United States Weather Bureaus, National Reactor Testing Station.

DECLASSIFIED

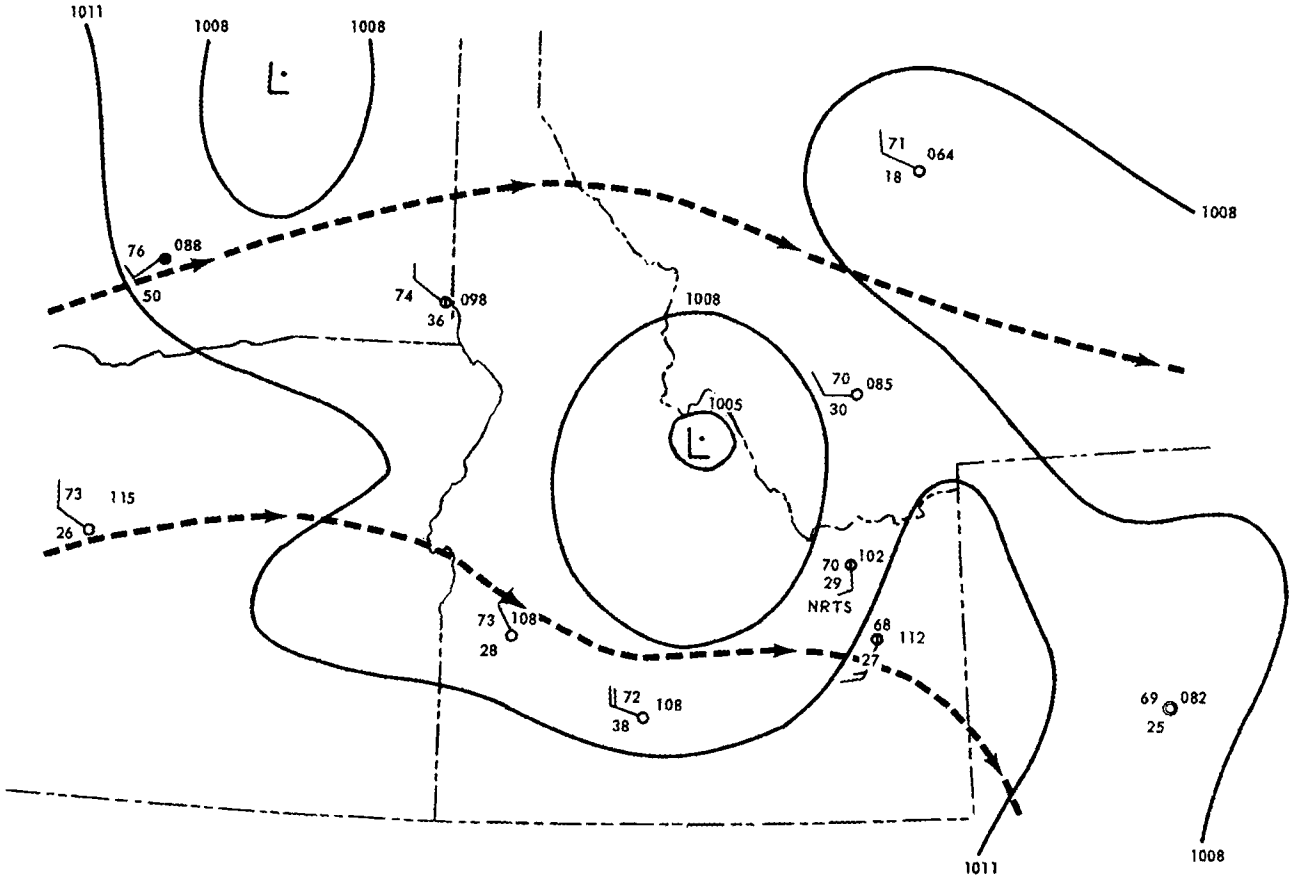

Fig. 51 – Mean air temperature profiles observed at the IET weather tower for time periods noted on May 2, 1958 compared to dry adiabatic lapse rate

DECLASSIFIED

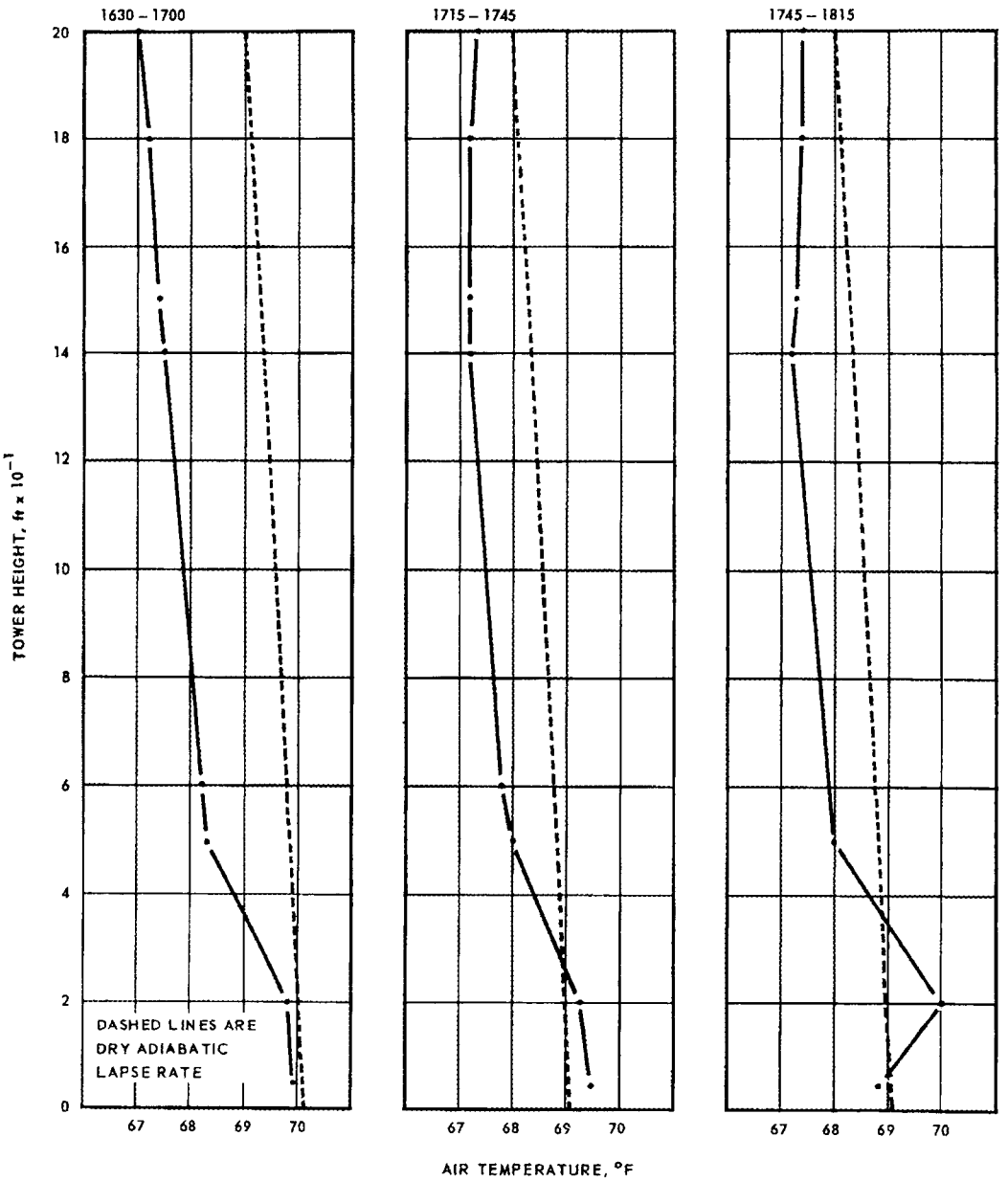

Fig. 52 – Synoptic surface weather chart with upper-level wind pattern indicated for 1700 MST, May 2, 1958

DECLASSIFIED

DECLASSIFIED

DELETED

DECLASSIFIED

DELETED

DECLASSIFIED

DELETED

DECLASSIFIED

DELETED

concentration through a cloud of this type would give a non-Gaussian distribution. Data from ground sampling equipment to be presented later show a distribution of this type. This, of course, is to be expected when thermal eddies exist in the atmosphere in which the effluent is released.

The smoke plume shown in Figure 56 illustrates strikingly the process by which strong concentrations may be brought to the ground close to the stack in an atmosphere characterized by "looping." Immediately to the left of the reference pole held by the observor smoke motion toward the ground and below the level of the stack can be seen. Further to the left nearly vertical rising smoke is seen. These two motions are typical of rising and subsiding air characteristic of thermal eddies.

Cloud Trajectory and Diffusion Parameters

Wind Distribution Over Grid and Trajectory - Wind speed and direction measurements taken at the IET weather tower and in the experimental area just prior to the initiation of the final power run were utilized to ascertain that an excellent opportunity existed for the radioactive cloud to transverse the grid nearly down the centerline. The tower data were further utilized to time the nearly instantaneous release with the existing fluctuating wind pattern which showed variations in azimuth wind direction from 140 to 230 degrees for short periods of time in the 1/2 hour preceding the release. The crude field wind measurements and the mean wind velocity from the 200-foot level of the tower for the 15-minute period prior to the release are shown in Figure 57. Also shown are the points of maximum activity, from fallout plates placed on the sector arcs, which substantiate the trajectory of the radioactive cloud. The sampling sector fallout and high-volume air-sampler isopleth patterns, which are presented later in Figures 69 and 75, also confirm the motion of the effluent.

Diffusion Parameters - The smoke releases prior to the experiment were utilized, in addition to describing the general character and probable path of the effluent, to obtain an approximation of the effective stack height. This height was arbitrarily taken to be the rise of the plume a short distance from the stack where it appears to nearly level off and not necessarily the maximum height reached by the plume. Such a procedure permits substitution of the effective stack height in diffusion equations and is an attempt at least to separate the effects due to the characteristics of the stack from the influence of the environment. Figures 58, 59, and 54 have been marked to note the selected heights which are respectively 195 feet, 215 feet, and 205 feet. The empirical stack height equation derived by Davidson* from Bryant's† wind tunnel experiments has been computed for comparison using the particular set of conditions existing at the time of the smoke release. The Bryant-Davidson expression and selected parameters are given below.

$$\Delta h = d\left(\frac{V_s}{\bar{u}}\right)^{1.4}\left(1 - \frac{\Delta T}{T_s}\right)$$

where

d = stack diameter, feet	d = 15 feet
V_s = stack draft velocity, ft/sec	V_s = 35 ft/sec
$\bar{u}$ = mean wind speed, ft/sec	$\bar{u}$ = 16 ft/sec
ΔT = excess temperature over ambient, ^{o}F	$\Delta T = 433^{o}F$
T_s = absolute temperature of stack gas, ^{o}R	$T_s = 959^{o}R$

*W. F. Davidson, "The Dispersion and Spreading of Gases and Dust from Chimneys," *Transactions of Conference on Industrial Wastes*, Fourteenth Annual Meeting, Industrial Hygiene Foundation of America, November 18, 1948, pp. 38–56.

†L. W. Bryant, "The Effects of Velocity and Temperature of Discharge on Shape of Smoke Plumes from a Funnel or Chimney," *Experiments in a Wind Tunnel*, National Physical Laboratory (Great Britain), 1949.

DECLASSIFIED

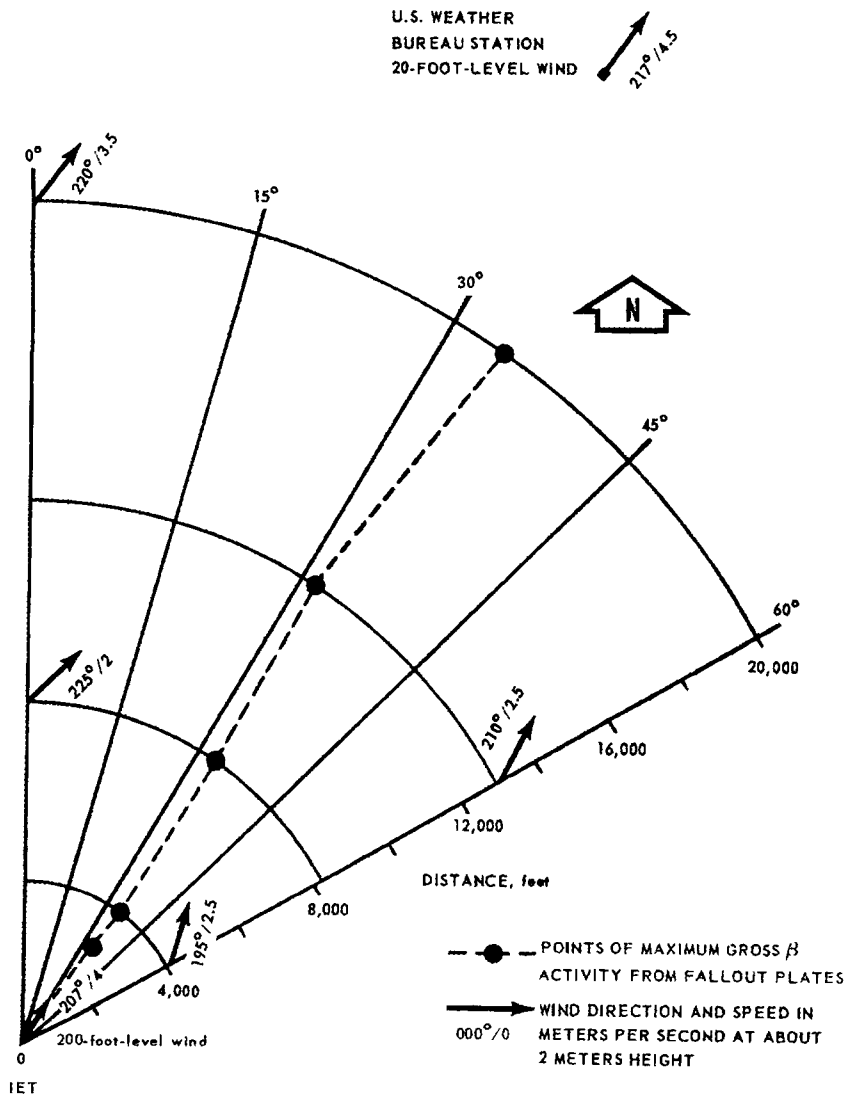

Fig. 57 – Wind speed and direction measurements over the experimental area just prior to release time and points of maximum fallout on sector arcs

DECLASSIFIED

DECLASSIFIED

DELETED

DECLASSIFIED

DELETED

DECLASSIFIED

The parameter V_s for the top of the stack was estimated from a velocity profile taken at the 80-foot level and is considered to be conservative. Figure 60 shows temperature and velocity measures being made at the IET stack. The stack gas temperature was measured at the 80-foot level and temperature and wind speed at the 150-foot level on the weather tower. The calculation results in an effective stack height of 211 feet which compares well with the heights obtained from the smoke photographs. It should be noted that the effect on plume rise of the stability of the atmosphere is not considered in the Bryant-Davidson relationship and was at least attempted to be isolated in the photography analysis. The influence of convective activity on initial plume rise can be seen in the smoke photographs. In Figure 58 the thermal effect at point A accounts for nearly one-stack-height rise. One minute and a half later the same modified smoke globule may be identified in Figure 59 at point B. If it is assumed that the smoke moves horizontally at the same velocity, it is evident that the rate of height increase of the parcel is not constant; i.e., the influence is a thermal eddy. At point C in Figure 59 smoke can be noted below the height of the stack, which of course is caused by the opposite effect of descending air motion. In Figure 54 the height of the smoke plume at a horizontal distance of five stack heights is about five stack heights. The inference from these photographs and calculations is that, in conditions of moderate to strong lapse, computations of effective stack height for facilities and parameters of the general nature of those described are of questionable value when atmospheric stability is neglected. Stability effects close to the stack in many cases can be the primary contributor to positioning the plume vertically at, below, or well above the physical stack height.

The dimensionless turbulence parameter, n, and diffusion coefficients C_x, C_y, C_z used in Sutton's diffusion equations were predicted for operational calculations for this experiment by the U.S. Weather Bureau at the NRTS. These values were $n = 0.20$ and $C = C_x = C_y = C_z = 0.285$ meters$^{n/2}$.

The wind speed data taken at the IET weather tower during the experiment were analyzed for use in determination of the stability parameter, n, using the equation developed by Sutton. This equation

$$\bar{u}_z = \bar{u}_{z_1} \left(\frac{z}{z_1}\right)^{\frac{n}{2-n}}$$

where

$\bar{u}_z$ = mean wind speed at height Z

u_{z_1} = mean wind speed at height Z_1

Z = height at top of layer of anemometer

Z_1 = height above surface of earth of anemometer

n = turbulence parameter

relates wind speeds and heights in appropriate units in the layer in which the diffusion process is occurring. The mean wind speed profiles presented in Figure 61 are for selected time periods before, during, and after the experiment. Also shown for comparison are mean temperature profiles for the same respective time periods and the dry adiabatic lapse rate. Calculations of n for the selected time periods are given in Table 7 along with mean temperature differences between the 200-foot and the 5-foot levels for the same periods.

DECLASSIFIED

DECLASSIFIED

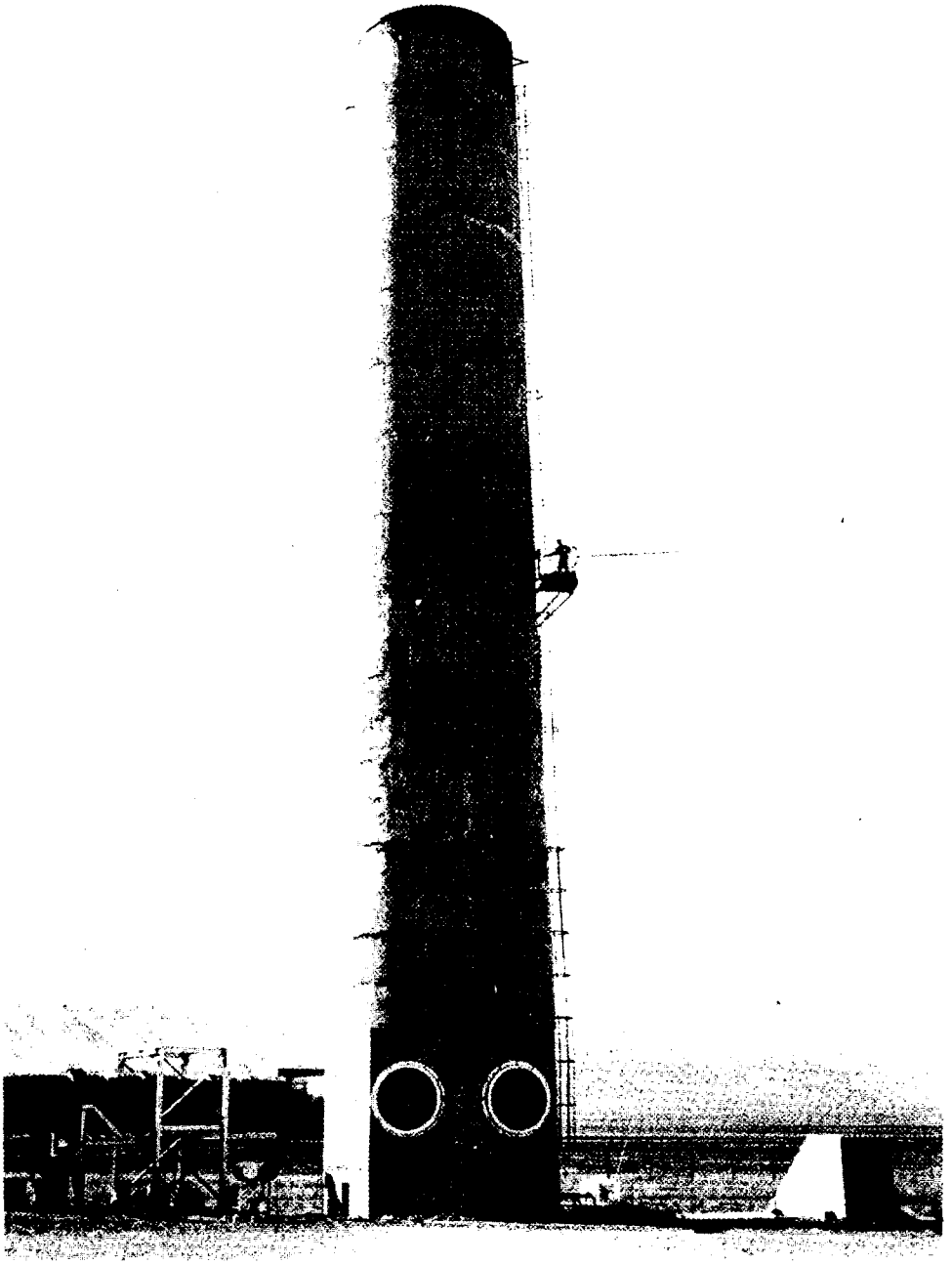

Fig. 60 – Velocity profile measurements being made at the 80-foot level of the IET stack

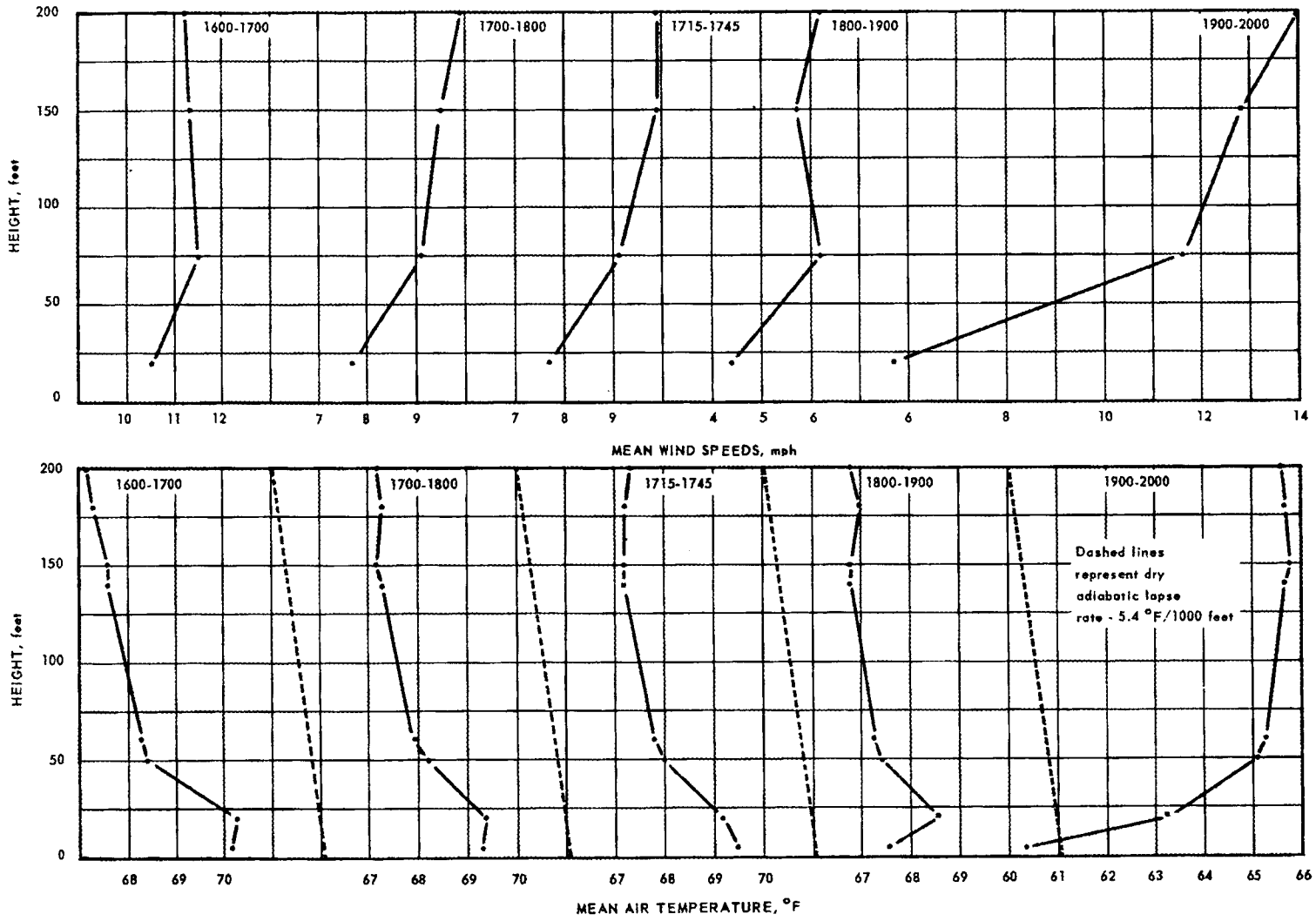

Fig. 61 – Profiles of mean wind speeds and air temperature for selected time periods from IET weather tower

DECLASSIFIED
DECLASSIFIED

DECLASSIFIED

The values compare favorably with those given by Sutton and others for similar conditions with somewhat greater values for the strong lapse and large inversion cases. The general relationship between the wind profile and stability can be noted as well as a rapid change in the turbulence parameter as the temperature gradient changed from strong lapse to large inversion in the 4-hour period. Such changes emphasize the atmosphere's everchanging capability to disperse contaminants and is of particular significance when it is recalled that the diffusion formulae are particularly sensitive to change in n since it appears as an exponent.

The diffusion coefficients C_x, C_y, C_z were originally given by Sutton for selected wind speed and stability conditions based on the relationship

$$C_y^2 = \frac{4\nu^n}{(1-n)(2-n)(\overline{u})^n}\left[\frac{\overline{(v')^2}}{\overline{u}^2}\right]^{1-n}$$

where

ν = kinematic viscosity of air, $\left(\frac{g}{m \times sec \times density}\right)$

n = turbulence parameter, dimensionless

$\overline{u}^2$ = mean wind speed squared, $(m/sec)^2$

$\overline{(v')^2}$ = mean squared values of the turbulent wind speed fluctuations, $(m/sec)^2$

C_x, C_y, C_z = diffusion coefficients, $meters^{n/2}$

Similar relationships for C_x and C_z are available by substituting $\overline{(u')^2}$ or $\overline{(w')^2}$ respectively for $\overline{(v')^2}$. Holland* developed a modified relationship based on theoretical work by Frenkiel,† reasoning that for isotropic turbulence

$$\frac{\overline{(w')^2}}{\overline{u}^2} = \frac{\overline{(v')^2}}{\overline{u}^2} \cong \sigma^2_{\tan\theta}$$

where θ is the instantaneous angular deviation of the horizontal wind direction from the mean wind and σ is the standard deviation. He further reasoned that for small angles ($\theta < 20^o$),

$$\sigma_{\tan\theta} \cong \tan\sigma_\theta$$

Therefore, an approximation for the equation for C_y given above is

$$C_y^2 \cong \frac{4\nu^n}{(1-n)(2-n)\,\overline{u}^n}\,(\tan\sigma_\theta)^{2(1-n)}$$

Using this equation, C_y was evaluated using the 200-foot-level wind data for a 30-minute period representative of the time the effluent was over the sampling network. Tan σ_θ and the other parameters (n, ν) were calculated from observed data taken at comparable time. The calculation was also made for a 5-minute period centered at release time.

*Meteorology and Atomic Energy, USWB for AEC, AECU 3066, July 1955.
J. F. Holland, "A Meteorological Survey of the Oak Ridge Area," AEC, Report ORO-99, 1953.

†F. N. Freinkel, "Frequency Distributions of Velocities in Turbulent Flow," *Journal of Meteorology*, 8, 316–320.

DECLASSIFIED

TABLE 7

TURBULENCE PARAMETER n AND TEMPERATURE DIFFERENCES FOR SELECTED TIME PERIODS

Time Period	n	$T_{200} - T_s$
1600 - 1700	0.09	- 3.0
1715 - 1745[a]	0.20	- 2.2
1700 - 1800	0.20	- 2.1
1800 - 1900	0.25	- 0.8
1900 - 2000	0.56	+ 5.2

[a]Estimated time cloud was over sampling network.

TABLE 8

ESTIMATES OF HORIZONTAL AND VERTICAL DIFFUSION COEFFICIENTS

Evaluation Period	n	$\overline{u}$	ν	C_y	C_z	C_z/C_y
30 minutes	0.20	4.5 m/sec	1.68×10^{-5}	0.176	0.174	0.989
5 minutes	0.20	4 m/sec	1.68×10^{-5}	0.131	0.130	0.989

DECLASSIFIED

In order to obtain an estimate of C_z, vertical wind-direction fluctuations must be known to evaluate $\overline{(w')^2}/\overline{u}^2$ in the above equation. Data from the bidirectional wind vane mounted at the 200-foot level of the weather tower have been utilized indirectly for this purpose. The instrument and recording system malfunctioned shortly before test time, and the data prior to failure are not completely consistent. However, a ratio of the mean value of the elevation angle fluctuation to the mean value of horizontal angle fluctuation for the period 1623 to 1653 is extractable and appears reasonable. Assuming that this ratio is approximately equal to the ratio C_z/C_y, and that similar conditions existed at test time, the value of C_z may be obtained. These assumptions are reasonable when it is considered that the vertical and horizontal components of the instantaneous wind velocity are relatable by the angular deviations and that the values are averaged over a 30-minute period. Further, the period 1623 to 1653 is reasonably similar to the test period since both were dominated by strong lapse conditions (see profiles presented in Figure 61). The estimates are presented in Table 8.

The value of near unity for the diffusion coefficient ratio C_z/C_y is what would be expected at levels near 200 feet for this type of meteorological condition (strong lapse) and indicates that an assumption of isotropic turbulence is for most practical purposes valid for strong lapse. It is also of interest to note that the 30-minute estimate of C_y (0.176) is somewhat less than would be selected from the values suggested by Barad and Hilst* (0.223) on the extension of Sutton's values. This may in part, at least, be attributable to the assumptions made in calculating C_y and to the fact that about 18 percent of the direction fluctuations (θ) were greater than 20 degrees over the 30-minute period averaged. This latter fact would question the advisability of using the relationship $\sigma_{\tan\theta} \simeq \tan \sigma_\theta$. The method, however, does give a reasonable estimate of the value of C_y which existed during the experiment and substantiates generally the suggested Sutton value of the parameter for this type of meteorological condition. It is considered that estimates of C_y and C_z over the 5-minute sampling period are not representative because of the short time period but are presented to illustrate the importance of the selection of the time interval for determination of parameters.

FIELD SAMPLING DATA

Fallout Plates

The flat fallout plate data are presented in Figures 62 through 69. The activities were all extrapolated from decay curves to time 5 hours after the melt (2215, 5/2/58). All plate activities were counted in a counter containing four G-M tubes in parallel and connected to a common scaler. Each G-M tube end window was covered with a 30-milligram-per-square-centimeter filter. The counter was calibrated with a Co^{60} source. Activities indicated in this report have already been corrected for indicated background activity.

It is rather obvious that an ideal sampling arrangement to ascertain complete fallout isopleths over an area as large as the one used in this experiment is very difficult to accomplish because of manpower limitations. In order to estimate fallout isopleths over the length of the arc, it was necessary to make assumptions and extrapolations beyond those which can be assumed to be truly justified. Speculations are often instructive; therefore, extreme extrapolations and assumptions were made concerning the distribution of fallout activities between points where data actually were taken.

*M. L. Barad and C. R. Hilst, HW-21415 and Supplement, Nucleonics Department, Hanford Works, General Electric Department, Richland, Washington, 1951.

DECLASSIFIED

DECLASSIFIED

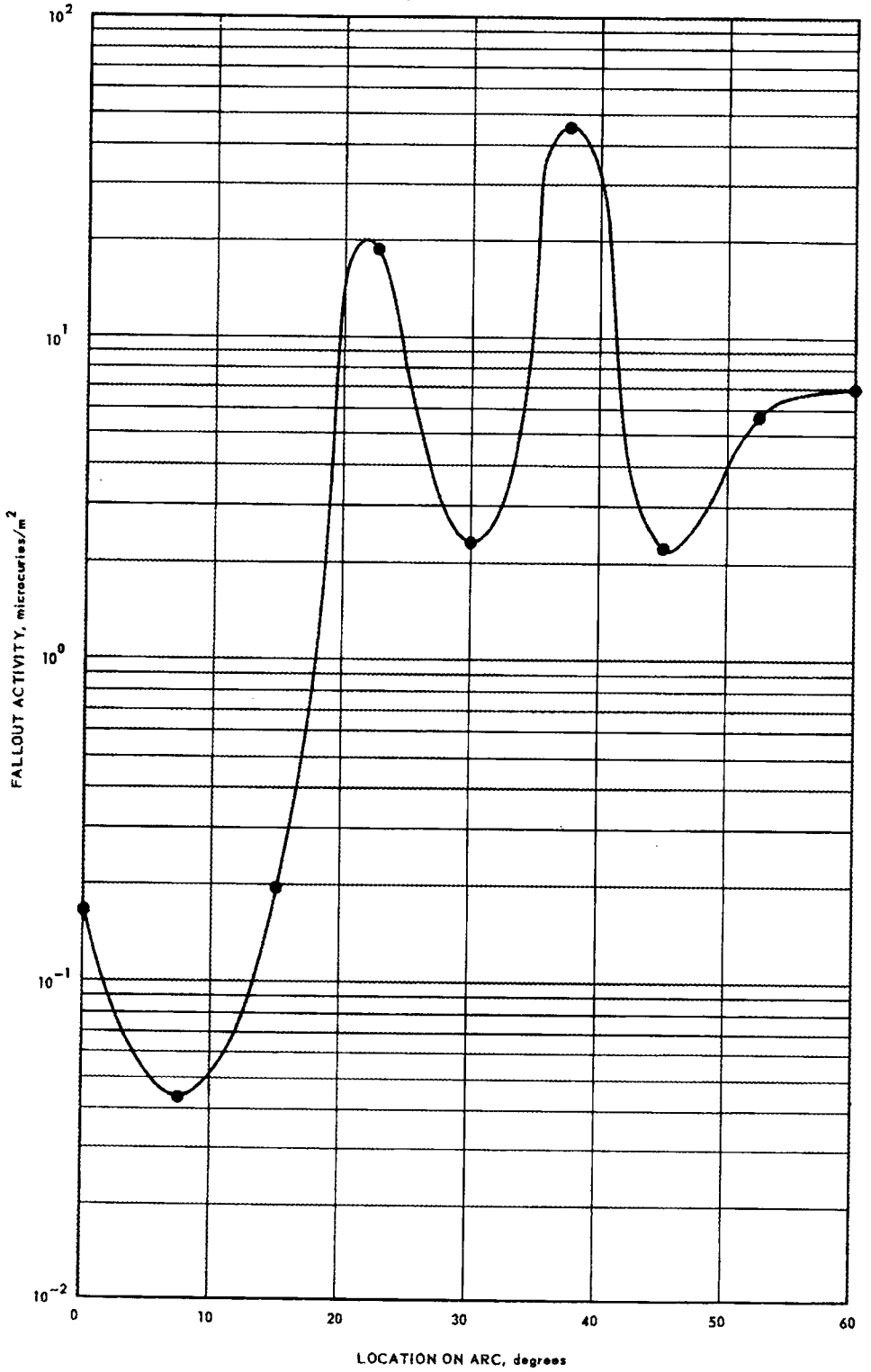

Fig. 62 – Fallout plate activity per square meter, 100 feet from stack (5 hours after melt)

DECLASSIFIED

DECLASSIFIED

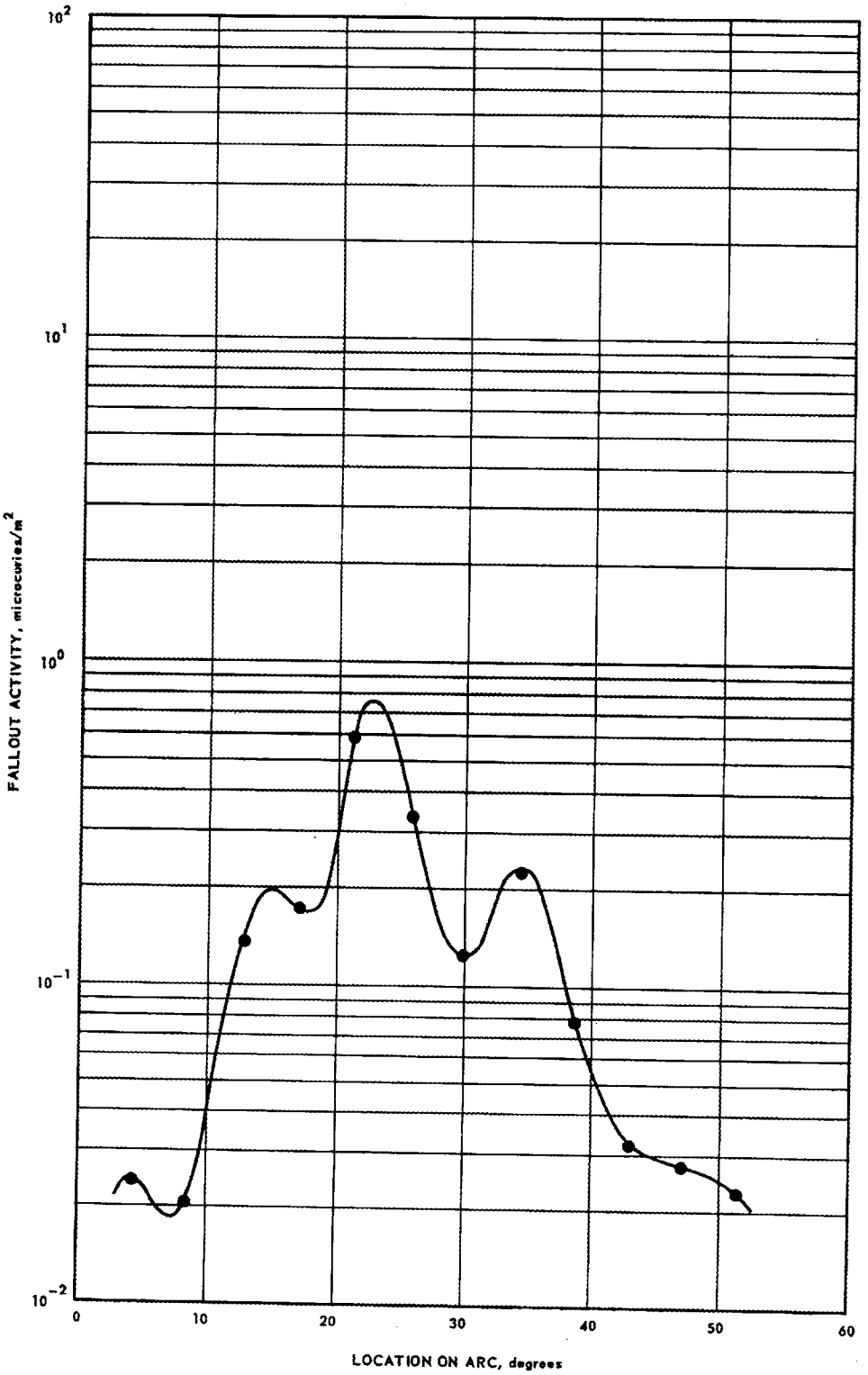

Fig. 63 – Fallout plate activity per square meter, 1500 feet from stack (5 hours after melt)

DECLASSIFIED

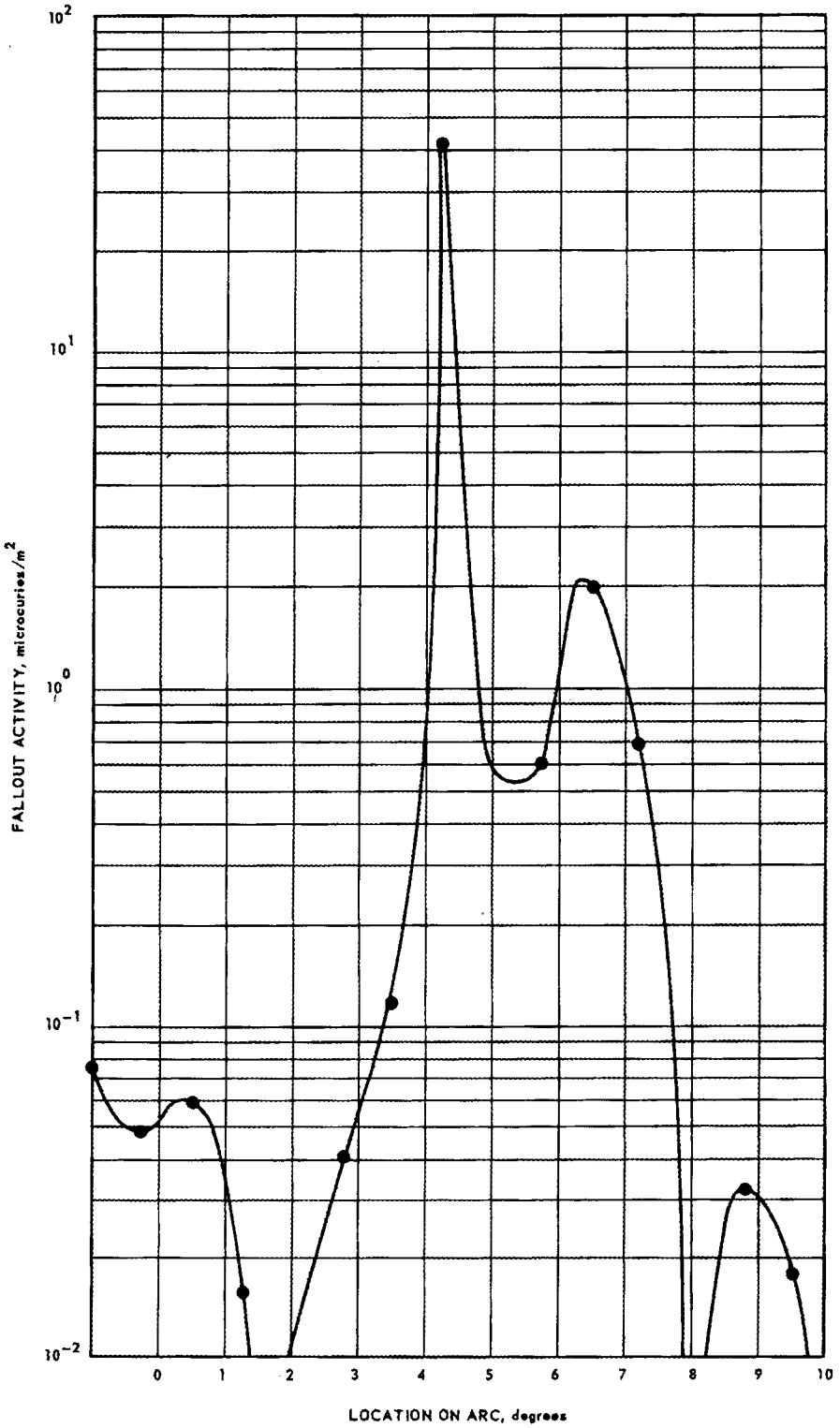

Fig. 64 – Fallout plate activity per square meter, 2000 feet from stack (5 hours after melt)

DECLASSIFIED

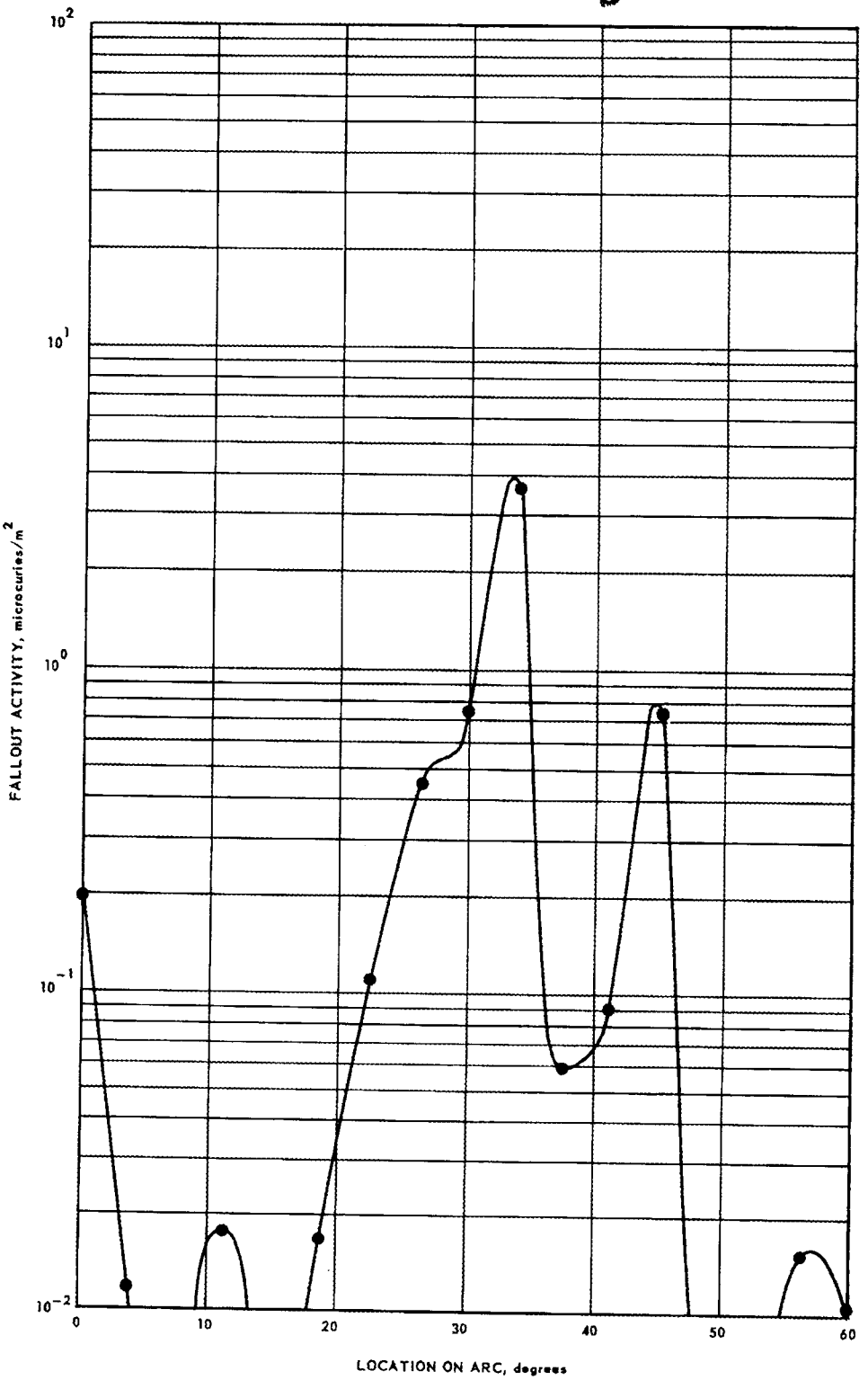

Fig. 65 – Fallout plate activity per square meter, 3000 feet from stack (5 hours after melt)

DECLASSIFIED

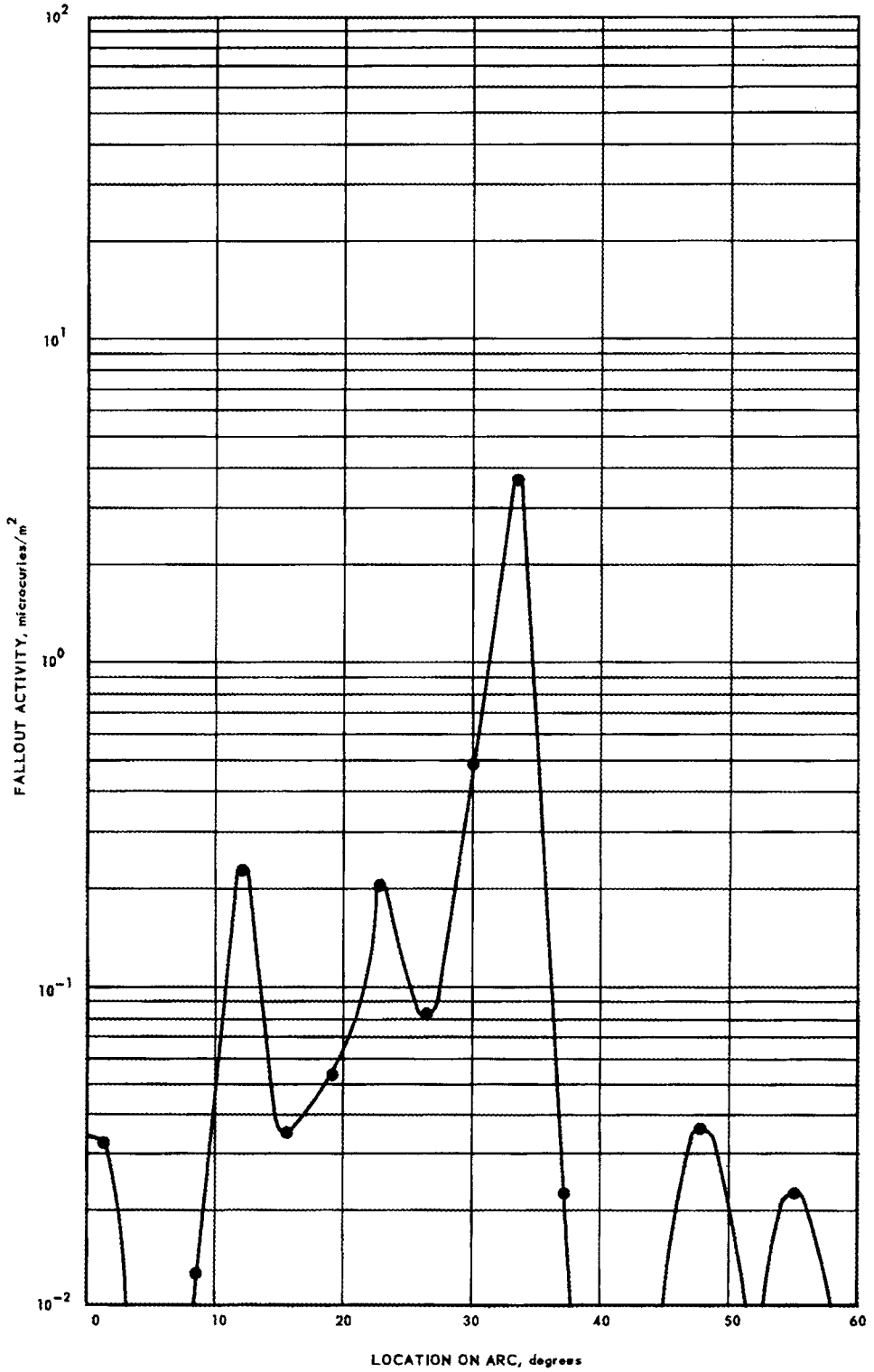

Fig. 66 – Fallout plate activity per square meter, 4000 feet from stack (5 hours after melt)

DECLASSIFIED

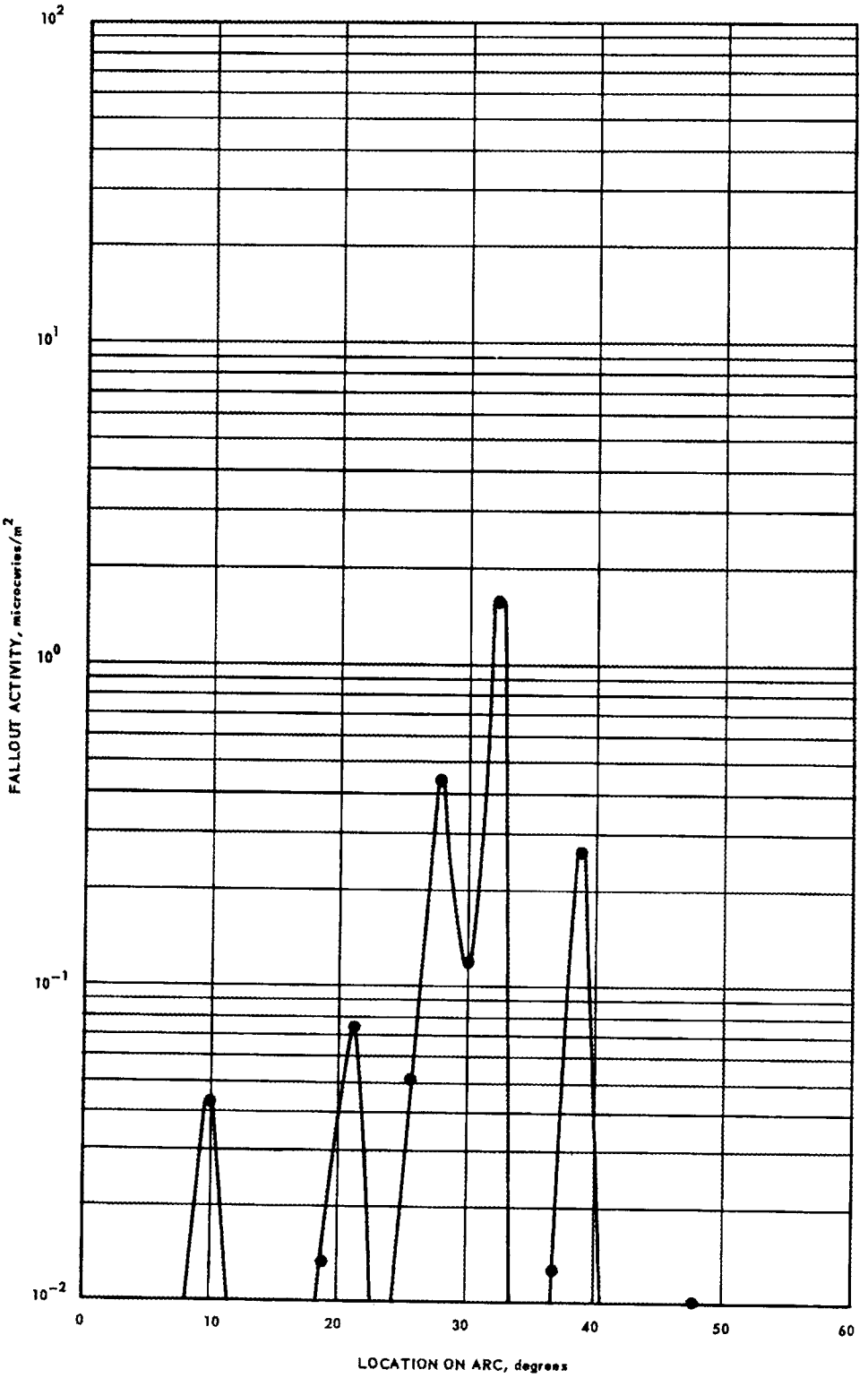

Fig. 67 – Fallout plate activity per square meter, 8250 feet from stack (5 hours after melt)

DECLASSIFIED

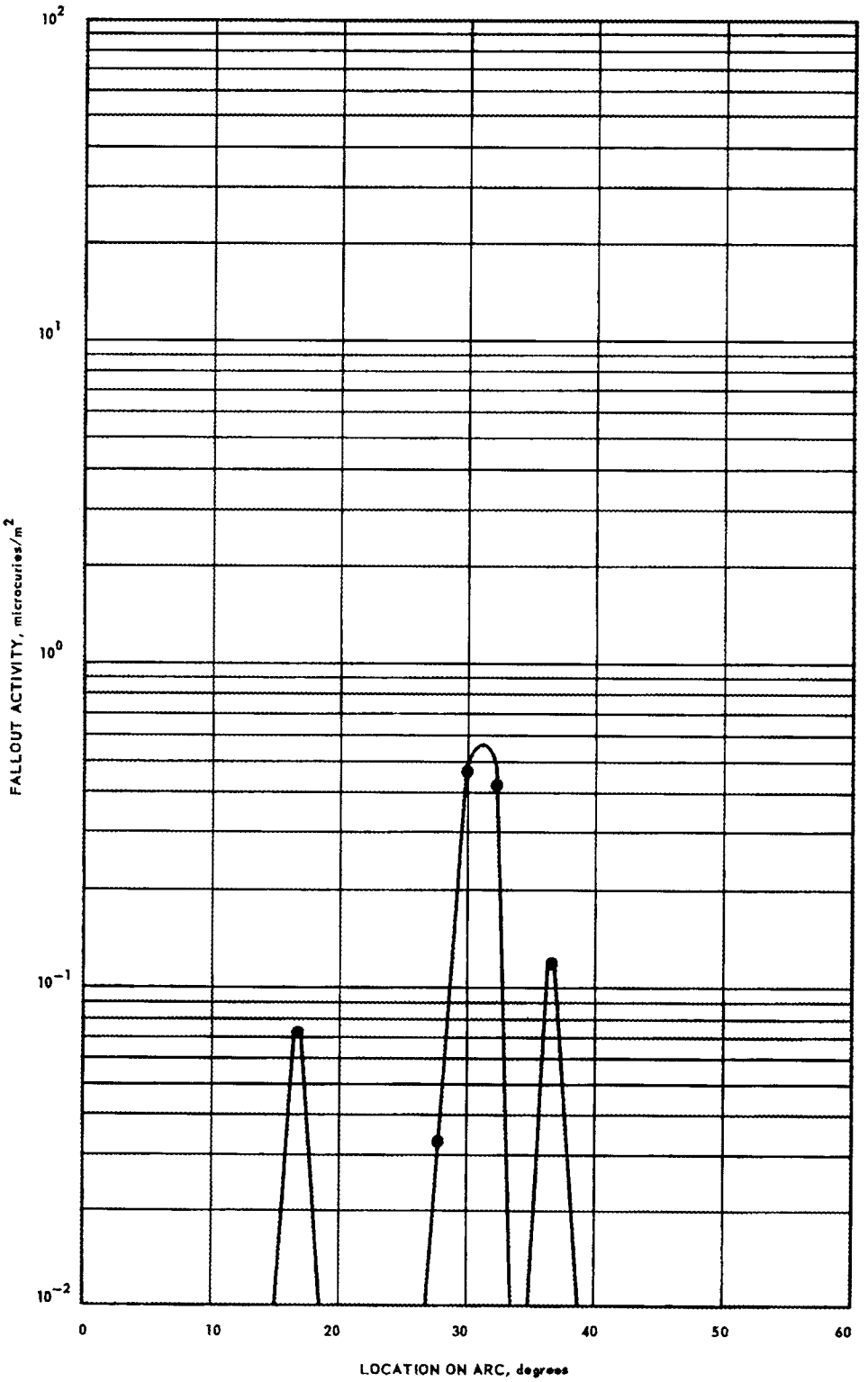

Fig. 68 – Fallout plate activity per square meter, 13,000 feet from stack (5 hours after melt)

DECLASSIFIED

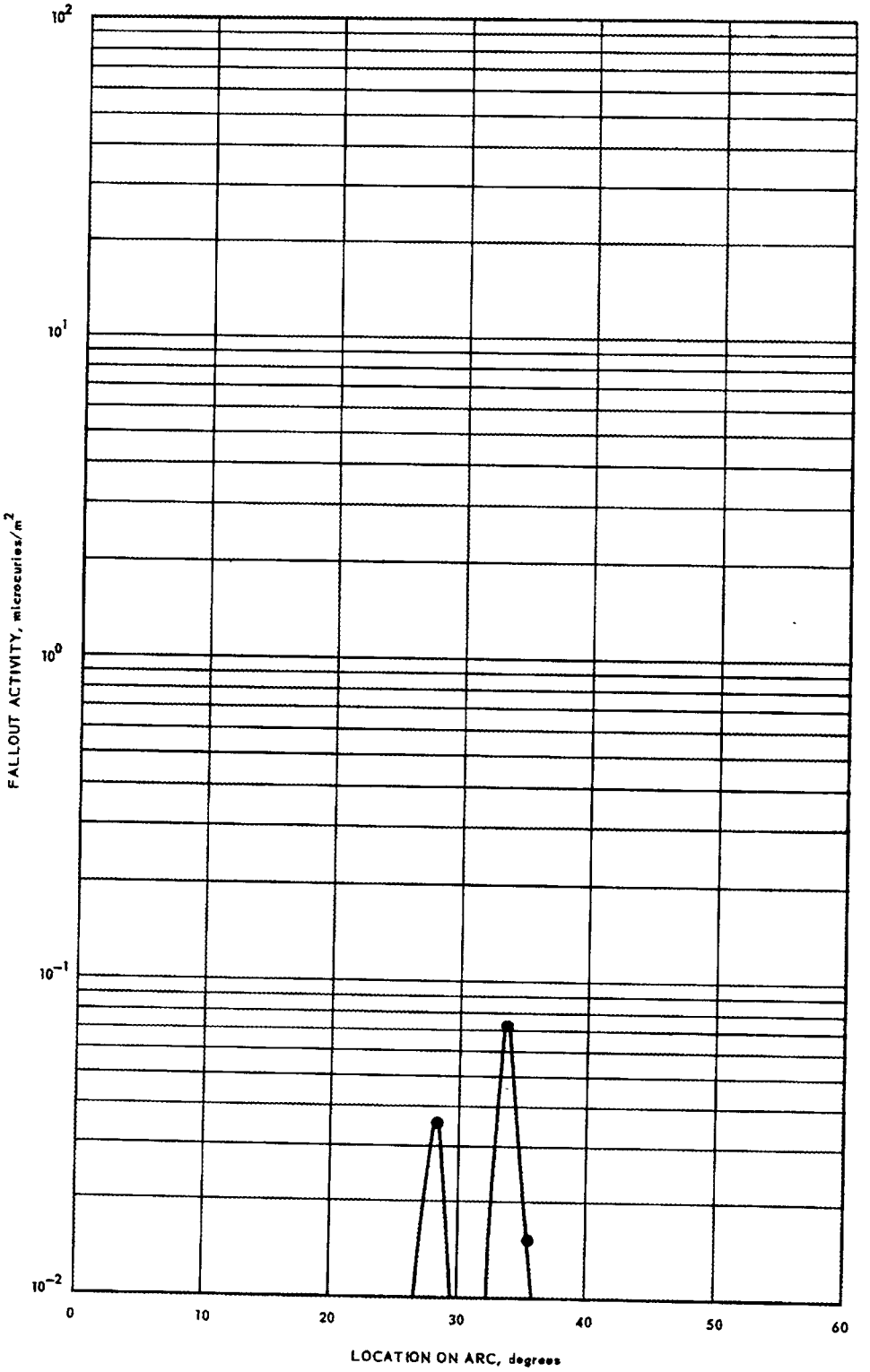

Fig. 69 – Fallout plate activity per square meter, 20,000 feet from stack (5 hours after melt)

DECLASSIFIED

DECLASSIFIED

Assuming the activities measured on the fallout plates were truly representative of the fallout activity in the region of the plates, a "reasonable" line was drawn to determine the distribution along a given radial sampling arc (these are the dashed curves connecting the measured activities in Figures 61 through 68). Points of equal activity deposition were located on the arcs from these distributions, and a rational location of isopleths was determined between sampling arcs. This extrapolation is not excessive out to 4000 feet because the sampling arcs were rather close together. Between 4000 feet and 20,000 feet the distances between arcs were quite large, but the same method of extrapolation was used. The results of these speculations are shown in Figure 70, which is a possible fallout isopleth pattern for the entire sampling network. It is not inconsistent with what one might expect for the meteorological conditions existing at the time of the release.

Radiographs were made from the plates containing sufficient activity. These showed that, by far, most of the activity was associated with sizable particulate material. The most active particle found on the fallout plates was approximately 30 microns in diameter and located on the 2000-foot sampling arc.

The major contribution to the gamma activity found on fallout plates was found spectrographically to be from I^{133}, Te^{132} - I^{132}, I^{131}, Mo^{99} - Tc^{99}, and Xe^{133}. The spectra were quite different from those from the cascade impactor sampling in the 76-inch duct loop, but no particular differences were noted between spectra from fallout plates located at various distances from the release point.

No significant differences could be found in the decay curves made from fallout plates.

Data from vertical cylindrical fallout plates on the 8250-foot arc show no definite correlation with horizontal flat fallout plates at the same locations. Data from cylindrical fallout plates located at various heights on the towers failed to indicate any significant vertical patterns. Very little significant fallout activity was found beyond the 4000-foot arc on any of the fallout plates.

High-Volume Air Samples (HVA)

The high-volume air sample data are presented in Figures 71 through 75. Extrapolations of these data were made similar to those made for fallout plates to indicate activity five hours after the melt. These samples were counted in G-M counters. Two counters with 3-milligram end window filters were used and were calibrated with a Ra D, E source.

Failure of a generator located near the center of the 4000-foot arc resulted in a loss of extremely valuable data from the several sampling devices which depended upon the generator for power. Supporting data indicate that these samplers were located very near the area of maximum air concentration for the cloud at ground level. From the supporting instruments extrapolations were made over the section of the arc covered by the inoperative HVA samplers.

Extrapolations of high-volume data in a manner similar to those made for fallout data produced the isopleths shown in Figure 76. Although the validity of the resultant isopleths may be questioned, the isopleths are at least interesting and possible for the particular meteorological conditions at the time of release. Statistically, the HVA data should be more representative of the area condition than fallout plates because most fallout activity is due to very few larger particulates containing considerable activity whereas the HVA filters collect smaller particulates rather uniformly distributed over the surface of the filter.

Radiochemical separation and spectral analyses of the filter papers indicated that the major contribution to the gamma activity was due to I^{131}, I^{133}, and I^{135} with possibly

DECLASSIFIED

DECLASSIFIED

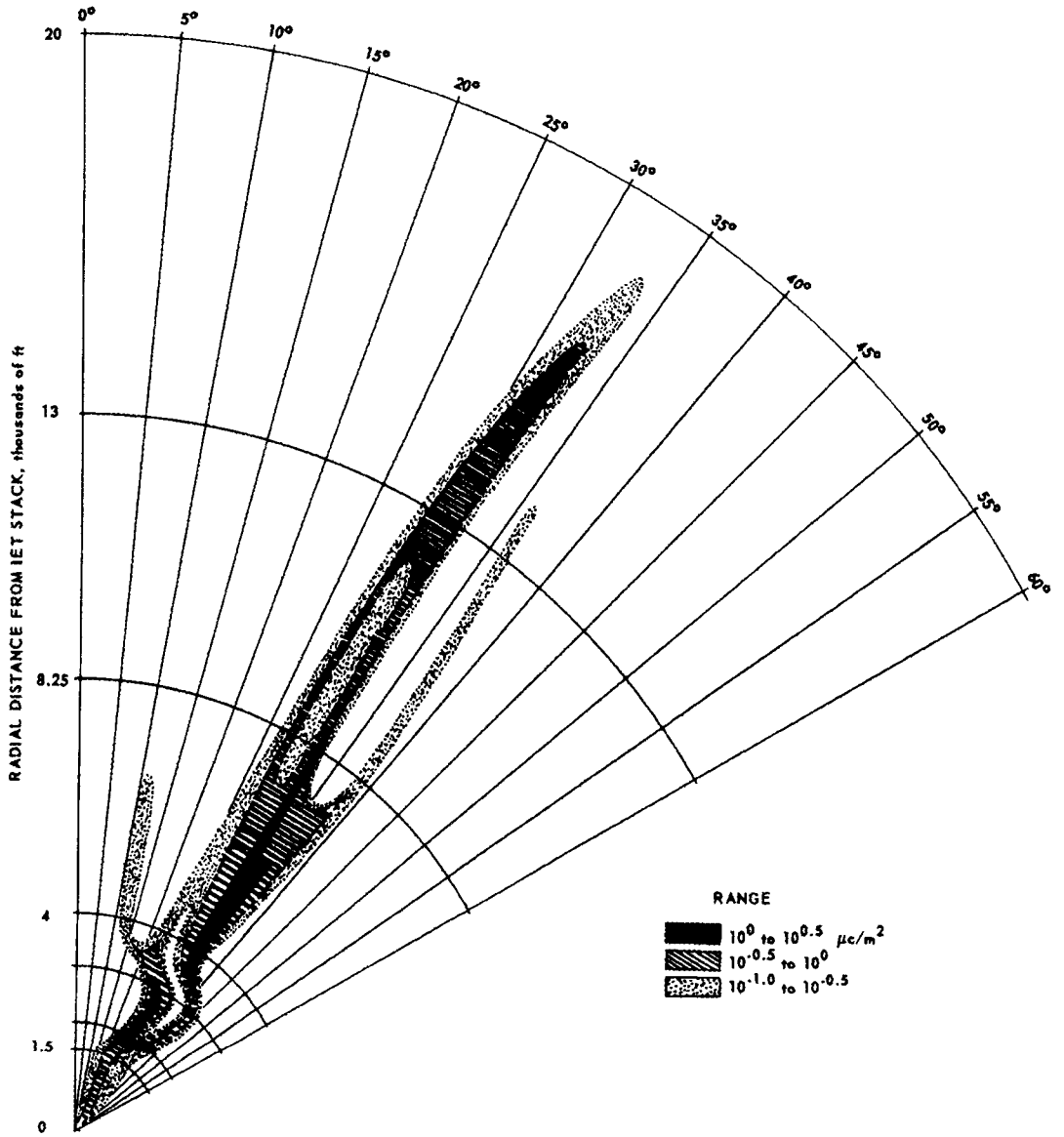

Fig. 70 – Estimated fallout activity isopleth pattern (normalized to 5 hours after melt)

DECLASSIFIED

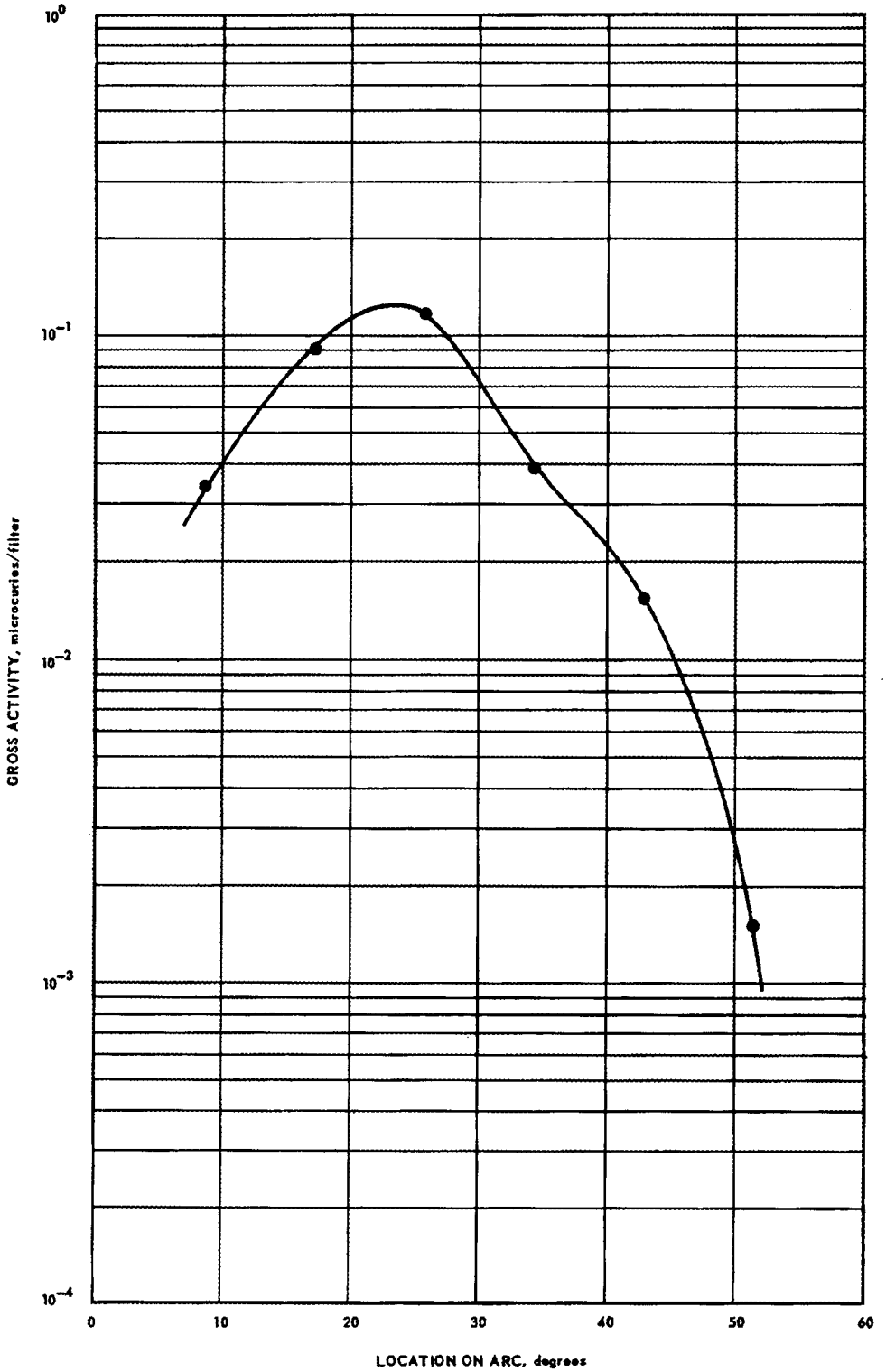

Fig. 71 – Gross activity per 35 cfm in HVA sampler, 1500 feet from stack (5 hours after melt)

DECLASSIFIED

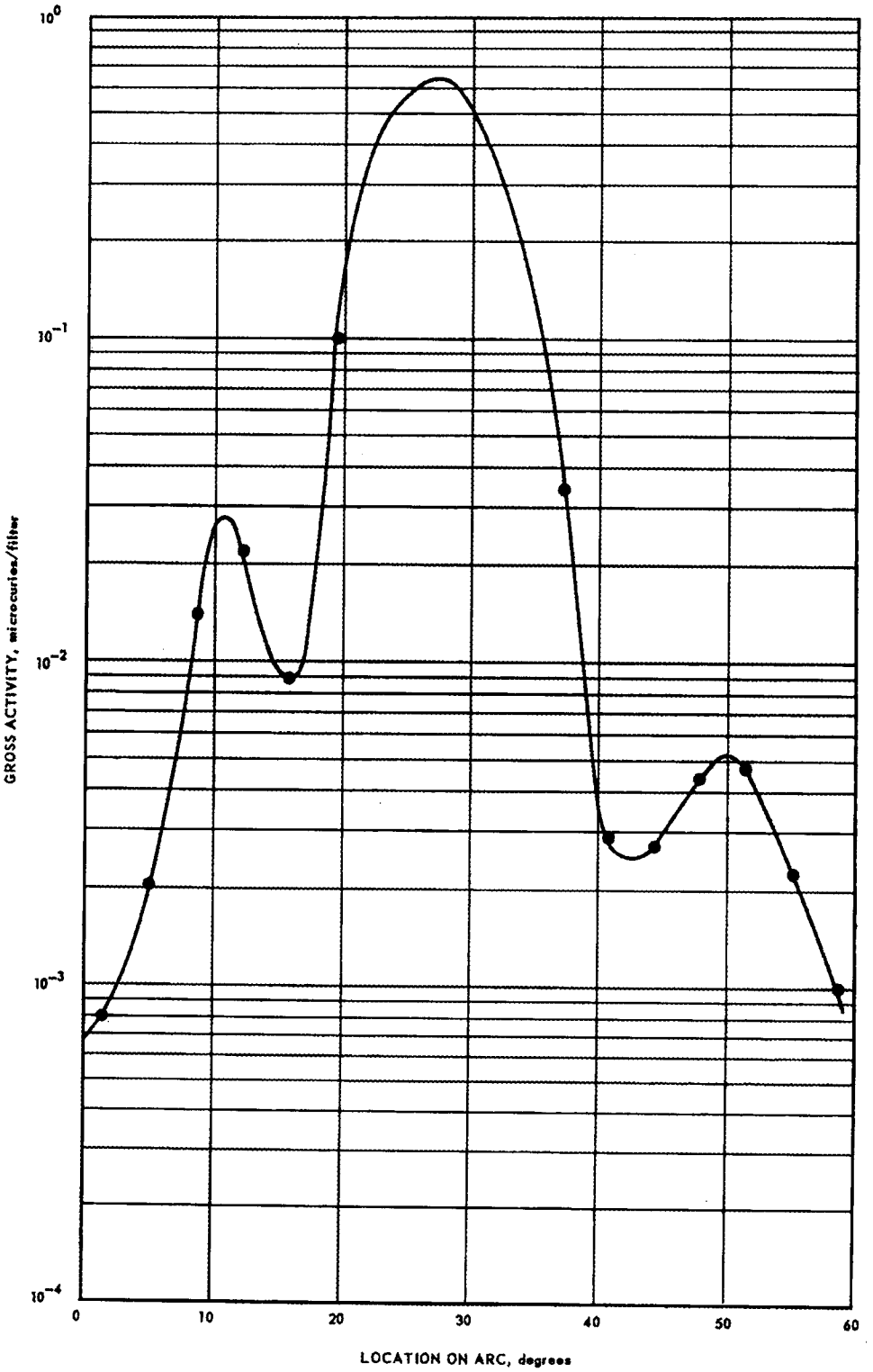

Fig. 72 – Activity per 35 cfm in HVA sampler, 4000 feet from stack (5 hours after melt)

DECLASSIFIED

DECLASSIFIED

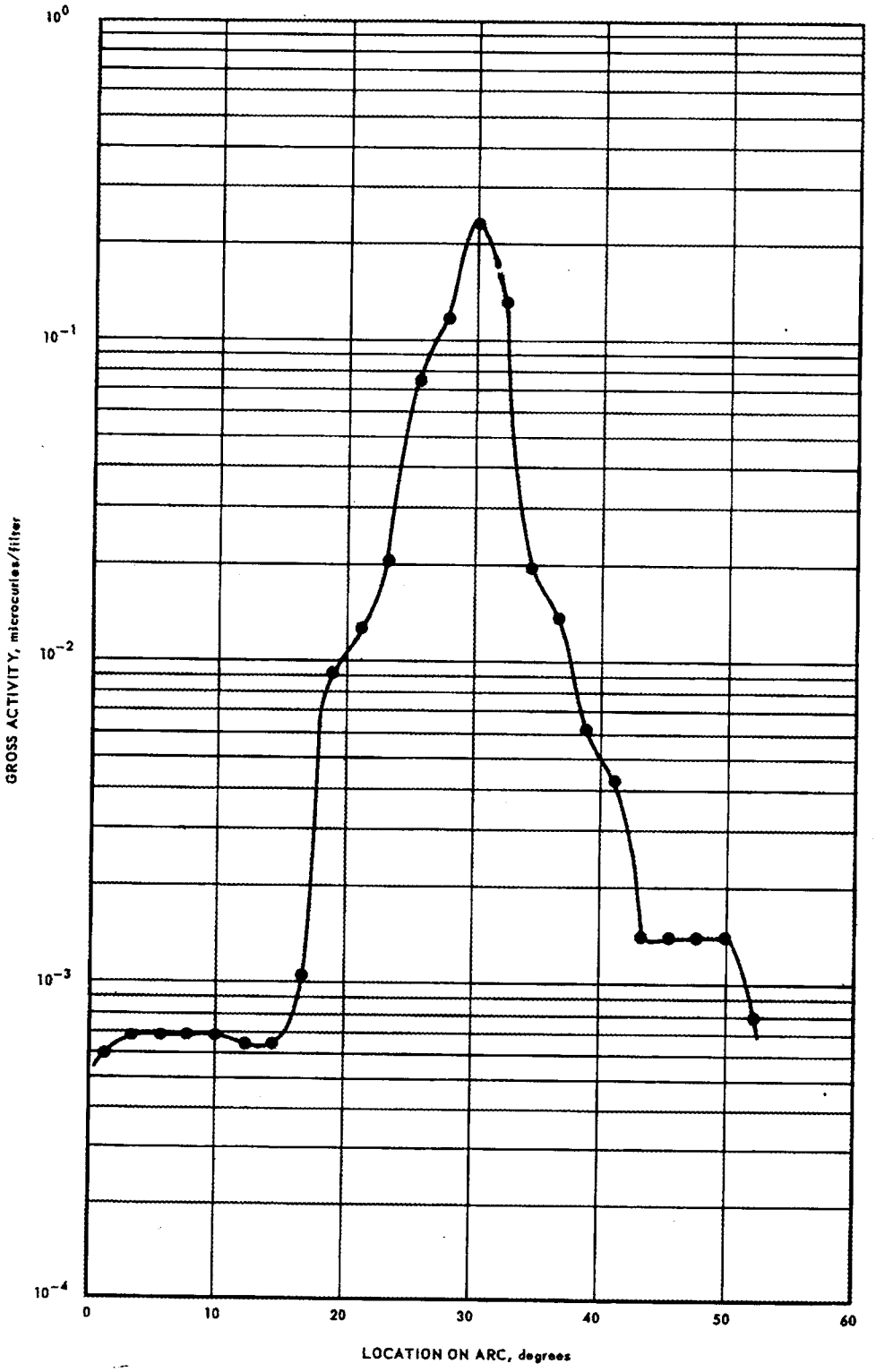

Fig. 73 – Activity per 35 cfm in HVA sampler, 8250 feet from stack (5 hours after melt)

DECLASSIFIED

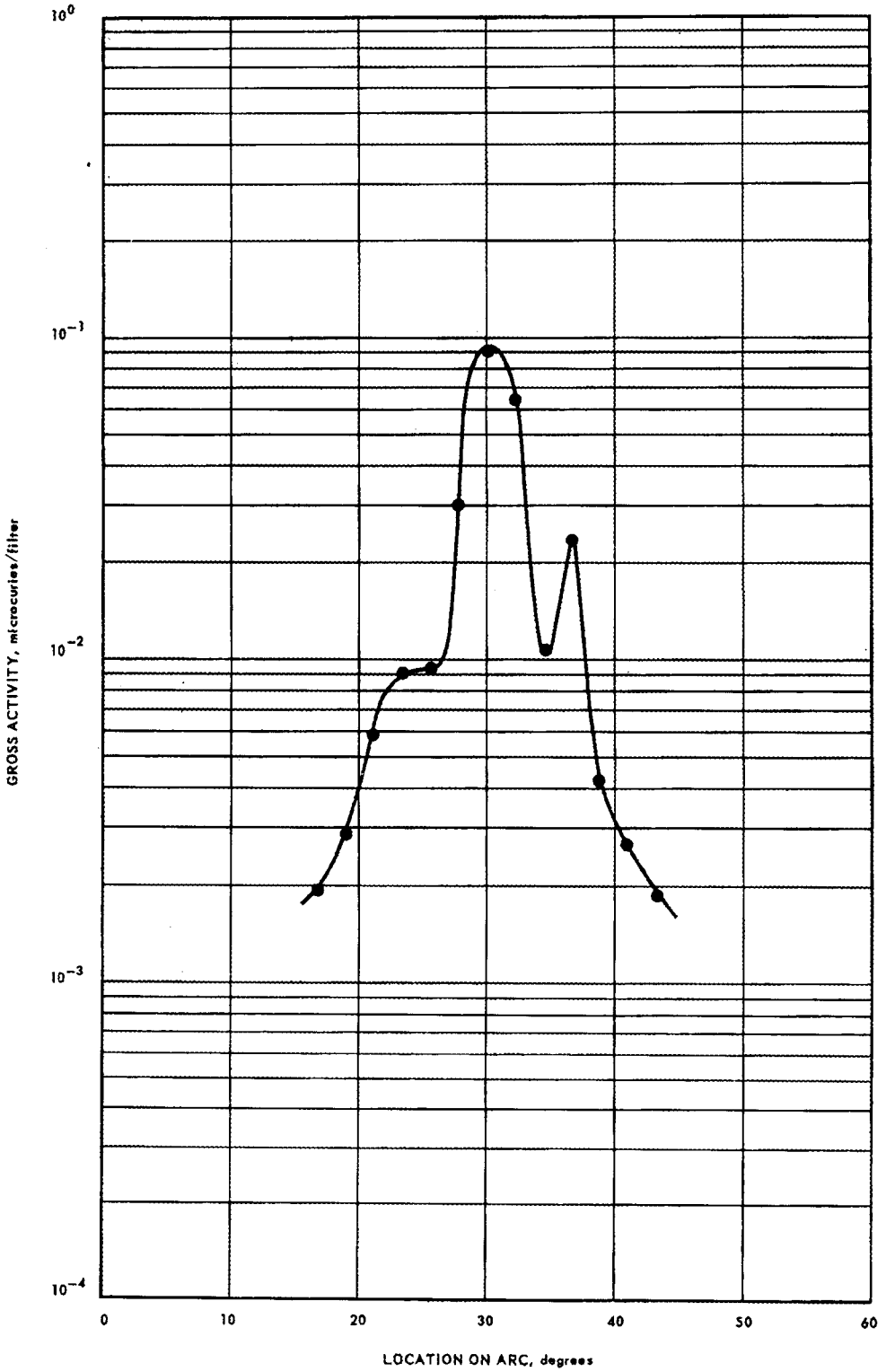

Fig. 74 – Activity per 35 cfm in HVA sampler, 13,000 feet from stack (5 hours after melt)

DECLASSIFIED

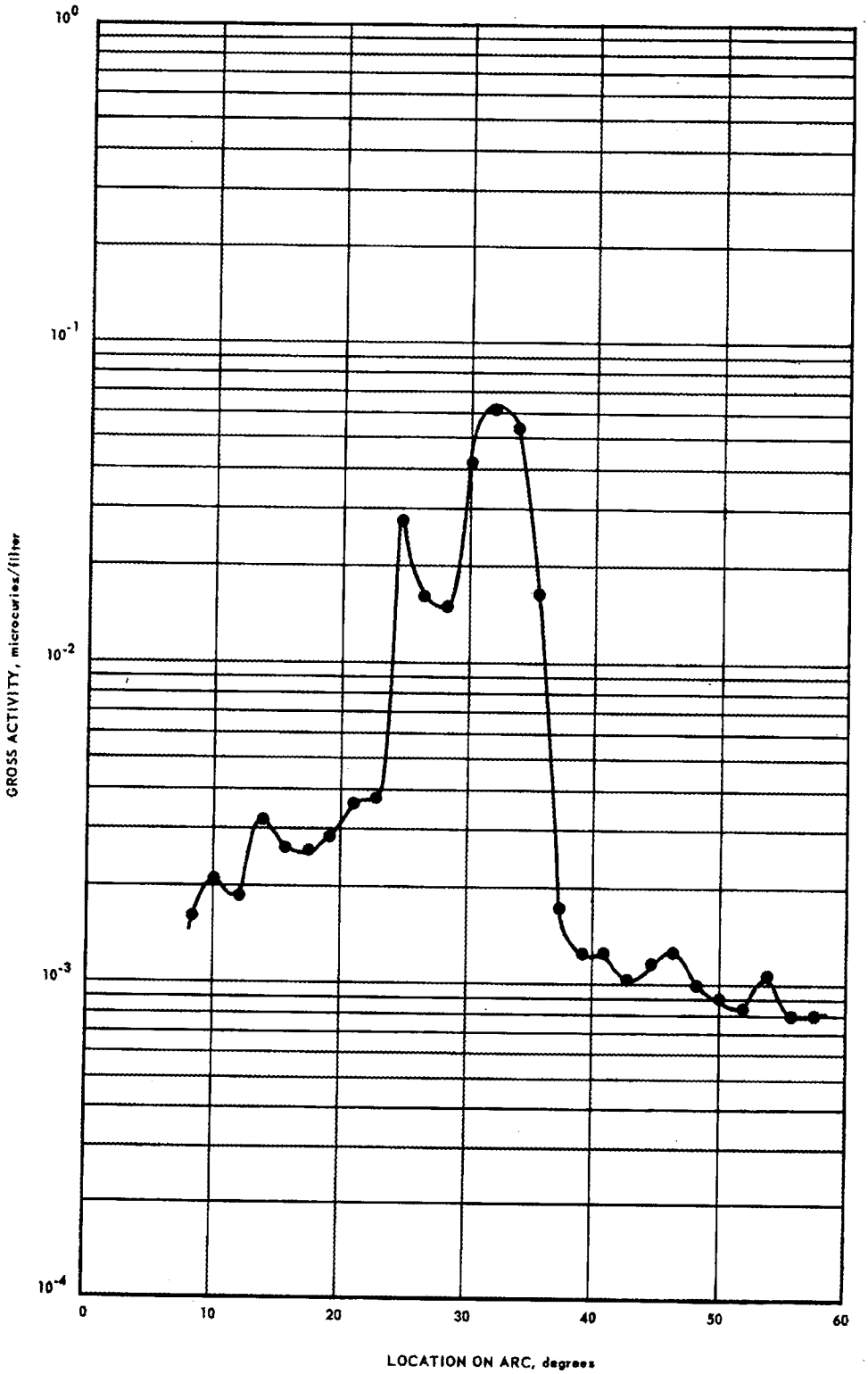

Fig. 75 – Activity per 35 cfm in HVA sampler, 20,000 feet from stack (5 hours after melt)

UNCLASSIFIED

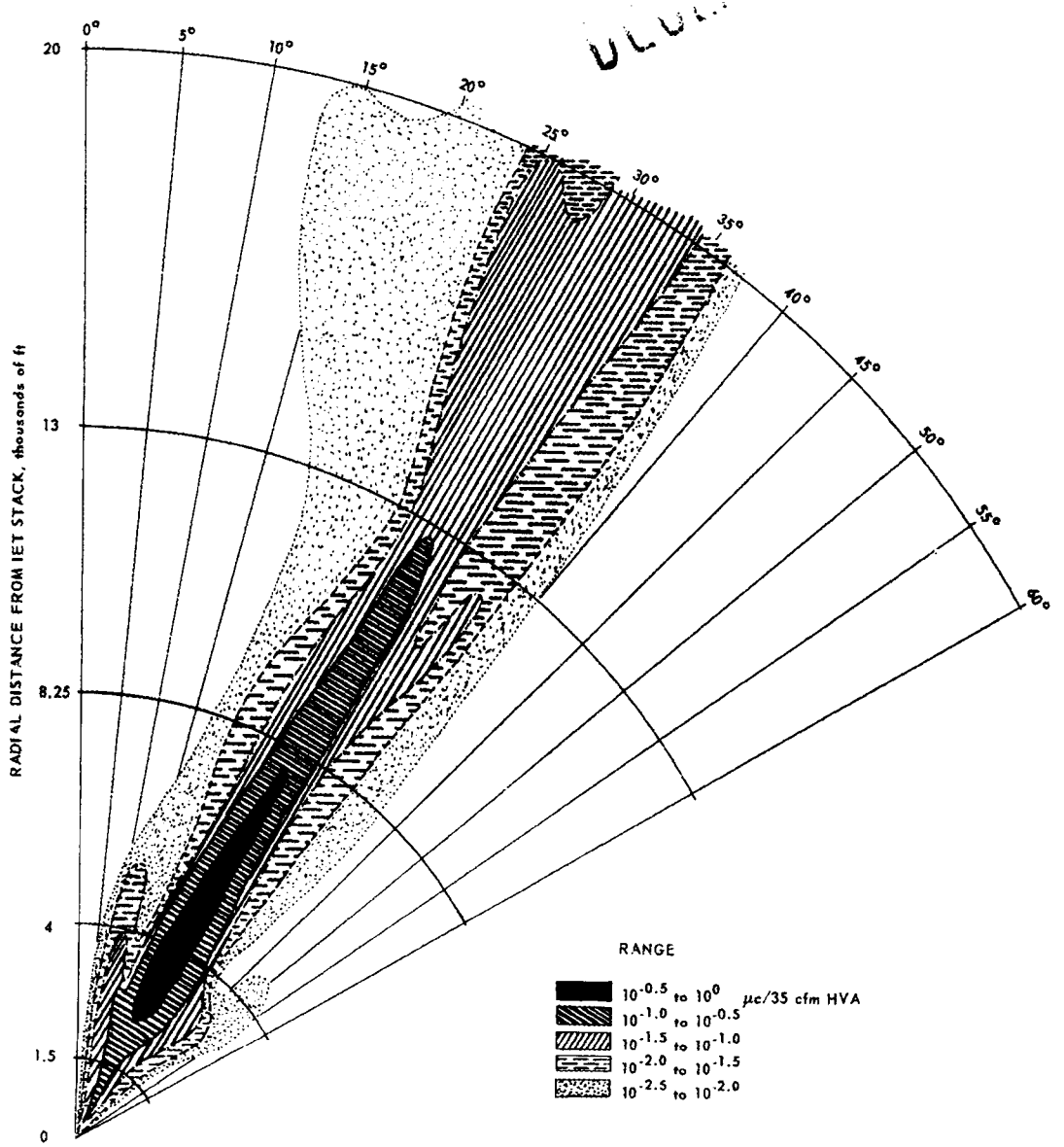

Fig. 76 – Estimated integrated airborne activity isopleth pattern (normalized to 5 hours after melt)

UNCLASSIFIED

some Mo^{99} - Tc^{99}. No significant differences were noted between spectra of samples taken at various distances from the stack, nor were any significant differences noted from decay curves.

Three HVA samples were analyzed spectrally and radiochemically for specific iodine isotopes in order to compare I^{131} field data with source data. One sample was taken from each arc at 1,500 feet, 8,250 feet, and 20,000 feet from the stack. The amount of I^{131} was determined in each case, and the ratio of I^{131} activity to gross activity was determined to be

Arc	I^{131}/gross activity
1,500 ft	0.073
8,250 ft	0.037
20,000 ft	0.056

This is a fairly large spread in these ratios; there are not sufficient samples to permit meaningful statistical treatments, but it does permit an estimate for the deposition pattern of I^{131} over the network. The conversion factor of 0.06 was assumed so that comparisons could be made between theoretical and measured deposition patterns. These will be discussed in a later portion of this document.

Vegetation Samples

Vegetation samples were collected before and after the test and counted for gross gamma activity. The activities associated with the two groups were so nearly alike that no conclusive differences could be found. By counting large samples of sagebrush for very long periods in the spectrograph, gamma spectra from the two groups were obtained. The sagebrush sample collected after the test showed the presence of some short-lived isotopes - the major portion of the activity due to Zr^{95}-Nb^{95}, Ru^{103}-Rh^{103}, and Ba^{140}-La^{140}. Seven days later the samples showed essentially the same spectrum as the background samples. These spectra are compared with a sagebrush sample from an area many miles from the site of the experiment for comparison in Figure 77. The background activity could be due to fallout from Russian bomb tests conducted just prior to this experiment.

Carbon Traps

Only two of the carbon traps in the field had sufficient activity for I^{131} analysis. The results of the carbon trap analyses were a factor of about 700 higher than the high-volume air sampler results at similar locations. While one might expect the charcoal traps to have a greater efficiency for iodine collection, a factor of 700 seems ridiculously high. There does not appear to be any valid reason for these observed differences, but comparison of this kind will be sought during future releases.

Pocket Ionization Chambers and Film Badges

The significant data from analyses of pocket ion chamber discharges and film badge exposures are shown in Figure 78. Only those badges and chambers on the 100-foot arc yielded data of any significance. The peaking observed is much sharper than could be expected for readings due only to gamma radiation from an airborne cloud. The readings must be due almost entirely to fallout material on the meters or in the nearby vicinity.

Inoperative Instrumentation

At the time of release some of the instrumentation in the sampling network was not operative. The field Jordan chambers had failed due to electrical difficulties, several air-sampling devices in the middle of the 4000-foot arc were inoperative because one

DECLASSIFIED

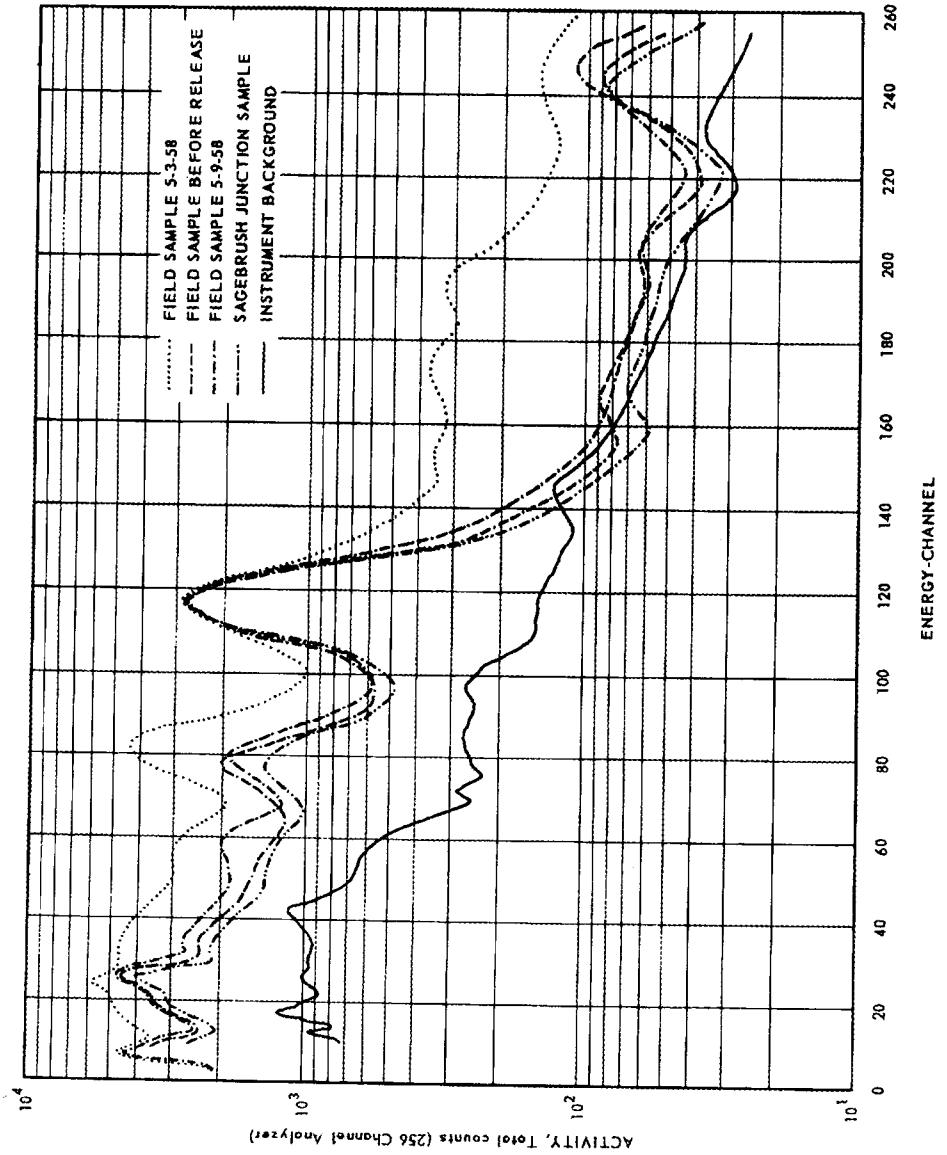

Fig. 77 – Comparison of sagebrush (vegetation) spectra

DECLASSIFIED

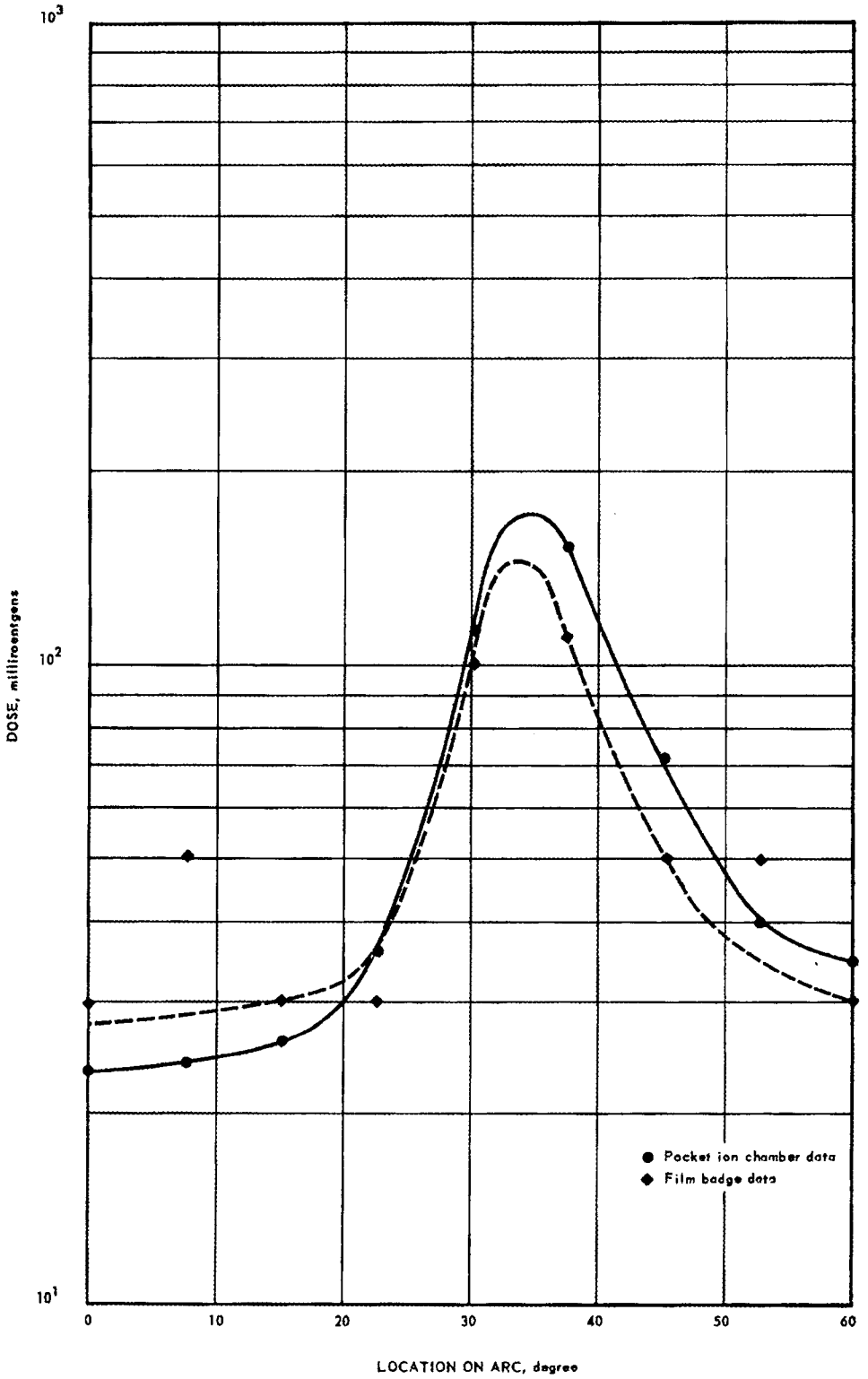

Fig. 78 – Total integrated doses along sampling arc, 100 feet from stack

DECLASSIFIED

mobile generator failed, and the tethered blimps on the 8250-foot arc were not ready in time to sample the cloud.

Other Measurements

In addition to the measurements discussed in this report, two more important pieces of information should be available but have not been reported at the time of this writing.

The field sampling personnel from the Idaho Operations Office, AEC made surveys and took air, vegetation, and milk samples beyond the field sampling network. They also attempted to follow the cloud trajectory and monitor the ground using a light aircraft with radiation detection devices.

As shown on the plan of the sampling network, Figure 22, a number of animals (rats) were placed in the network 2000 and 3000 feet from the IET stack. According to post-experimental analysis of HVA data, the animals were located in a very favorable location with respect to high ground-level air concentrations. These animals were analyzed by personnel from the University of Rochester.

These data could be very useful in clearing up some of the discrepancies noted in measured release source and field data.

I^{131} RELEASE FRACTION ESTIMATE BY RESIDUE ANALYSIS

Chemical Separations

Samples of the residue were taken from the basket (Figure 49), the plug (Figure 47), and the stage 18 ring 11 (Figure 46) for chemical analyses in an attempt to determine the fractional release of I^{131} during the melt. Each sample was analyzed for uranium, Zr^{95}, and I^{131}. Chemical separations were made, and at least two determinations were made on each sample. Results of these analyses are given in Table 9.

Using the average power of the insert, theoretical values were calculated for both I^{131} d/m-μg U and Zr^{95} d/m-μg U. All experimental determinations for Zr^{95} were within (±) a factor of two of the theoretical value. The power distributions within the cartridge likewise vary (±) a factor of two. Since there is no way of telling where a specific sample of molten slag originated, the experimental findings appear to be in very good agreement with what might be expected theoretically.

Assuming that no zirconium was released from the residue, the theoretical I^{131} to Zr^{95} ratio was determined for the time of the iodine counting and this ratio was used in conjunction with the measured Zr^{95} concentrations to give the full I^{131} inventory that should have been present in the sample. The actual concentrations of I^{131} were subtracted from the full inventory values, and the difference was divided by the full inventory values to determine the fractional release value for I^{131}. These figures are given in Table 10, and the inventory of Zr^{95} and I^{131} based on average power is given in Figure 79.

The average fractional release from the basket, plug, and stage-18 samples are 0.672, 0.713, and 0.473, respectively. Since the basket and plug samples are in good agreement, it appears fair to estimate the fractional release as approximately 0.7 for material that has been melted sufficiently to lose its original form and is partially oxidized (as is the condition of the true slag) and the fractional release of 0.5 for the partial stages which are left apparently (visually) intact after other portions of the stage have been removed by thermal damage.

Stages 8 and 9 were not sampled or analyzed. These stages show degrees of blistering - stage 8 slightly, and stage 9 extensively. Fractional release of I^{131} was estimated to be 0.04 and 0.25 respectively for these two stages.

DECLASSIFIED

TABLE 9

RESULTS OF RESIDUE ANALYSIS OF I^{131} RELEASE FRACTION

Sample Location	Counting Time	I^{131} d/m-μgU[a]	Counting Time	Zr^{95} d/m-μgU[a]
Basket				
6-180	5-20-58	1.13×10^4	5-23-58	2.58×10^4
6-181	5-21-58	4.40×10^3	5-23-58	2.05×10^4
6-182	5-21-58	7.80×10^3	5-23-58	2.77×10^4
Plug				
6-183	6-10-58	1.00×10^3	6-11-58	1.68×10^4
6-184	6-10-58	6.24×10^2	6-11-58	1.83×10^4
6-185	6-10-58	3.80×10^2	6-11-58	1.51×10^4
6-186	6-10-58	2.04×10^3	6-11-58	1.91×10^4
Stage 18				
6-187	6-13-58	1.17×10^3	6-16-58	1.77×10^4
6-188	6-13-58	9.4×10^2	6-16-58	1.28×10^4
6-189	6-13-58	1.96×10^3	6-16-58	1.80×10^4

[a]Disintegrations per minute per microgram of uranium.

TABLE 10

DETERMINATION OF FRACTIONAL RELEASE VALUES FOR I^{131}

Sample No.	Time	Zr^{95} (measured)	I^{131} (theory)	I^{131} (measured)	Indicated Fractional Release
6-180	5-20-58	2.68×10^4	2.55×10^4	1.13×10^4	0.56
181	5-21-58	2.10×10^4	1.86×10^4	4.40×10^3	0.765
182	5-21-58	2.83×10^4	2.50×10^4	7.80×10^3	0.69
183	6-10-58	1.70×10^4	3.27×10^3	1.00×10^3	0.693
184	6-10-58	1.86×10^4	3.58×10^3	6.24×10^2	0.83
185	6-10-58	1.58×10^4	2.96×10^3	3.80×10^2	0.875
186	6-10-58	1.94×10^4	3.74×10^3	2.04×10^3	0.455
187	6-13-58	1.83×10^4	2.79×10^3	1.17×10^3	0.58
188	6-13-58	1.32×10^4	2.01×10^3	9.4×10^2	0.532
189	6-13-58	1.86×10^4	2.84×10^3	1.96×10^3	0.31

DECLASSIFIED

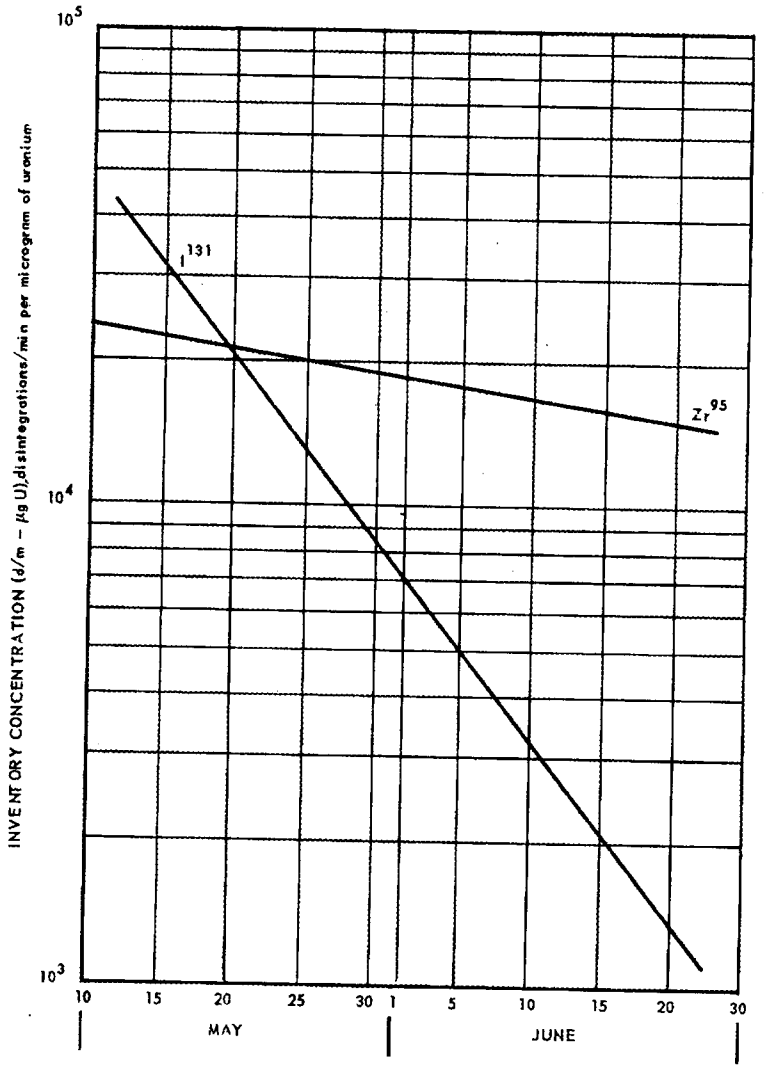

Fig. 79 – Theoretical inventory of I^{131} and Zr^{95} per microgram of uranium remaining at various times after melt

DECLASSIFIED

DECLASSIFIED

I^{131} Fractional Release Estimation

During disassembly of the cartridge, the slag and individual stages were removed and weighed. The results of this investigation are given in Table 11.

The original gross weight of the last nine stages was approximately 2000 grams. Since only about 1157 grams could be accounted for, about 843 grams (approximately four stages) could not be accounted for and are assumed to have passed along to or through the exhaust system.

If the estimated I^{131} values for fractional release determined by chemical separation are assigned to the specific amounts of cartridge affected, an estimate can be made for the fractional release of I^{131} from the entire cartridge inventory. The weightings are given in Table 12.

Dividing the product of fractional release and gross weight by the original gross weight of the cartridge yields the estimated fractional I^{131} release (F.R.) of the entire cartridge, Σ F.R. (I^{131}) $\doteq$ 0.3. This value disagrees with the measured release fractions by about a factor of 10. The assumptions made in the estimated fractional release shown above do not appear to be subjected to very gross errors if the samples are representative. The apparent difference between the two release values is not resolved.

CONTAMINATION OF FACILITIES

Just prior to the time the IET facility was used for conducting Operation BOOT, the facility was used for another test which also involved the release of fission products; therefore, there was some residual contamination of the ducting before Operation BOOT. A series of gamma radiation surveys were made in and about the IET facility between May 1 and 5, 1958. The fission product release in Operation BOOT took place at 1715, May 2, 1958. Table 13 lists the locations surveyed and the dose rates encountered at various times. These data might be of interest to personnel planning similar experiments.

DECLASSIFIED

DECLASSIFIED

TABLE 11

WEIGHT ANALYSIS OF INDIVIDUAL STAGES AND SLAG

Location	Gross Weight, grams	Refer to Figure Number
Stage 8	intact	37
Stage 9	227[a]	38
Stage 10	40	39
Stage 11	35	40
Stage 12	18	41
Stage 13	21	42
Stage 14	26	43
Stage 15	53	44
Stage 16	44	45
Stage 17	42	46
Stage 18	40 (est.)	47
Plug	798	48
Basket	40 (est.)	49
Last nine stages	1157	

[a]Not included in total

TABLE 12
ESTIMATED FRACTIONAL RELEASE OF I^{131} FROM ENTIRE CARTRIDGE INVENTORY

Location	Estimated Gross Weight, grams	Estimated Fractional Release of I^{131}	Product
Stages 1-7	1560	0.00	0
8	223	0.04	9
9	227	0.25	57
10-18	300	0.50	150
Basket	40	0.50	20
Rings	300	0.50	150
Slag	500	0.70	350
Missing slag	843	0.70	590
			1326

DECLASSIFIED

TABLE 13

GAMMA SURVEY

Detector Location	Date, Time	Dose, mr/hr	Date, Time	Dose, mr/hr	Date, Time	Dose, mr/hr	Date, Time	Dose, mr/hr	Date, Time	Dose, mr/hr
Engine 2 turbine	5/1, 1030	57.8								
Engine 2 hot duct above unit combustor	5/1, 1034	136.0								
Engine 2 unit combustor	5/1, 1039	918.6								
Hot torus, forward right	5/1, 1047	106.3			5/3, 1124	120.4	5/5, 1107	104.9	5/6, 0937	98.7
Hot torus, forward left	5/1, 1051	95.9			5/3, 1128	94.0	5/5, 1111	88.6	5/6, 0941	83.7
Junction, hot torus and No. 2 hot duct	5/1, 1102	153.9			5/3, 1135	307.1	5/5, 1117	210.5	5/6, 0948	194.8
Junction, hot torus, and No. 1 hot duct	5/1, 1056	103.4			5/3, 1131	187.6	5/5, 1114	132.9	5/6, 0944	120.0
Engine 1 hot duct above unit combustor	5/1, 1113	30.2			5/3, 1105	79.1	5/5, 1038	45.0	5/6, 0858	38.7
Engine 1 unit combustor	5/1, 1119	49.4			5/3, 1110	1252.0	5/5, 1044	919.1	5/6, 0903	717.3
Engine 1 turbine	5/1, 1123	24.5			5/3, 1057	501.5	5/5, 1033	322.4	5/6, 0930	262.5
33.6 ft down exhaust duct from engine 2 turbine	5/1, 1128	39.0								
60.1 ft down exhaust duct from engine 2 turbine	5/1, 1130	18.4								
76-in. duct, 90 ft from engine No. 2	5/1, 1134	40.5	5/2, 1913	189.1	5/3, 1041	58.2	5/5, 1051	47.1	5/6, 0908	44.4
32.5 ft down exhaust duct from engine 1 turbine	5/1, 1142	7.3	5/2, 1919	302.0	5/3, 1047	41.4	5/5, 1059	26.6	5/6, 0923	22.5
61.4 ft down exhaust duct from engine 1 turbine	5/1, 1139	3.8	5/2, 1916	205.0	5/3, 1044	28.7	5/5, 1055	15.1	5/6, 0920	12.7

DECLASSIFIED

Comparison of Measured Data with Theoretical Predictions

AIRBORNE ACTIVITY DISTRIBUTION

Calculations of theoretical ground-level isopleths of fractional values of maximum concentration for airborne activity of I^{131} that could have been observed by sampling devices have been made. The computations are based on an I^{131} inventory of 32 curies for the entire cartridge and a fractional release range of 0.03 to 0.3 (see sections, "CTF Source Data" and "I^{131} Fractional Release Estimation" for discussion of release term range). The computations suggest a source term from 0.96 to 9.6 curies (decayed to five hours) for three selected sets of meteorological parameters that could be representative of the atmospheric conditions during the test. The following relationship based on a modification of Sutton's* diffusion equations was used.

$$A_{x,y,0} = \frac{2\,RC(t_e)\,C_z}{\pi u h_e^2\,C_y} \exp\left[-\frac{y^2}{\sigma_y^2}\right] f(\sigma_z, h_e, h')$$

where

$A_{x,y,0}$ = number of curies collected by a sampling device located near the ground x meters downwind and y meters crosswind from the release point

R = sampling flow rate, meters^3/second

t_e = time of sample evaluation, seconds

C_y, C_z = diffusion coefficients in the y and z directions, respectively

u = average wind velocity in x direction, meters/second

$\sigma_y^2 = C_y^2 (x)^{2-n}$

$\sigma_z^2 = C_z^2 (x)^{2-n}$

n = atmospheric stability parameter

$C(t_e)$ = number of curies emitted at time t_e

$= 0.872\, P_o \Sigma F \gamma (1 - e^{-\lambda T})\, e^{-\lambda t_e}$

P_o = average nuclear power generated in the cartridge that is melted, watts

F = fraction of fission products which are released from the cartridge

$= F_m \times F_r \times F(L) \times F(S)$

F_m = fraction of cartridge that melts

F_r = fraction of fission product inventory contained in the melt fraction (slag) that are released as a consequence of the melting

$F(L)$ = function which corrects for nonuniform power distribution over the cartridge length

$F(S)$ = function which corrects for the fraction of fission products lost from the cloud by scrubbing action of vegetation

*O. G. Sutton, *Micrometeorology*, McGraw-Hill, New York, p. 333.

DECLASSIFIED

DECLASSIFIED

γ = fission yield for isotope
λ = decay constant of isotope, seconds^{-1}
T = reactor operating time, seconds

$$f(\sigma_z, h_e, h') = \frac{h_e^2}{\sigma_z^2} \sum_{m=0}^{\infty} \left\{ \exp\left[-\frac{2mh' + h_e}{\sigma_z}\right]^2 + \exp\left[-\frac{2(m+1)h' - h_e}{\sigma_z}\right]^2 \right\}$$

h' = height at which inversion layer starts, meters
h_e = effective stack height, meters
$= h + \Delta h$
h = stack height, meters

$$\Delta h = d\left[\frac{v}{u}\right]^{1.4} \left[1 + \frac{(T_s - T_a)}{T_a}\right]$$

d = diameter of stack, meters
T_s = temperature of exhaust gas in stack, ^{o}R
T_a = temperature of ambient air, ^{o}R
v = velocity of exhaust gas in stack, meters/second

$$= \left[\frac{q T_s p_{sl}}{\rho_a T_a \frac{\pi}{4} d^2 p_{its}}\right]$$

q = flow rate of coolant air through the reactor, lb/sec
ρ_a = density of air, lb/meter
p_{sl} = standard atmospheric pressure, mmHg
p_{its} = atmospheric pressure at ITS, mmHg

The values for the respective parameters used in the above equation and comments pertaining to them are given in Table 14. $A_{x,y,0}$ was evaluated for maximum ground airborne centerline concentration

$$\left(\exp - \left[\frac{y^2}{\sigma_y^2}\right] = 1 \quad \text{since } y = 0\right).$$

Fractional values of this maximum value ($10^{-0.5}$, $10^{-0.1}$, $10^{-0.15}$, etc.) were then used in the equation to determine particular values of y for selected distances of x so that isopleths could be constructed. In addition, for comparison purposes, the high-volume air sampler data presented in Figures 70 through 74 have been adjusted to show values of I^{131} using a 6 percent correction factor from analysis of selected field samples (see section "High-Volume Air Samples (HVA)" for discussion of this value) and have been redrawn with reasonable smooth-fitting curves. The individual arc maximum points were then centered on an azimuth bearing of 30 degrees which was approximately the direction of the mean wind. This adjustment provides a basis for drawing a smooth isopleth pattern to compare with the theoretical curves discussed above. The smoothed curves before and after centering the maximum points are presented in Figures 81 and 82. The isopleth pattern constructed from the adjustment of the field data and the isopleth patterns from the theoretical calculations are presented in overlaid Figures 83, 84, and 85. Values for pertinent parameters of the three sets of graphs are given on the figures. It should be noted that the isopleth values given are for a release of 9.6 curies of I^{131} and should be reduced by a factor of 10 for the 0.96 curie release.

From qualitative examination of the curvature of the isopleths (neglecting absolute value) on the three selected sets with the observed and adjusted pattern it is possible to deduce that Figure 85 makes the best comparison. Figure 84 also well describes the

TABLE 14

VALUES OF PARAMETERS USED IN CALCULATION OF GROUND-LEVEL DISTRIBUTION OF I^{131}

Factor	Units	Value	Comments
R	m^3/sec	1.65×10^{-2}	Sampling rate of high-volume air samplers.
C_y, C_z	$m^{n/2}$	0.176, 0.174	Calculated from meteorological data.
		0.223	Theoretical value for conditions that existed.
		0.285	Predicted by USWB for experiment.
$\bar{u}$	m/sec	4.5	Observed mean wind speed.
n	--	0.2	Calculated from observed wind speed profile.
$C(t_e)$	curies	9.6 to 0.96	Based on I^{131} inventory of 32 curies (section, "Reactor Operating History and Iodine Inventory") and fractional release, F, of 0.3 to 0.03 (sections, "CTF Source Data" and "I^{131} Fractional Release Estimation").
$f(\sigma_z, h_e, h')$	--		See Figure 80.
h_e	m	65	Observed from smoke plumes (see section, "Cloud Trajectory and Diffusion Parameters").
h'	m	∞	Inversion not present in diffusing layer.
$A_{x,y,0}$	curies/HVA	--	Calculated for maximum ground concentration.
$\exp\left[-\frac{y^2}{\sigma_y^2}\right]$	m^2	--	Evaluated for values of y.

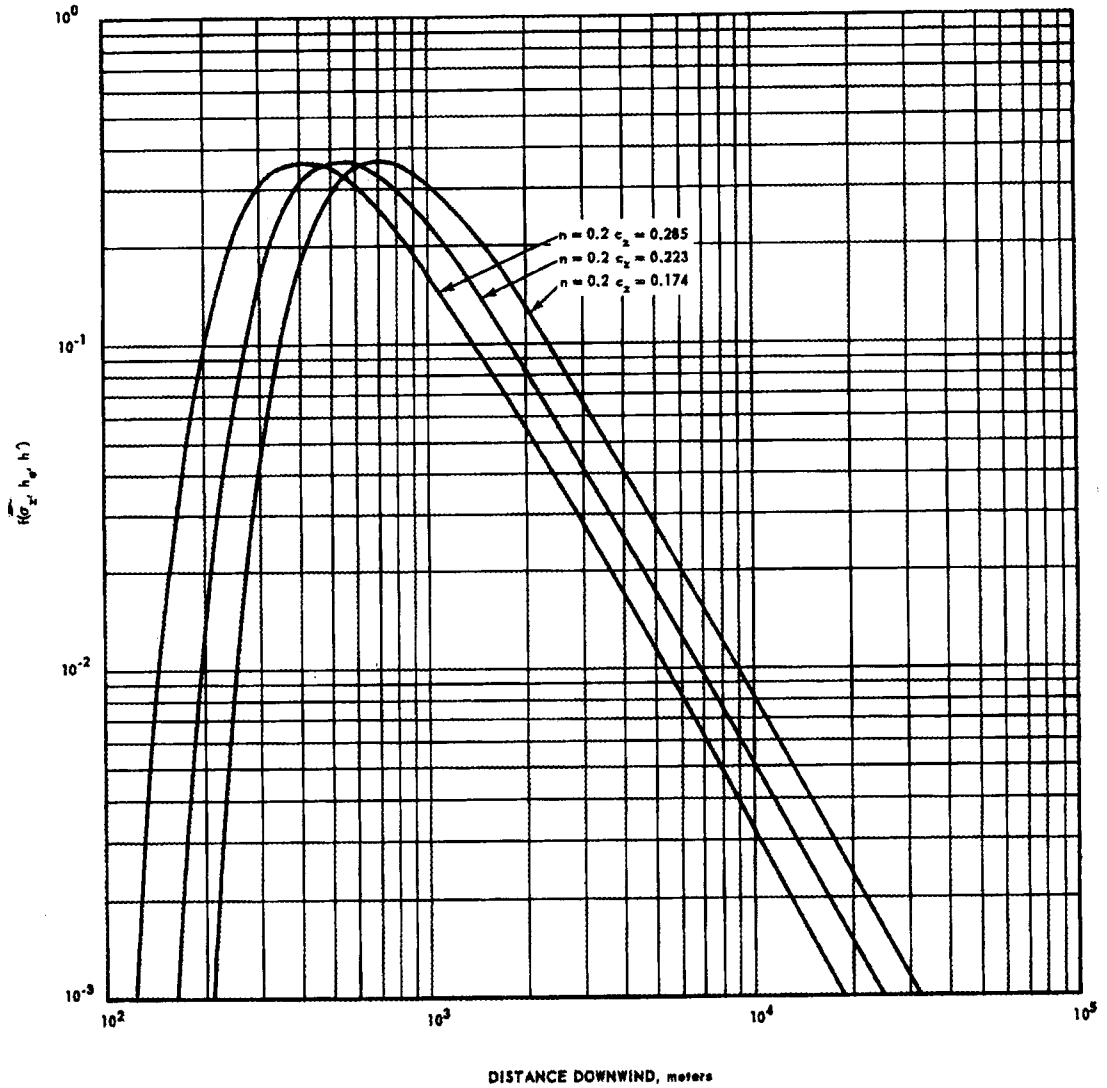

Fig. 80 – Values of $f(\sigma_z, h_e, h')$ for selected n and C_z values

DECLASSIFIED

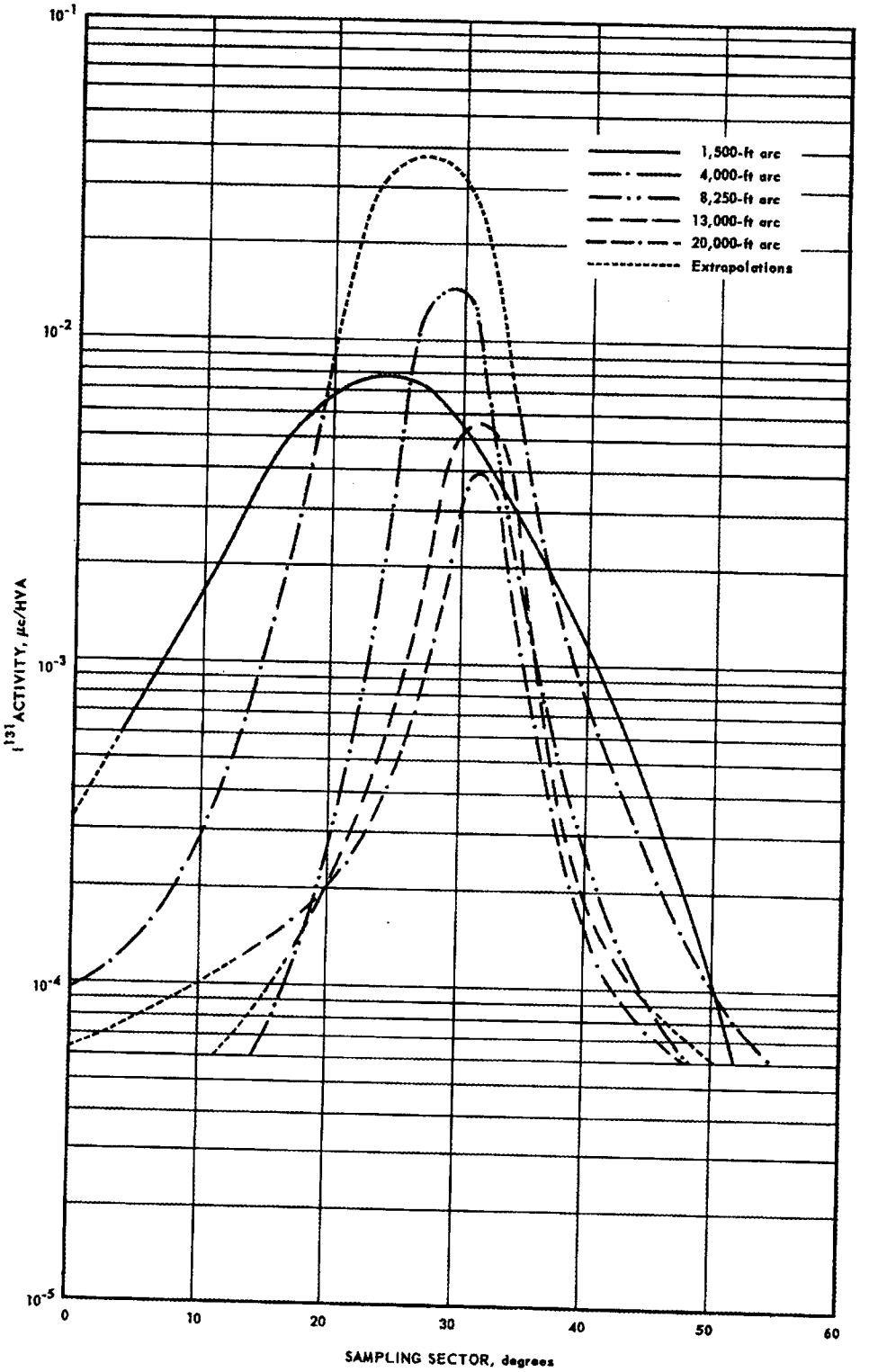

Fig. 81 – Smoothed curves of I^{131} activity from high-volume air samplers for sampling arcs (decayed to 5 hours after melt)

DECLASSIFIED

DECLASSIFIED

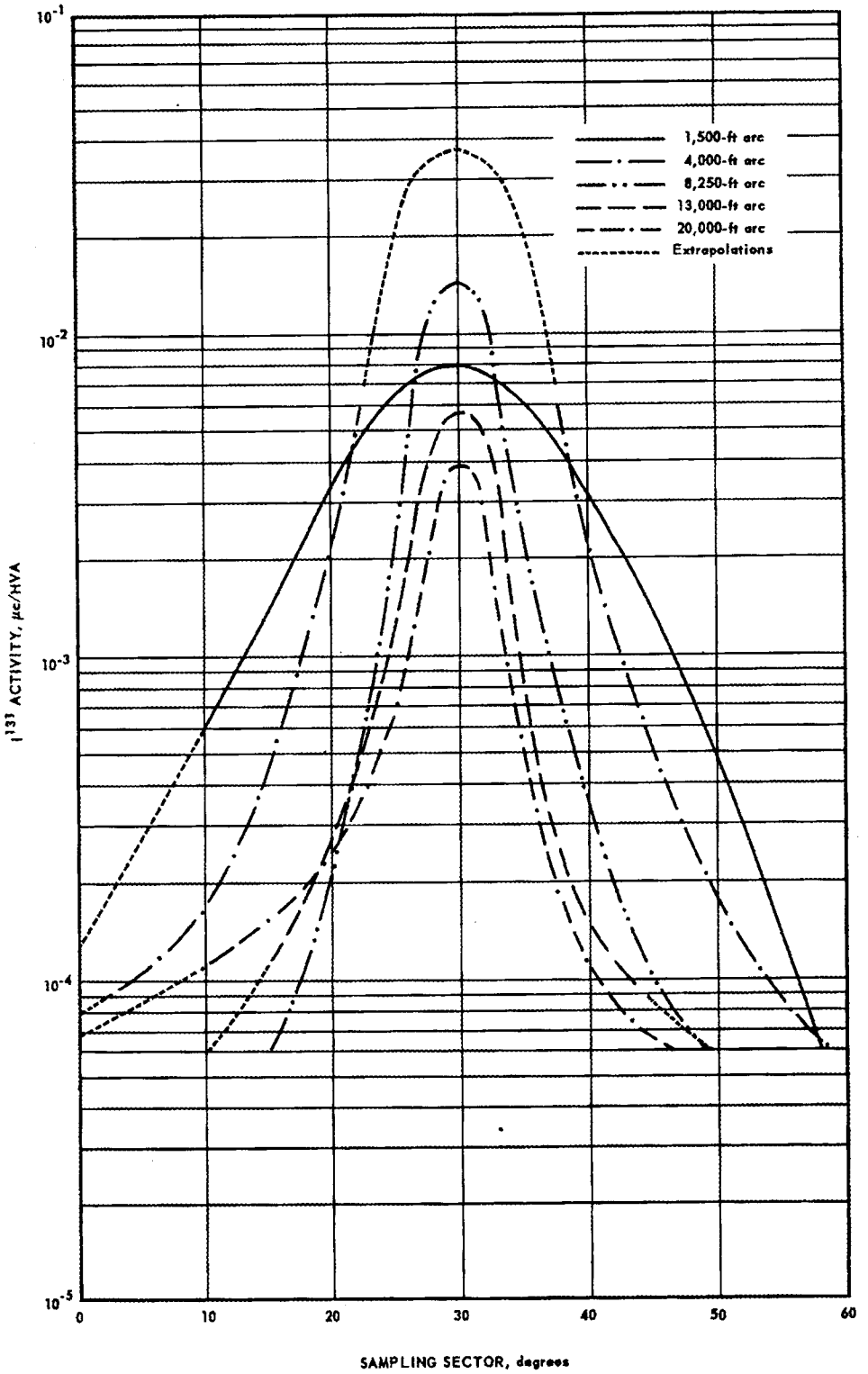

Fig. 82 – Adjusted and smoothed I^{131} activity from high-volume air samplers for sampling arcs (decayed to 5 hours after melt)

DECLASSIFIED

DECLASSIFIED

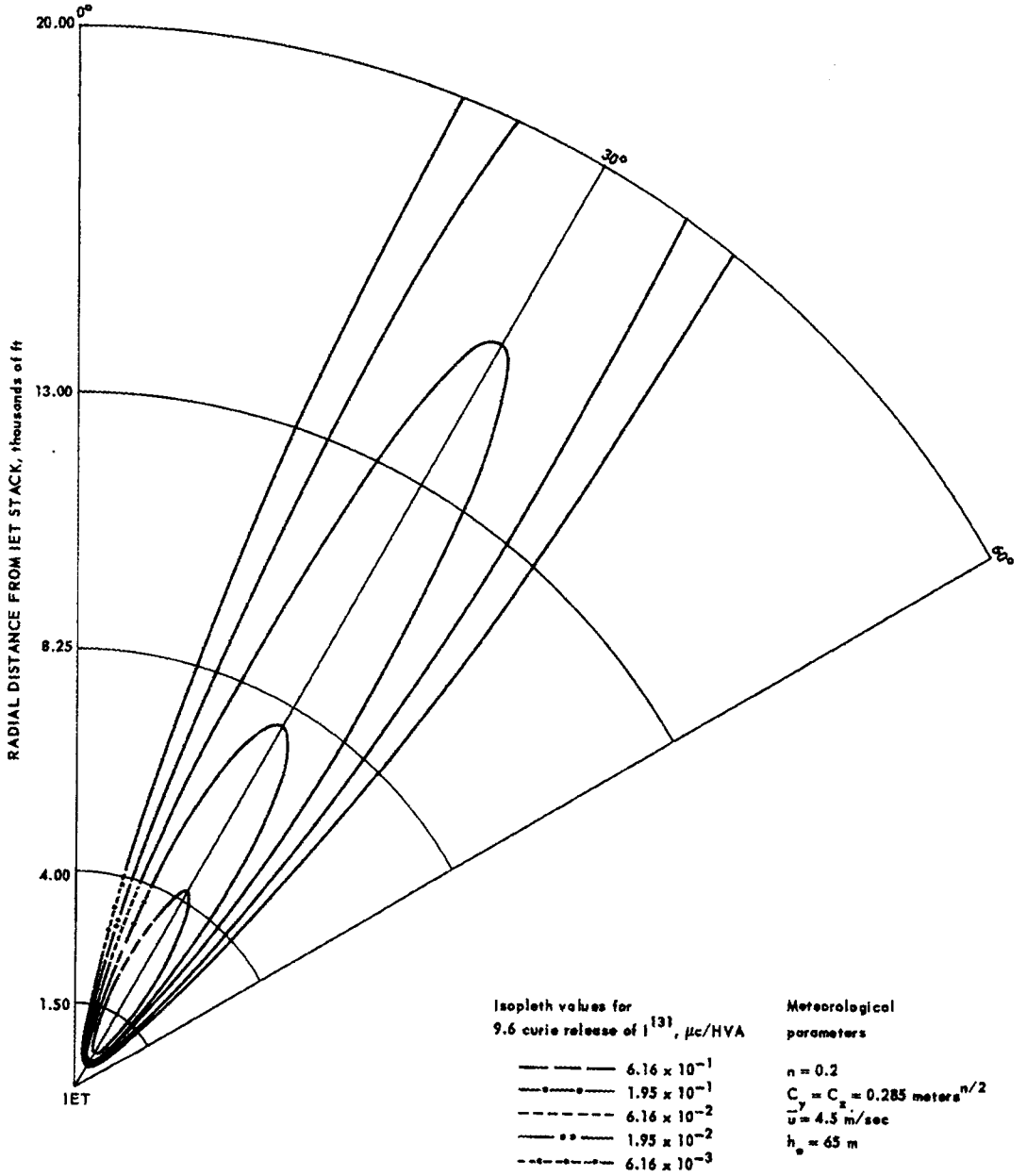

Fig. 88 – Theoretical isopleth pattern for I^{131} source terms of 9.6 and 0.96 curies for predicted meteorological parameters

DECLASSIFIED

DECLASSIFIED

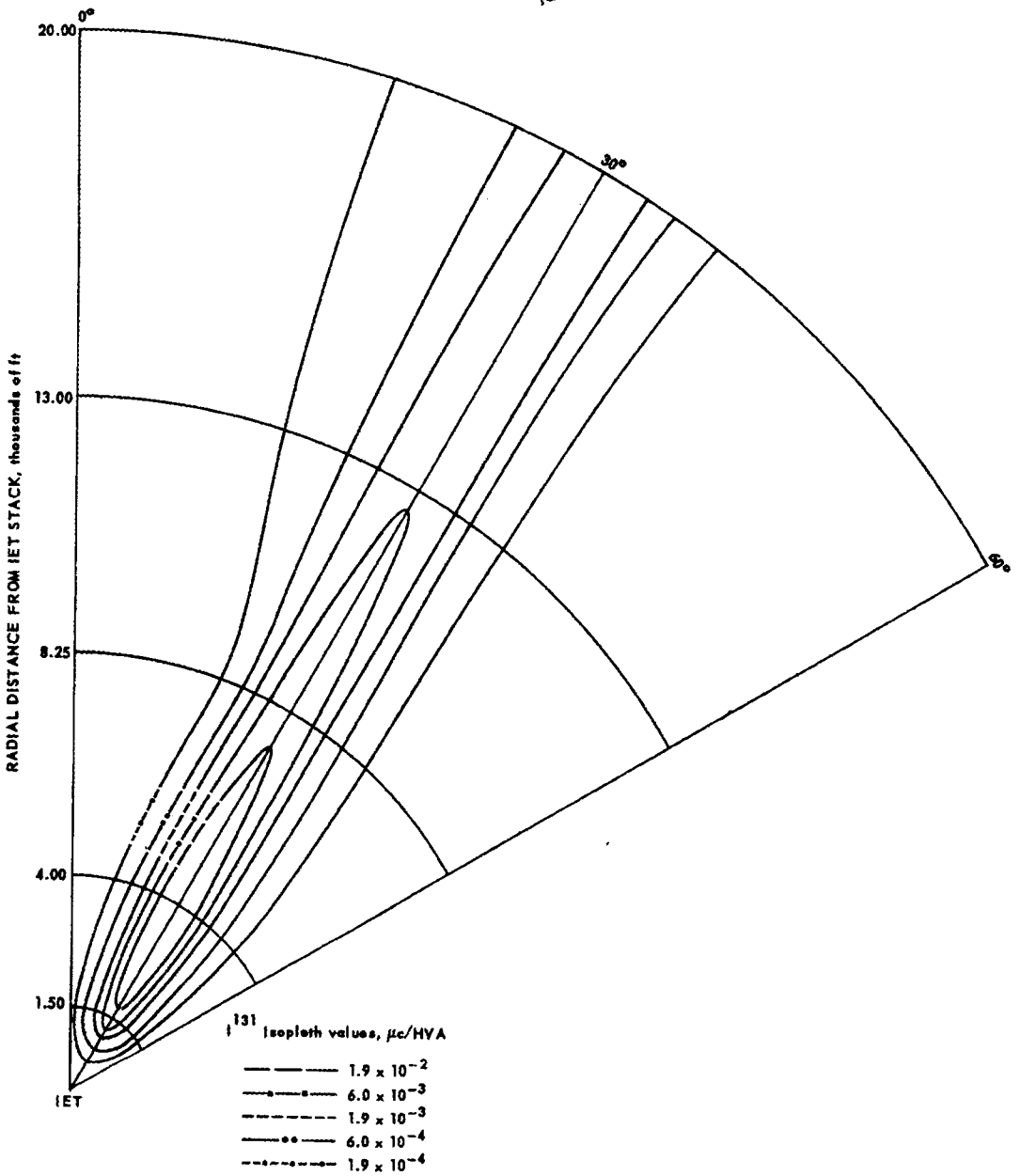

Fig. 88A – Adjusted and smoothed integrated airborne activity isopleth pattern observed for I^{131} (normalized to 6 hours after melt)

DECLASSIFIED

DECLASSIFIED

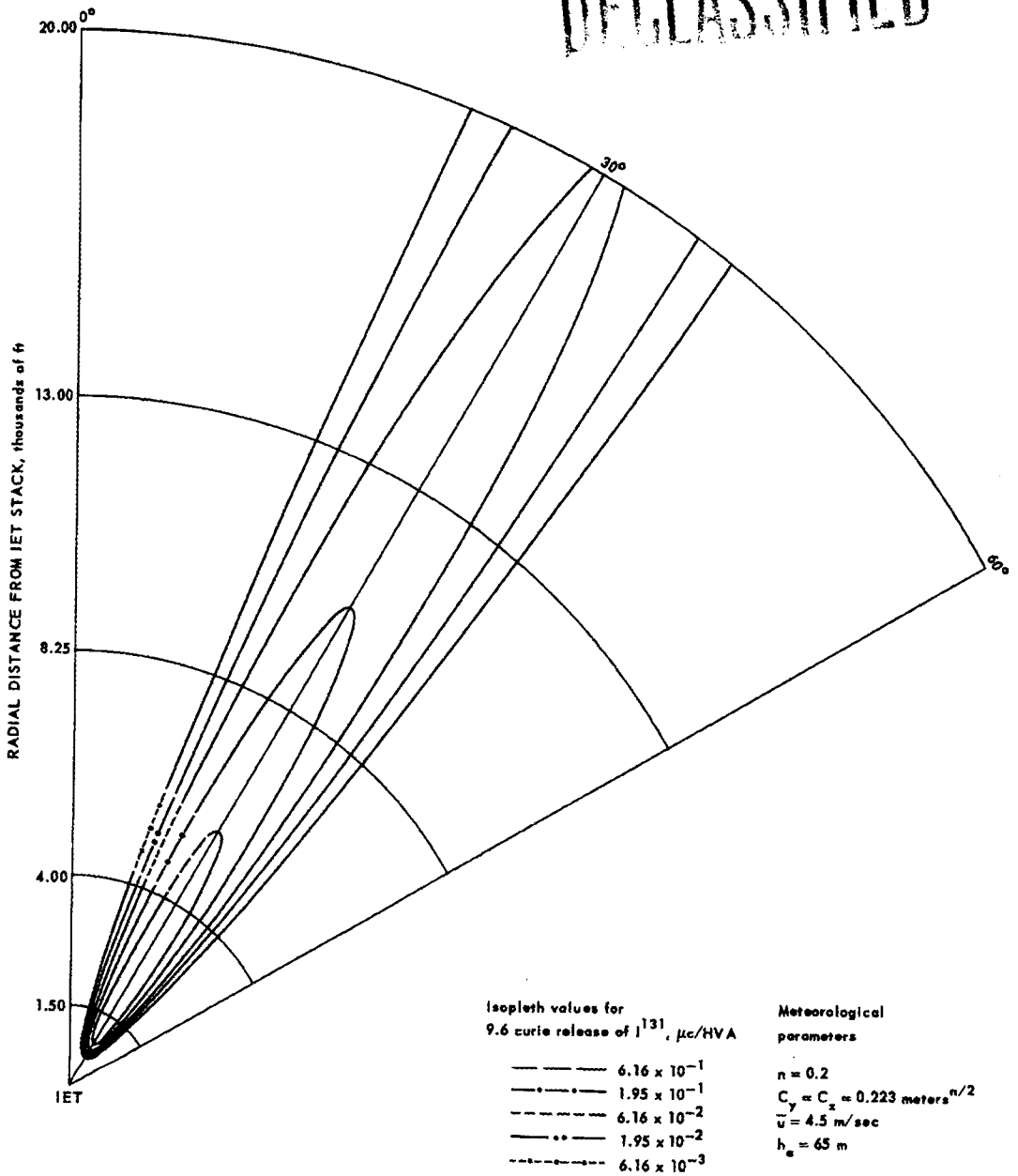

Fig. 84 – Theoretical isopleth pattern for I^{131} source terms of 9.6 and 0.96 curies for meteorological parameters suggested by theory

DECLASSIFIED

DECLASSIFIED

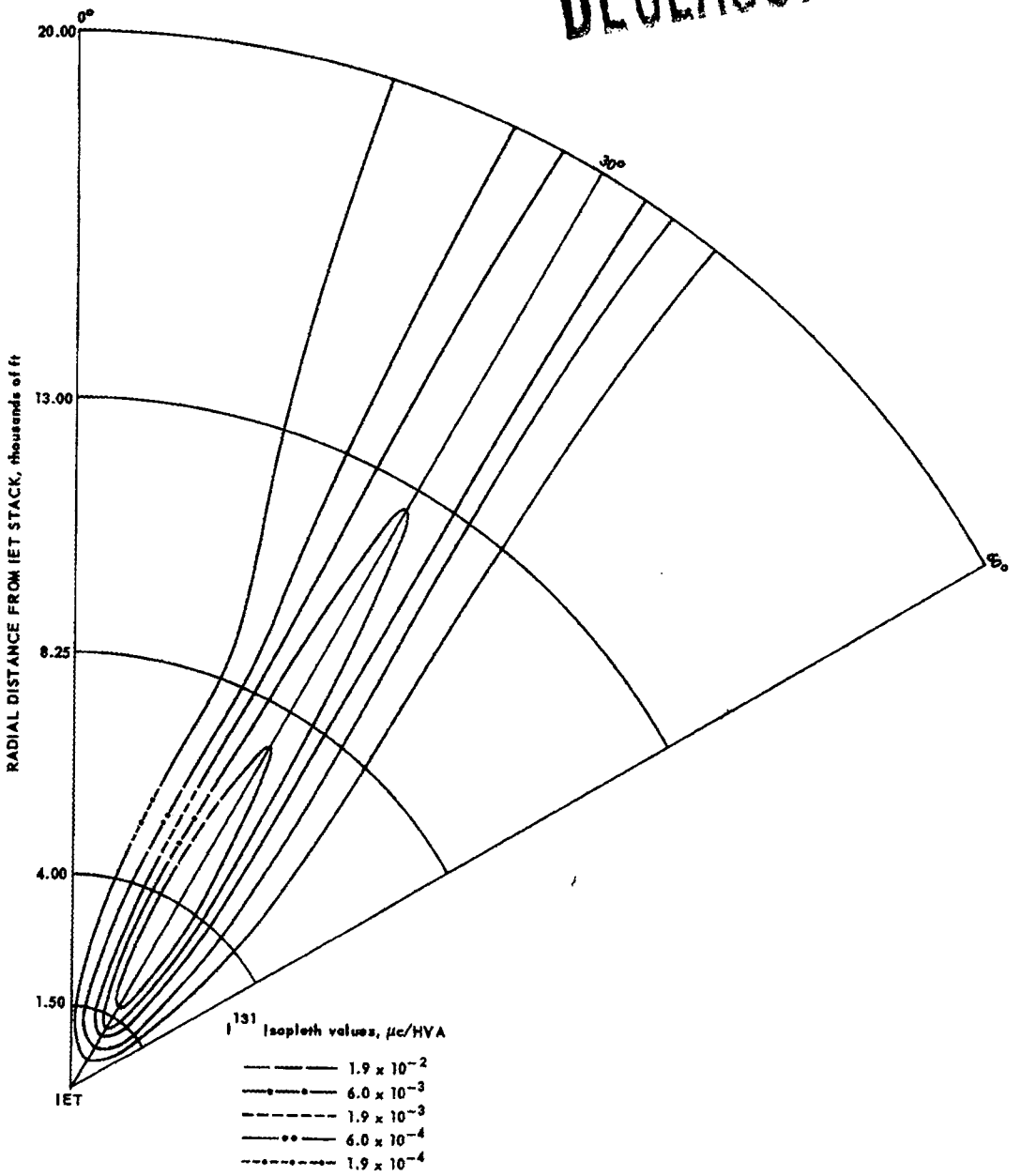

Fig. 84A – Adjusted and smoothed integrated airborne activity isopleth pattern observed for I^{131} (normalized to 6 hours after melt)

DECLASSIFIED

DECLASSIFIED

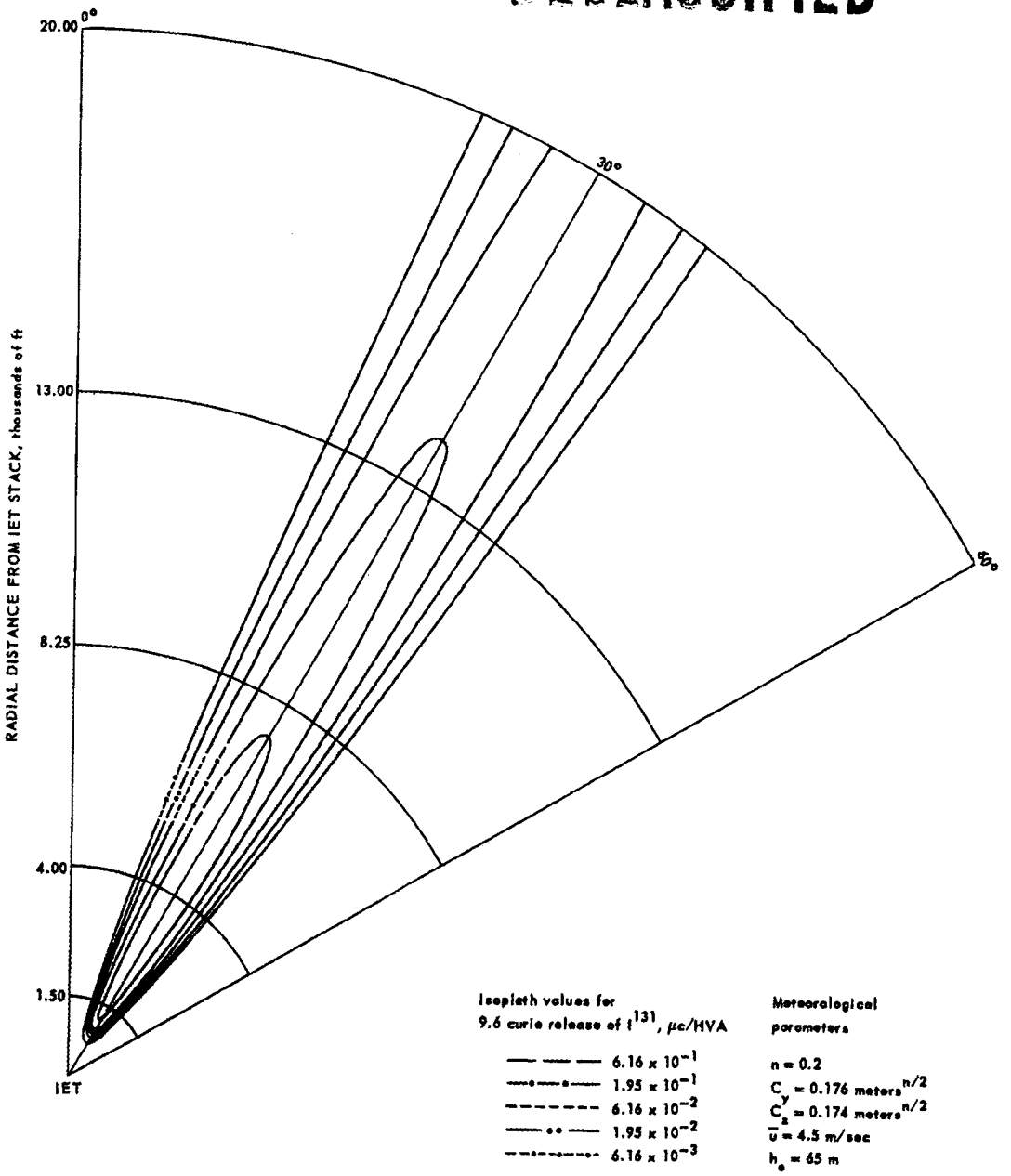

Fig. 85 – Theoretical isopleth pattern for I^{131} source terms of 9.6 and 0.96 curies for meteorological parameters observed during experiment

DECLASSIFIED

DECLASSIFIED

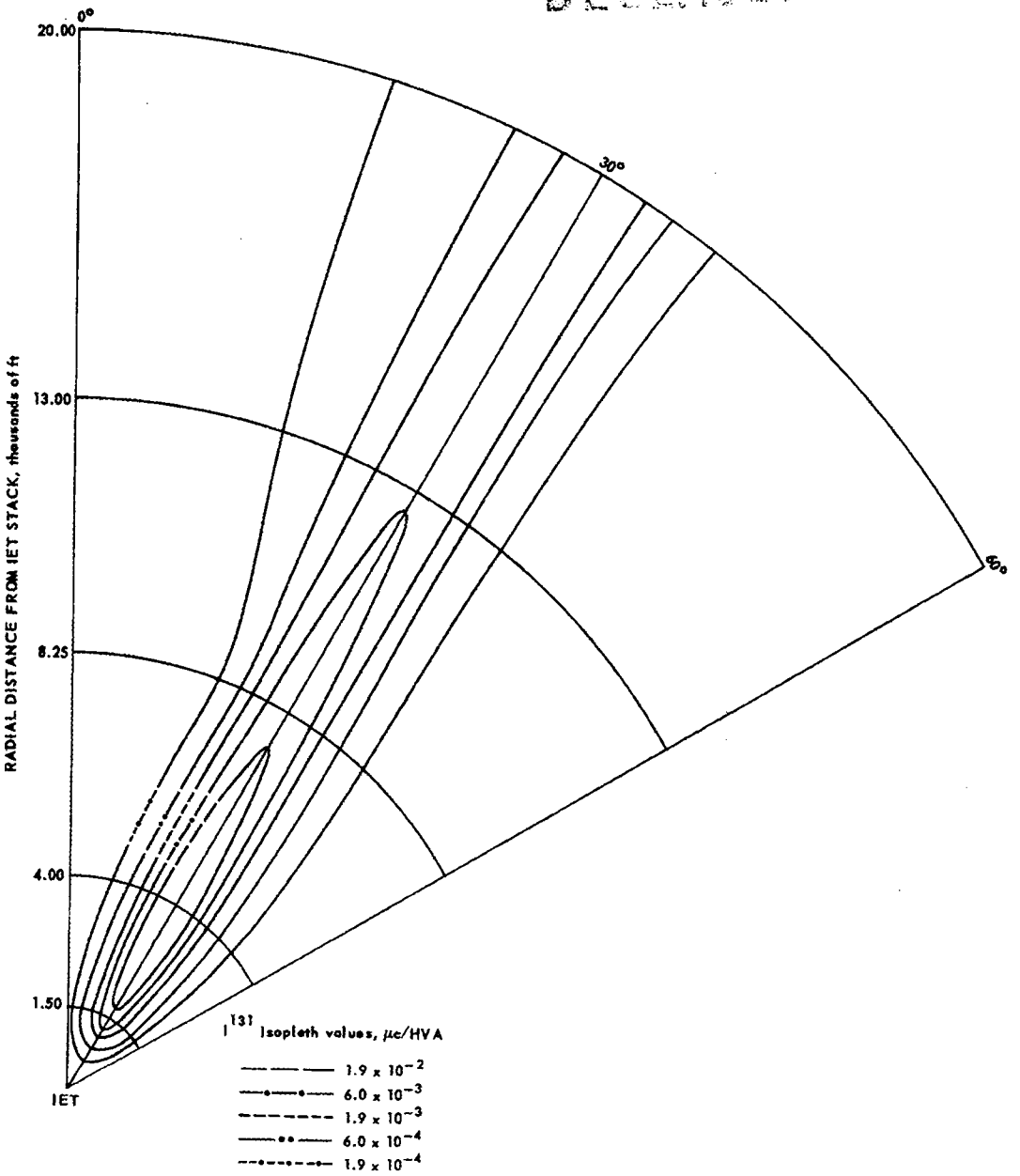

Fig. 85A – Adjusted and smoothed integrated airborne activity isopleth pattern observed for I^{131} (normalized to 6 hours after melt)

DECLASSIFIED

DECLASSIFIED

general pattern. It is of interest to note that the theoretical pattern in Figure 85 was constructed from the estimated value of C_y obtained from wind velocity data obtained during the experiment.

Since the source term cannot be resolved to values less than a factor of about 10 as previously discussed, it is not possible to make accurate comparisons of activity disbursement. In order to obtain some idea of the possible range of theoretical versus observed, however, maximum centerline activity at near ground level has been plotted for Figure 85 and the observed data using both values of source term. This comparison is presented in Figure 86. It can be seen that the curves for both values of source term overpredict the observed by varying amounts depending on the selected distance. If the meteorological diffusion equations are assumed to describe correctly the process occurring, they tend to support the 0.96 curie release. Possible explanation of this overprediction may be in the selection and measurement of the parameters, i.e., development of more suitable instrumentation for measurement of diffusion parameters may reduce these factors. Another possible explanation may be in the disbursement of material by thermal or mechanical eddies to greater heights than considered in the theoretical equations. Information on the magnitude of this vertical disbursement was expected to be obtained from sampling instrumentation on the four towers located on the 8250-foot arc and the tethered blimps. However, only the tower data were obtained in this plane due to the inoperative condition of the blimps. The observation from the high-volume air samplers located on the towers and from near ground level on the 8250-foot arc are presented in Figure 87 with a speculation of portions of an isopleth pattern which could have existed.

Further information of the degree of vertical displacement of material by atmospheric processes has been obtained from the series of aerial photos taken of plumes of chemical smoke released from the IET stack prior to and after the melt. Figures 53, 54, 55, and 56 are representative. These photos indicate that the main body of the plumes had attained an altitude of about 900 feet by the time they were 4000 feet downwind of the stack. It should be noted that Sutton's diffusion equations are based upon clouds moving in the horizontal plane. Because it appears that the radioactive cloud was moving in a plane other than horizontal and the suggestion that the center of activity was higher than expected (Figure 87), it appears that vertical diffusion for strong lapse conditions may well be greater than predicted by theory.

ACTIVITY AND WIND-DIRECTION-FLUCTUATION DISTRIBUTION

Figure 88 compares the distribution of gross beta activity from high-volume air samplers from three arcs of the sampling network with the frequency distribution of wind direction from vanes at heights of 150 feet at the source and 20 feet at approximately 29,400 feet downwind.* The wind direction distribution for the source vane was taken at the height nearest the point of emission (150 feet) and is for a period of 5 minutes corresponding to the time over which most of the radioactive material was released. The wind direction distribution at the downwind location was for a period of 45 minutes selected to cover at least the period of time that the radioactive cloud needed for passage over the wind-data recording site.

The general shape of the activity curves for the three travel distances compares favorably with the wind-direction frequency curves with less correspondence at greater distances. Maximum activity points on the three arcs illustrated, as well as the other instrumented arcs, all fall within the 20-degree sector from 200 to 220 degrees (see

*The data at 29,400 feet were recorded by USWB equipment.

DECLASSIFIED

DECLASSIFIED

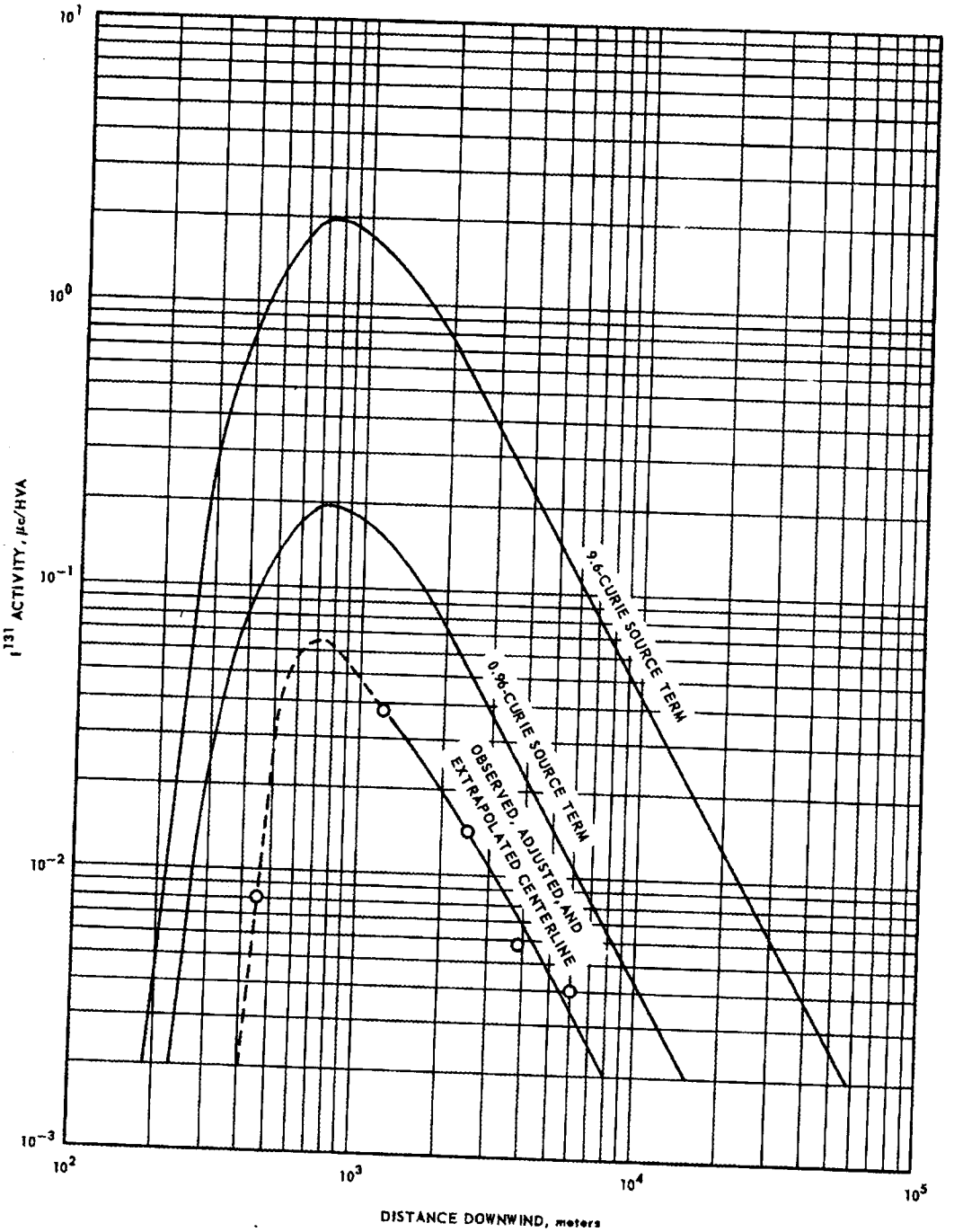

Fig. 86 – Theoretical maximum ground-level centerline activity for release terms of 9.6 and 0.96 curies of I^{131} (decayed to 5 hours) compared with observed and adjusted centerline

DECLASSIFIED

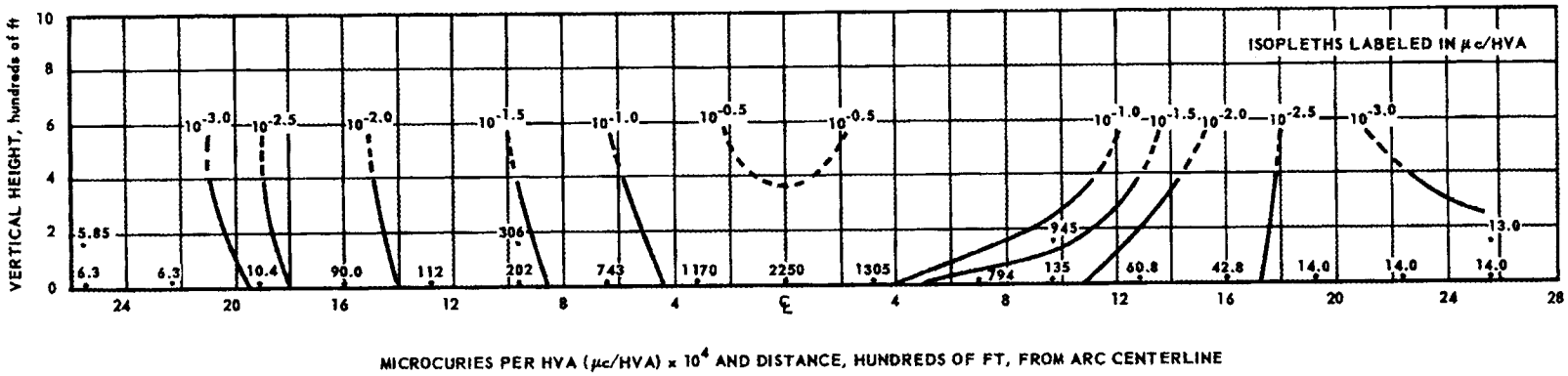

Fig. 87 – Vertical cross section of gross beta activity from high-volume air samplers for 8250-foot arc. Dotted lines are suggested extrapolations.

DECLASSIFIED

DECLASSIFIED

DECLASSIFIED

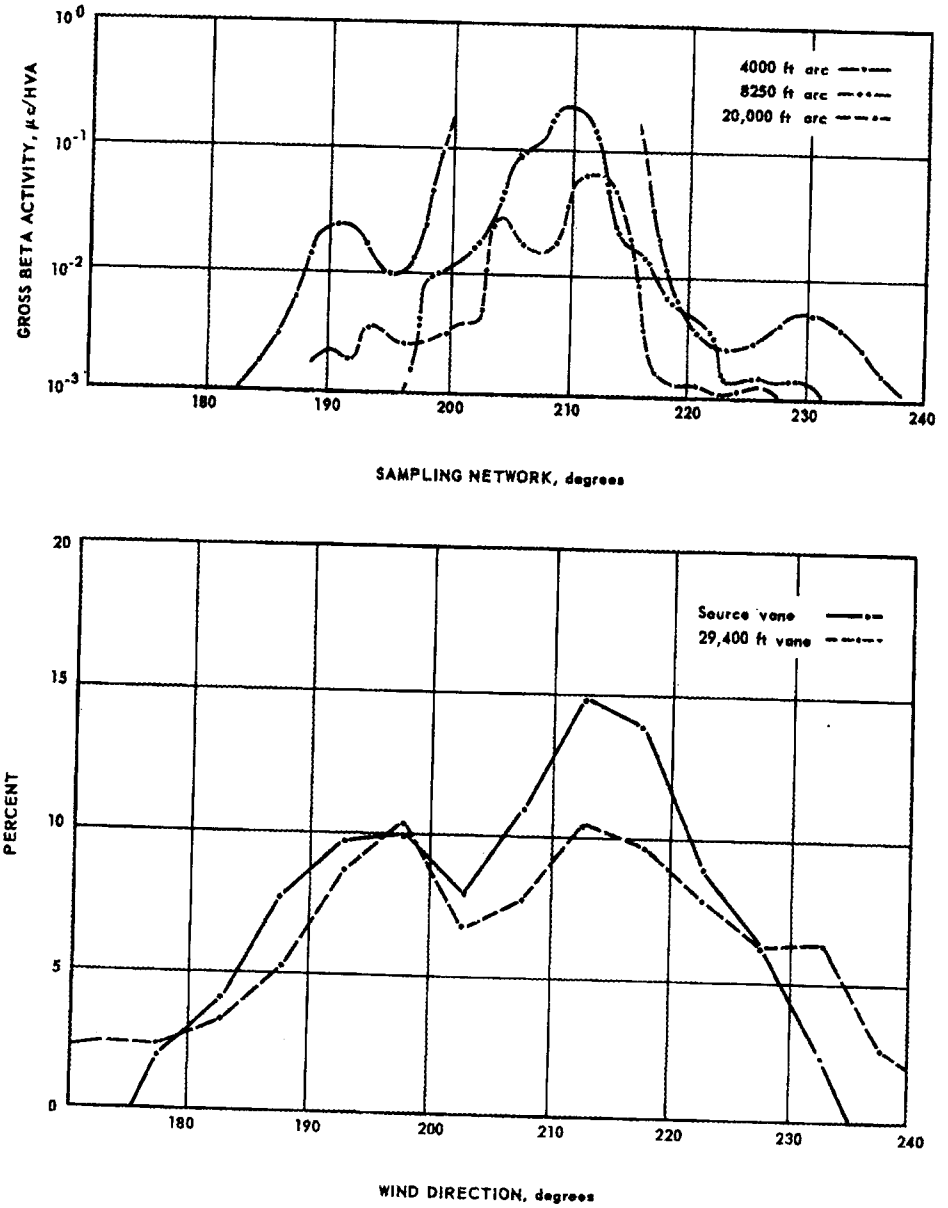

Fig. 88 – Gross beta activity for three selected arcs (upper) and frequency distribution of wind direction from source and downwind vane (lower)

DECLASSIFIED

DECLASSIFIED

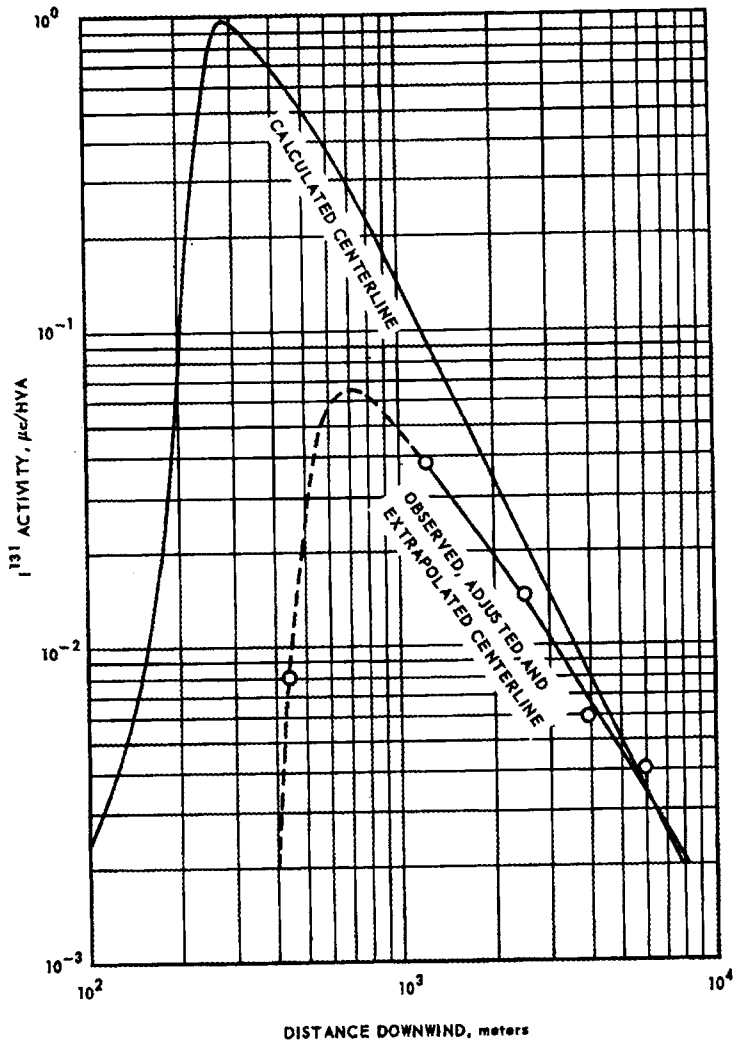

Fig. 89 – Calculated and observed ground airborne centerline activity versus downwind distance for 9.6-curie release

DECLASSIFIED

DECLASSIFIED

Figures 70 through 74), which is also the sector showing the greatest frequency of wind direction. A secondary maximum point is apparent on the 4000-foot-activity curve, and suggestions of similar points on the other activity curves, which may well correspond to the secondary maximum point on the wind direction curve, can be noticed. Isopleths of airborne gross beta activity distribution over the sampling sector shown in Figure 75 also show activity displacement corresponding to this secondary maximum point.

It can be inferred from these data that the shape of the radioactive cloud was determined by the wind-direction-fluctuation regime into which the material was emitted and that the cloud maintained this basic form as it diffused and moved with the mean wind.

Use of direct meteorological measurements such as wind direction fluctuations for parameters in diffusion formulae is suggested by the comparisons noted above. Previous investigators* have noted similar correspondence between wind direction fluctuations and airborne material disbursement. Generally, however, their work has been with experiments of a smaller scale than the one being described. Cramer, et. al,* using about 100 ground-level, point-source experiments over distances of the order of a kilometer, have proposed a model utilizing the standard deviation of the horizontal (σ_A) and vertical (σ_E) wind-direction fluctuations as diffusion parameters. Substantiating experimental data for elevated sources and greater distances, however, have not been available for evaluation.

In order to obtain some idea of the possible use of wind-direction fluctuations for diffusion parameters for distances of the order of those in this experiment, a calculation using the relationship and parameters suggested by Cramer et. al for distances of about a kilometer and conditions similar to those of this experiment ($\sigma_A = 15^{\circ}$) of ground centerline airborne activity has been made. This calculation for a 9.6-curie release of I^{131} compared with the observed and adjusted centerline curve (as previously discussed) is presented in Figure 89. It can be seen that at greater distances good agreement exists for the 9.6-curie source term, with large differences at shorter distances. Further work in future experiments using these more directly measurable parameters is indicated.

*H. E. Cramer, F. A. Record, and H. C. Vaughan, "The Study of the Diffusion of Gases or Aerosols in the Lower Atmosphere," ASTIA Document No. 152582, p. 70.

"Meteorology and Atomic Energy," AECU 3066, U.S. Dept. of Commerce, 1955, pp. 63–70.

DECLASSIFIED

DECLASSIFIED

Discussion

Operation BOOT was designed to investigate the degree of reactor damage, fractional release of fission products, adequacy of diffusion theory, and environmental changes associated with fuel element failure due to insufficient cooling.

REACTOR DAMAGE

The occurrence of the unexpected reactor scram, 15 seconds after the valve was closed, limited the damage of the cartridge being tested. The damage was to the cartridge that was purposely overheated and had no noticeable effect, other than loss of reactivity, upon the reactor as a whole. Theoretical predictions of the degree of damage which could be expected were essentially confirmed. Since the analytical studies were necessarily based upon steady-flow conditions, this was encouraging.

Temperature measurements of the damaged cartridge were somewhat disappointing in that many of the thermocouples had failed prior to the time of melt and those in working order attained off-scale readings, which had to be extrapolated.

Damage to the cartridge was quite extensive. The residue from the reactor can be arbitrarily separated into several categories according to physical appearance:

1. Undamaged.
2. Blistered.
3. Partially oxidized, but retaining original shape.
4. Heavily oxidized slag.

SOURCE MEASUREMENTS AND FRACTIONAL RELEASE

Radioiodine release generally constitutes the major potential radiological hazard associated with the release of fission products from high-performance reactors similar to those tested at the ITS. Attempts were made to ascertain the amount of radioiodine released during the melt; and, since the inventory of iodine was known at all times, the fraction released would also be determined.

Independent determinations of radioiodine release (specifically I^{131}) were attempted by:

1. Radiochemical analyses of fuel element residue.
2. Radiochemical analyses of effluent samples taken in the duct during release.
3. Estimating the source strength necessary, according to diffusion theory, to produce the measured isopleth patterns.

Each of these determination methods have intrinsic uncertainties associated with it, and none was truly definitive enough that other results could be discounted. The fractional release for the entire cartridge I^{131} inventory indicated by each of these methods is as follows.

DECLASSIFIED

Method	Fractional Release (I^{131})	
Residue analyses	0.30	(Total)
Effluent samples (duct)	0.026	(BOOT I)
	0.0063	(BOOT II)
	0.031	(Total)
Diffusion theory and isopleths	0.025	(BOOT I)

Consideration must be given to the attempt made to melt cartridge 2_1 after cartridge 6_1 had been melted. During the attempt to go to power some additional iodine was released from cartridge 6_1. Effluent samples taken in the duct indicated that 0.0063 was released during the second attempt as compared to 0.026 during the initial run. If it is assumed that these measurements are both valid, it seems rational to assume that the residue analyses release fraction determination given above should be modified by 0.026/0.031 = 0.84 to yield the release fraction for the time of BOOT I.

The release fractions, for comparison (BOOT I), would then be:

Method	Fractional Release (I^{131})
Residue analyses	0.25
Effluent samples (duct)	0.026
Diffusion theory and isopleths	0.025

The spread of a factor of ten in fractional release is difficult to resolve with the information available from the experiment at this time. It is well to discuss some of the major shortcomings of each method.

Residue Analysis

This method of analysis is reasonably straightforward and appears to suffer from relatively few uncertainties. The estimation depends upon the analysis of nine random samples taken in three significant regions. It is, of course, possible that the random samples were not representative of the regions.

The I^{131} : Zr^{95} and Zr^{95} : U ratios were used to determine the I^{131} fractional release. It was assumed that the uranium and zirconium remained together before and after the melt occurred. Zirconium is known to be very tenacious over a wide range of conditions; this is also true for uranium in this particular type of fuel element. However, it should be pointed out that since the theoretical and measured ratios were used to determine the theoretical and actual I^{131} content, if for any reason an appreciable amount of either uranium or Zr^{95} did indeed leave the element, the I^{131} release fraction would be different.

Effluent Samples (Duct)

This is a standard method for the determination of iodine concentrations in effluent, i.e., the use of sampling probes and chilled carbon traps. The method does, however, suffer from several uncertainties: (1) the sampling probes must be located in positions where representative samples of gaseous and particulate materials occur, (2) material can be trapped in the lines from the probes to the carbon traps, (3) the traps must be efficient for retaining I^{131} either in gaseous form or contained in or on particulate material.

Past experience has shown that a complex situation exists when iodine is released while chemical augmentation of power is being used. Some of the iodine is absorbed or adsorbed by the incompletely oxidized jet fuel so that part of the iodine is collected with particulates

and part is gaseous iodine. Nonisokinetic sampling, separation of particulate and gases in the ducting enroute to the stack, entrapment of material in the lines between the sampling points and the traps, and preferential entrapment for gases or particles by the traps can all give erroneous values for fractional release. The rather large variations between the second samples taken by several individual probe-trap combinations in the same general area of the 76-inch duct suggests that some of the factors mentioned above did indeed occur and the values reported are therefore subject to question.

Diffusion Theory and Isopleths

It is presumptuous to use a theory the validity of which was being tested, to ascertain one of the parameters of the investigation. The isopleth patterns also involved extensive extrapolations. The requirement that the release had to be made during a period of strong lapse rather than a neutral atmospheric condition added uncertainty to the isopleth pattern determination because of the nature of the strong-lapse condition. Much cleaner isopleth determinations could be expected for neutral conditions. Because of these extrapolations and rationalizations the fractional release value for I^{131} estimated by these comparisons may only be of academic interest, and the agreement between this estimate and the duct effluent samples may be entirely coincidental. The agreement between the two methods was better than could be expected and, if indeed the theory does adequately describe the distribution of the effluent, the estimate of fractional release by this method could be correct.

General

The spread of values for I^{131} fractional release is not resolved. It is possible to rationalize the observed data to justify either I^{131} release fraction (0.025 or 0.25) for the time of melt and that neither value be selected with any certainty. There are many other factors which may or may not be important, for example, the possibility that an appreciable fraction of the iodine released from the reactor might become affixed to the inside surfaces of the ducting and apparatus leading to the release point. It is also possible that the duct effluent samples were in error and that the bulk of the iodine was carried off at an altitude higher than expected. Data from off-site surveys by the Idaho AEC health physics personnel and from Rochester animals which were placed within the network may support one of the arguments, but these data have not been reported at the time of this writing.

Some Sr^{91} was found in the carbon traps sampling the 76-inch duct. The indicated Sr^{91} release fraction was about 0.006 and none was found spectrographically on any other samples. It should be noted, however, that Sr^{91} would not necessarily be seen on these spectra because no other chemical separation of strontium was made, and it could be masked by other isotope activities when gross spectra were measured.

ENVIRONMENTAL MEASUREMENTS

Vegetation

Vegetation samples taken prior to and after the release indicated that surprisingly little activity was absorbed or adsorbed during the passage of the cloud. It is known that sagebrush generally picks up a considerable amount of iodine from the atmosphere when it is available in the vapor form. It is entirely possible that much of the iodine isotope release during the test was associated with particulate material, which was not as readily "scrubbed" by the vegetation as it would have been had it been vaporous iodine.

The amount of activity found on the vegetation was too small to permit quantitative determinations of quantities of individual isotopes. The gamma spectra from vegetation

DECLASSIFIED

taken in the path of the cloud before the release and after the release are essentially the same spectra as those from vegetation samples taken completely out of the test area. Apparently there was negligible contribution to vegetation activity as a consequence of this experiment.

Milk samples and vegetation samples taken downwind of the release point and outside the ITS boundaries were taken by Idaho AEC personnel after the release. These data have not been reported, but it is expected that they will confirm these findings.

Fallout Activity

Activity found on fallout plates was also quite small and did not permit determination of quantities of individual isotopes. Spectral analysis did indicate some of the isotopes present, and these isotopes are mentioned in the appropriate section of this report. By the very nature of this type of measurement, representative fallout values are difficult to ascertain with any degree of certainty because much of the activity found on any given plate is generally from one or two rather large particles, and average surface contamination values are greatly influenced by the probability of these relatively few large particles being trapped by the sticky paper. Many fallout stations were used, and the data appear consistent if the fallout isopleths are compared with the HVA isopleths.

Particle Size Distribution

Particle size distribution estimates made from cascade impactor samples in the ducting indicate unusually large numbers of relatively large and small particles with relatively few between. Analyses of material collected by the electrostatic precipitator and carbon trap in series with a sampling probe in the same area indicated that I^{131} was not associated with particulate material at this point because it was found in the carbon rather than on the precipitron liners. These samples were taken in the hot duct between the hot torus and the unit combustor before the reactor effluent came in contact with the chemical fuel byproducts. If similar samples were taken in the 76-inch duct (where the other duct samples were taken), the results might have been considerably different.

HVA Samples

Samples taken using HVA samplers appeared to be quite satisfactory and consistent. It was very unfortunate that, of all the generators used during the test, the one supplying current to the samplers located most favorably for the measurement of the highest ground-level concentration should fail at the time of release. The sampling efficiency of the HVA filters for the effluent released is not known. Past experience with the sampling of effluent in the stack has indicated that the HVA filters are satisfactory for iodine sampling at that location since this location is downstream of the combustor and much of the iodine is apparently in particulate form when it reaches that location.

There was a huge discrepancy noted between samples collected by carbon traps in the field and HVA samples. The two values for I^{131} are in disagreement by a factor of about 700. The field carbon trap results have been discounted because one can rationalize that, to obtain the indicated concentrations, more I^{131} would have to be released than there was available in the cartridge inventory. The discrepancy between the values will be investigated further during future experiments.

CONCLUSIONS

The HTRE power system and insert arrangement is a very satisfactory arrangement for the study of reactor damage and as a source of fission products to investigate meteorological diffusion phenomena and radiological studies. Instrumentation presently within

DECLASSIFIED

DECLASSIFIED

the IET facility does not appear to be sufficiently adequate to determine accurately release values for this type of fission product release, i. e., when the entire release takes place in a matter of seconds. Contamination of the facility by the release was not excessive and did not create any unusual problems.

Field measurements taken during the passage of the cloud indicate that the shape of the isopleth pattern may be described by Sutton's diffusion theory; but, because the source strength at the point of release was not definitely established, it is possible that the absolute values of the individual isopleths are incorrect. Meteorological parameters of the diffusion equation were determined sufficiently well to describe the shapes of the isopleth pattern. Further, because of the source term uncertainty, it is not possible to definitely determine the degree to which Sutton's diffusion equations describe the distribution of airborne material during conditions of strong lapse for the distances considered.

There were no measurements that would indicate that any biological hazard was produced as a consequence of the release - either from inhalation of the effluent, by ingestion, or by direct exposure. Activities collected on most field samples were too low for accurate quantitative analysis of specific isotopes because there was insufficient inventory of fission products to produce significant concentrations at the distances of interest for the meteorological condition required at the time of release.

DECLASSIFIED

[redacted]

DECLASSIFIED

AIRCRAFT NUCLEAR PROPULSION DEPARTMENT

GENERAL ELECTRIC

RECEIVED
AEROJET NUCLEAR CO.
JUL 16 1974
NRTS
TECHNICAL LIBRARY

DECLASSIFIED

[redacted]